Hine, A.C., Feary, D.A., and Malone, M.J. (Eds.)
Proceedings of the Ocean Drilling Program, Scientific Results Volume 182

3. Neogene Planktonic Foraminiferal Biostratigraphy of Sites 1126, 1128, 1130, 1132, and 1134, ODP Leg 182, Great Australian Bight[1]

Qianyu Li,[2] Brian McGowran,[2] and Charlotte A. Brunner[3]

ABSTRACT

Planktonic foraminifers from Ocean Drilling Program Leg 182, Holes 1126B and 1126C, 1128B and 1128C, 1130A and 1130B, 1132B, and 1134A and 1134B confirm the neritic record that during the early Miocene the Great Australian Bight region was in a cool-temperate regime with abundant *Globoturborotalita woodi*. Warm marine environments started to develop in the later part of the early Miocene, and the region became warm temperate to subtropical in the early middle Miocene with abundant *Globigerinoides, Orbulina,* and *Globorotalia,* corresponding to global warming at the Miocene climatic optimum. Fluctuations between cool- and warm-temperate conditions prevailed during the late Miocene, as indicated by abundant *Globoconella conoidea* and *Menardella* spp. A major change in planktonic foraminiferal assemblages close to the Miocene/Pliocene boundary not only drove many Miocene species into extinction but also brought about such new species as *Globorotalia crassaformis* and *Globoconella puncticulata*. Warm-temperate environments continued into the early and mid-Pliocene before being replaced by cooler conditions, supporting numerous *Globoconella inflata* and *Globigerina quinqueloba*.

Based on data from this study and published results from the Australia–New Zealand region, we established a local planktonic foraminifer zonation scheme for separating the southern Australian Neogene (SAN) into Zones SAN1 to SAN19 characterizing the Miocene and Zones SAN20 to SAN25 characterizing the Pliocene. The Neogene sections

[1]Li, Q., McGowran, B., and Brunner, C.A., 2003. Neogene planktonic foraminiferal biostratigraphy of Sites 1126, 1128, 1130, 1132, and 1134, ODP Leg 182, Great Australian Bight. *In* Hine, A.C., Feary, D.A., and Malone, M.J. (Eds.), *Proc. ODP, Sci. Results,* 182, 1–67 [Online]. Available from World Wide Web: <http://www-odp.tamu.edu/publications/182_SR/VOLUME/CHAPTERS/005.PDF>. [Cited YYYY-MM-DD]

[2]Department of Geology and Geophysics, The University of Adelaide, Adelaide SA 5005, Australia. Correspondence author: qianyu.li@adelaide.edu.au
[3]Department of Marine Science, University of Southern Mississippi, Stennis Space Center MS 39529, USA.

Initial receipt: 21 April 2001
Acceptance: 30 September 2002
Web publication: 30 June 2003
Ms 182SR-005

from the Great Australian Bight are bounded by hiatuses of ~0.5 to >3 m.y. in duration, although poor core recovery in some holes obscured a proper biostratigraphic resolution. A total of 15 hiatuses, numbered 1 to 15, were identified as synchronous events from the base of the Miocene to the lower part of the Pleistocene. We believe that these are local manifestations of major third-order boundaries at about (1) 23.8, (2) 22.3, (3) 20.5, (4) 18.7, (5) 16.4, (6) 14.8, (7) 13.5, (8) 11.5, (9) 9.3, (10) 7.0, (11) 6.0, (12) 4.5, (13) 3.5, (14) 2.5, and (15) 1.5 Ma, respectively. This hiatus-bounded Neogene succession samples regional transgressions and stages of southern Australia and reveals its stepwise evolutionary history.

INTRODUCTION

Among the four allostratigraphic Cenozoic supersequences from neritic southern Australia, the last two comprise the late Oligocene to middle Miocene and late Miocene to Quaternary, respectively (McGowran et al., 1997b, fig. 6). These are second-order sequences, representing transgression-regression and warming-cooling at 10^7-yr scale and each containing a bundle of third-order marine transgressions at 10^6-yr scale. The third supersequence, exemplified by the Miocene oscillation, has been the subject of a series of studies on planktonic and benthic foraminifers in the Lakes Entrance section from southeastern Australia (McGowran and Li, 1994, 1997; Li and McGowran, 2000). These and other similar studies indicate that the neritic realm in southern Australia reflects a substantial global component in its regional geohistorical and biohistorical records (McGowran et al., 1997b). One of the objectives of Ocean Drilling Program (ODP) Leg 182 was to test the completeness of this neritic record in sediments from oceanic settings in the Great Australian Bight.

Nine sites were drilled during Leg 182 in the western Great Australian Bight (Fig. F1B). Neogene sediments were recovered from all sites, with Sites 1126 and 1134 containing similar relatively complete Neogene sequences. Planktonic foraminifers are common to abundant and fair to well preserved in sites from deeper water (Sites 1126, 1128, 1130, and 1134). However, they are rare and poorly preserved in sediments from shallower sites, especially Sites 1127, 1129, and 1131 on the upper slope from the eastern transect. Reasons for their rarity and poor preservation may include a higher sedimentation rate driven by prolific bryozoans, abundant chert, and an early diagenesis resulting from the presence of a brine (Swart et al., 2000). By analyzing planktonic foraminifers in sediments from selected sites, we aimed to establish a biostratigraphic framework for the region. The results may also suffice for us to address the following issues: how many datum levels can be reliably applied to Neogene sections from offshore to onshore? How rapid did the planktonic foraminiferal assemblage respond to changes in climate and water mass from one mode to another? What is the faunal evidence of major oceanographic events in the region, such as transgressions/regressions, erosions, activities of the Leeuwin Current, and high productivity?

F1. Circulation around southern Australia and Cenozoic basins, p. 29.

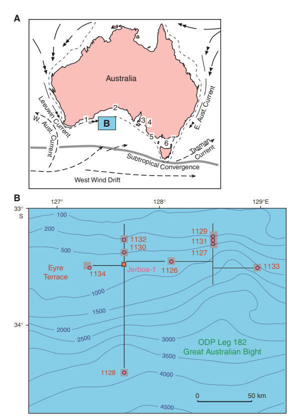

MATERIALS

We studied a total of 406 samples from Neogene sections recovered at Sites 1126, 1128, 1130, 1132, and 1134 (Table T1). Among them, 164

T1. Site parameters and Neogene samples, p. 42.

core catcher samples were washed, dried, and examined on board and reexamined after the cruise. Other samples collected postcruise, mostly at a spacing of 1–3 m, were processed with standard techniques. About 300–400 planktonic foraminifer individuals were picked and identified from a small fraction of each sample. Identification of species was mainly with reference to Blow (1979), Kennett and Srinivasan (1983), Bolli and Saunders (1985), and Hornibrook et al. (1989). We used the first occurrence (FO) or last occurrence (LO) and relevant common occurrences (first common occurrence [FCO] or last common occurrence [LCO]) of species found widely in southern Australia as datum levels (Fig. F2). These levels were tied to calibrated ages listed in Berggren et al. (1995) and updated by the Shipboard Scientific Parties of Leg 181 (Carter, McCave, Richter, Carter, et al., 1999, table T3) and Leg 182 (Feary, Hine, Malone, et al., 2000, table T3).

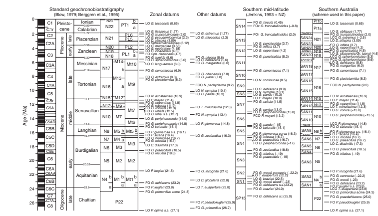

F2. Neogene and Quaternary geochronostratigraphy, p. 30.

NEOGENE PLANKTONIC FORAMINIFERAL STUDIES

Neogene planktonic foraminifers in the southern Indo-Pacific region were studied notably by Jenkins (1971, 1985; mainly from New Zealand), Brönnimann and Resig (1971; southwest Pacific, Deep Sea Drilling Project [DSDP] Leg 7), Jenkins and Srinivasan (1986; southwest Pacific, DSDP Leg 90), Srinivasan and Kennett (1981; South Pacific), Kennett et al. (1985; Indo-Pacific), Wright and Thunell (1988; Indian Ocean), Huber (1991; Kerguelen Plateau, Ocean Drilling Program [ODP] Leg 119), Berggren (1992; Kerguelen Plateau, ODP Leg 120), and Chaisson and Leckie (1993; equatorial western Pacific). In southern Australia, McGowran et al. (1971) first attempted the correlation of local assemblages to tropical zonations and McGowran (1986) emphasized species datum levels while reviewing planktonic foraminiferal biostratigraphy of the southern Indo-Pacific region. McGowran and Li (1997) reported their detailed study on the Lakes Entrance section in southeastern Australia, from which Jenkins (1960) pioneered a local planktonic foraminiferal zonation.

In southern Australia, the (sub)tropical zonations of Blow (1979) and Berggren et al. (1995) cannot be directly recognized because of the rarity or absence of many zonal markers. The southern mid-latitude zonation of Jenkins (1993) (Fig. F2) appears to be relevant, but three reasons prevented its use in this study: (1) lack of chronologic constraint on many datum levels, (2) difficulties in correlating it with other schemes (see also Hornibrook et al., 1989), and (3) at least some datum levels probably from a more incomplete stratigraphy than previously realized. Examples of the latter two points include the FO of *Globoconella puncticulata,* which has been used to date the Miocene/Pliocene boundary by Jenkins (1971, 1993; as *Globorotalia puncticulata*). Jenkins (1993) also recognized the overlying Zone SN12 (including *Globorotalia pliozea* and *Globorotalia puncticulata* Subzones) as representing the early Pliocene, with the top defined by the LO of *Globorotalia inflata*. The succession, as summarized in Jenkins (1993), from the FO of *G. puncticulata* (also FO of *G. pliozea*) to the LO of *G. pliozea* to the FO of *G. inflata* could not be ratified by Hornibrook et al. (1989, p. 144), who showed that *G. pliozea* ranged as high as the LO of *Globorotalia margaritae*. Based on a magnetostratigraphy, Berggren et al. (1995) dated the FO of *G. pliozea* at 5.6 Ma, the FO of *G. puncticulata* at 4.5 Ma, the LO of *G. margaritae* at 3.58

Ma, and the FO of *G. inflata* at 2.09 Ma. Although this mainly Mediterranean record may not be considered as a standard also for southern mid-latitudes, the sequence of these events may remain consistent should it not be disturbed by an incomplete local statigraphic section or by variations in the distribution of species. Consequently, we proposed a new zonation scheme, a hybrid of the existing subtropical and temperate zones. We hoped our scheme not only served a better biostratigraphy in this study but for the entire southern Australian region at large.

Datums and Zones

Figure F2 summarizes the integrated Neogene geochronostratigraphy, showing standard planktonic foraminiferal Neogene (N-) zones of Blow (1979) and Miocene (M-), Miocene transitional (Mt-), and Pliocene (PL-) zones and datum levels of Berggren et al. (1995). Jenkins' (1971, 1985, 1993) southern mid-latitude zones were correlated by recalculating the zonal markers. Stratigraphically useful datum levels found in southern Australia, as tabled in McGowran (1986) and McGowran et al. (1997b), were tied to the standard zonal scheme to highlight their synchronous nature. The new southern Australian Neogene SAN zones were recognized with species datums as detailed below, together with brief discussions on the regional assemblages.

Early Miocene Zones

Zone SAN1

Zone SAN1 (= N4a), 23.8–23.2 Ma, base = FO of *Paragloborotalia kugleri* sensu stricto (s.s.), top = LO of *Globoquadrina dehiscens*. The LCO of *Turborotalia euapertura* can be used as a proxy to the FO of *P. kugleri* in locating the Oligocene/Miocene boundary dated at 23.8 Ma by Berggren et al. (1995). Although Berggren (1992) reported the LO of *T. euapertura* coinciding the boundary in mid- to high-latitude sites, rare specimens of *T. euapertura* have been identified from the early Miocene of Australia (Li and McGowran, 2000; Li et al., 2000) and New Zealand (Jenkins, 1993). The common occurrence of *Globigerinoides primordius* can also be used to recognize the base of the Miocene. In southeastern Australia where *P. kugleri* and *G. primordius* are often absent, the LCO of *T. euapertura* may be more helpful for locating the base of Zone SAN1.

Zone SAN2

Zone SAN2 (≈ N4b), 23.2–21.6 Ma, base = FO of *G. dehiscens* (23.2 Ma), top = *Globoconella incognita*. However, *G. dehiscens* is rare in its early range and needs careful distinction from its predecessor *G. praedehiscens.* In New Zealand, these two morphotypes are often lumped as *G. dehiscens,* with an estimated FO as early as 25 Ma (Morgans et al., 1996). The FO of *Globoturborotalita brazieri* at ~24 Ma (Hornibrook et al., 1989) can also be used to justify the Oligocene/Miocene boundary, especially when accompanied by *G. dehiscens, G. primordius,* and *Dentoglobоqudrina globularis* (Li et al., 1999). Within Zone SAN2, two other datums also occur: the FO of *Globoturborotalita woodi* and the FO of *G. connecta*. Ages estimated for these two datums range between 23 and 22.6 and 22 Ma and between 22.2 and 20.9 and 21 Ma by Hornibrook et al. (1989), Chaproniere et al. (1996), and Li and McGowran (2000), respectively. Li and McGowran (2000) also regarded the FO of *G. connecta* close to the Zone SAN2/SAN3 boundary at ~21.6 Ma, but this placement of the datum appears too high compared to that documented by Hornibrook et al. (1989). In this study, we placed the FO of *F. connecta* in upper Zone SAN2, at ~22.2 Ma, as did Carter, McCave, Richter, Carter, et al. (1999) (Fig. F2).

Zone SAN3

Zone SAN3 (≈ N5), 21.6–19 Ma, base = FO of *G. incognita,* top = FO of *Globigerinoides trilobus* sensu lato (s.l.). The zonal species *G. incognita* first appeared at 21.6 Ma (Berggren, 1992) and is mainly restricted to Zone N5 equivalents (= SAN3) in Australia (Li et al., 2000) and New Zealand (Hornibrook et al., 1989, fig. 27), even though it has been recorded as young as Zone N7 elsewhere (Kennett and Srinivasan, 1983; Berggren et al., 1995). Similar to the underlying Zone SAN2 assemblage, the cancellate-spinose *G. woodi–G. connecta* group is predominant but may be replaced in some intervals in relative abundance by the spinose *Globigerina bulloides* and microperforate tenuitellids that signal cooler and more fertile water (McGowran and Li, 1997; Li and McGowran, 2000).

Zone SAN4

Zone SAN4 (= uppermost N5 to lower N6), 19–18.5 Ma, base = FO of *G. trilobus,* top = FO of *Globorotalia praescitula*. These two datum levels appear to be diachronous, as Jenkins (1985, 1993) found the latter preceding the former and Hornibrook et al. (1989) reported their occurrences from a single level.

Zone SAN5

Zone SAN5 (= upper N6), 18.5–17.3 Ma, base = FO of *G. praescitula,* top = LO of *Catapsydrax dissimilis*. However, to separate this zone from the overlying Zone SAN6 is difficult because the marker species *C. dissimilis* is often rare and its datum is ambiguous locally. We discuss the characteristics of these two zonal assemblages together below.

Zone SAN6

Zone SAN6 (= N7), 17.3–16.4 Ma, base = LO of *C. dissimilis,* top = FO of *Praeorbulina sicana*. Both *G. praescitula* and *Globoconella zealandica* characterize the assemblage in Zones SAN5 and SAN6, although *G. praescitula* rarely ranges into the uppermost Zone SAN6. Other common species include *G. trilobus, G. woodi, G. bulloides,* and *G. dehiscens*. *G. conoidea* occurs sporadically within Zone SAN6. Subzones SAN6a and SAN6b (= Mt4a and Mt4b, respectively) can be recognized by the FO of *Globoconella miozea* at 16.7 Ma. A decline in the abundance of *G. trilobus* and *G. woodi* toward the top of Zone N7 is countered by an increase in *G. bulloides* in the Lakes Entrance section (Li and McGowran, 2000). Scott et al. (1990) reported from New Zealand that the FO of *Fohsella peripheroronda* was in the lower part of Zone N7, at ~17 Ma, but in southern Australia it often arrived much later, in Zone SAN8.

Middle Miocene Zones

Zone SAN7

Zone SAN7 (= N8a), 16.4–16.1 Ma, base = FO of *P. sicana,* top = FO of *Praeorbulina glomerosa* s.s. Apart from the marker species, both *Globigerinoides* (many species including *G. trilobus* and *G. quadrilobatus*) and *Globoconella* (mainly *G. miozea, G. conica,* and *G. conoidea*) are abundant in Zone SAN7 and range into younger intervals. *Globigerina,* however, declines to a minimum and is often represented by some large specimens of *G. bulloides*.

Zone SAN8

Zone SAN8 (= N8b), 16.1–15.1 Ma, base = FO of *P. glomerosa* s.s., top = FO of *Orbulina suturalis*. The assemblage is dominated by various species of *Praeorbulina, Globigerinoides,* and *Globoconella*.

Zone SAN9

Zone SAN9 (= N9), 15.1–14.8 Ma, base = FO of *O. suturalis,* top = LCO of *P. glomerosa*. Although many species are similar to those in Zone N8, the keeled globorotaliids began to become common in Zone N9, especially *Globoconella panda, G. scitula,* and the *Menardella archeomenardii–Menardella praemenardii* bioseries.

Zone SAN10

Zone SAN10 (= lower N10), 14.8–13.5 Ma, base = LCO of *P. glomerosa,* top = LO of *F. peripheroronda*. The age of 13.5 Ma for the latter datum is here proposed pending further studies, although it has been dated at 14.0 Ma by Berggren et al. (1995) and 13.0 Ma by Morgans et al. (1996). Other important events occurring within Zone SAN10 include the FO of *M. praemenardii* and the FO of *Sphaeroidinellopsis kochi* (both close to base of N10, according to Kennett and Srinivasan, 1983).

Zone SAN11

Zone SAN11 (= upper N10), 13.5–13 Ma, base = LO of *F. peripheroronda,* top = LO of *Globoconella conica*. Morgans et al. (1996) considered the later datum close to 13 Ma, as quoted also in Carter, McCave, Richter, Carter, et al. (1999). Two other datums are significant: the FO of *Neogloboquadrina nympha* at 13.4 Ma (Berggren, 1992) and the FCO of *Paragloborotalia mayeri* at 13.2 Ma (Scott et al., 1990). Jenkins (1993) recognized his Zone SN7 using the FO of *P. mayeri,* a datum he found from below the LO of *F. peripheroronda*.

Zone SAN12

Zone SAN12 (≈ N11–N13), 13–11.8 Ma, base = LO of *G. conica,* top = FO of *Globoturborotalita nepenthes*. Within this interval also occur the FOs of *Menardella menardii, Globorotalia lenguaensis,* and *Globigerinatella siphonifera* (all lower N12; ~12 Ma) (Kennett and Srinivasan, 1983) and the LO of *Tenuitella minutissima* (~12.3 Ma) (Li et al., 1992). *P. mayeri* is the dominant species.

Zone SAN13

Zone SAN13 (= N14), 11.8–11.4 Ma, base = FO of *G. nepenthes,* top = LO of *P. mayeri*. Scott et al. (1990) estimated the latter datum in New Zealand to be at 10.9 Ma, which is 0.5 Ma younger than that estimated by Berggren et al. (1995). The FO of *Globorotalia scitula* is close to the upper limit of Zone SAN13 at ~11.5 Ma. Abundant *P. mayeri* characterizes Zones SAN11 through SAN13 in an interval equivalent to Zone SN7 of Jenkins (1993).

Late Miocene Zones

Zone SAN14

Zone SAN14 (= N15), 11.4–10.9 Ma, base = LO of *P. mayeri,* top = FO of *Neogloboquadrina acostaensis*. According to Kennett and Srinivasan

(1983), typical *Globigerinoides ruber* first occurred within this interval (~11 Ma).

Zone SAN15

Zone SAN15 (= lower N16), 10.9–9.2 Ma, base = FO of *N. acostaensis,* top = FCO of *Neogloboquadrina pachyderma* (9.2 Ma) (Berggren, 1992). Other important datums include the LO of *G. panda* (~10.3 Ma) (Scott et al., 1990) and a temporary LO of *G. dehiscens* (9.9 Ma) (Morgans et al., 1996).

Zone SAN16

Zone SAN16 (= upper N16), 9.2–8.3 Ma, base = FCO of *N. pachyderma,* top = FO of *Globorotalia pleisiotumida* or FO of *Globigerinoides extremus*. The LO of *Neogloboquadrina continuosa* was within this interval at ~8.5 Ma. *G. conoidea–Globoconella miotumida* complex remained common to abundant.

Zone SAN17

Zone SAN17 (= lower N17), 8.3–7.1 Ma, base = FO of *G. pleisiotumida* or FO of *G. extremus,* top = FO of *Globoconella conomiozea*. Note that the latter datum was dated at 6.9 Ma by Berggren et al. (1995), ~0.2 Ma younger than the age given in Morgans et al. (1996), which is adopted here. Common in Zones SAN17 and SAN18 include such keeled globorotaliids as *M. menardii* and *G. conoidea–G. miotumida*. The FOs of *Globoconella juanai* and *Globoconella cibaoensis* were from this interval, both at ~7.8 Ma.

Zone SAN18

Zone SAN18 (= mid N17, = upper Mt9), 7.1–6.0 Ma, base = FO of *G. conomiozea,* top = FO of *G. margaritae* or LO of *G. lenguaensis*.

Zone SAN19

Zone SAN19 (= upper N17), 6.0–5.3 Ma, base = FO of *G. margaritae* or LO of *G. lenguaensis,* top = LCO of *Globoconella sphericomiozea*. The FCO of *Globoconella sphericomiozea* or the FO of *Globorotalia tumida* (both at 5.6 Ma) can be used to separate between Subzones SAN19a and SAN19b, the latter being an analog to the *Globorotalia sphericomiozea* Subzone of Hornibrook et al. (1989). As in the underlying SAN18, Subzone SAN19a contains frequent *M. menardii, Globigerinoides* spp., *Neogloboquadrina* spp., *Globorotalia plesiotumida, G. conoidea, G. juanai–G. cibaoensis* complex, and *G. miotumida*. *G. dehiscens* last occurred within Subzone SAN19a, at ~5.8 Ma (Chaproniere et al., 1996). It occurs below the FCO of *Globoconella sphericomiozea* rather than concurs at 5.6 Ma, as reported by Berggren et al. (1995). *Globoconella pliozea* first appeared in Subzone SAN19b and ranged up to the Pliocene.

Pliocene Zones

Zone SAN20

Zone SAN20 (≈ N18, ≈ PL1a), 5.3–4.6 Ma, base = LCO of *Globoconella sphericomiozea,* top = LO of *Globorotalia cibaoensis*. Other common species include *Globorotalia crassaformis, G. margaritae, Globoconella pliozea,* and *G. extremus*.

Zone SAN21

Zone SAN21 (≈ N19, ≈ PL1b), 4.6–4.2 Ma, base = LO of *Globorotalia cibaoensis,* top = LO of *G. nepenthes*. *Globoconella puncticulata* first appeared close to the base of Zone SAN21 at ~4.5 Ma. Most common species are *Globoconella puncticulata, G. crassaformis, Globoturborotalita* spp., *Globigerinoides* spp., *G. bulloides,* and *Globigerina falconensis.*

Zone SAN22

Zone SAN22 (≈ N20, ≈ PL2), 4.2–3.7 Ma, base = LO of *G. nepenthes,* top = FO of *Globoconella inflata* at ~3.7 Ma (Morgans et al., 1996). As in the underlying Zone SAN21, *G. crassaformis* and *Globoconella puncticulata* are common to abundant.

Zone SAN23

Zone SAN23 (= lower N21, = PL3–PL4), 3.58–3.1 Ma, base = LO of *G. margaritae,* top = LO of *Dentoglobоquadrina altispira.* The local assemblage is characterized also by abundant *G. ruber* and *Globoconella inflata,* as well as frequent *G. bulloides, G. falconensis,* and *G. quinqueloba.*

Zone SAN24

Zone SAN24 (upper N21, ≈ PL5–PL6), 3.1–2.0 Ma, base = LO of *D. altispira,* top = FO of *Globorotalia truncatulinoides.* The LCO of *G. extremus* was within Zone SAN24 at ~2.5 Ma, close to the FO of *Globorotalia tosaensis.* Species common to Zone SAN24 are *Globoconella inflata, G. ruber, G. crassaformis, G. bulloides,* and *G. quinqueloba.*

Zone SAN25

Zone SAN25 (= uppermost N21), 2.0–1.77 Ma, base = FO of *G. truncatulinoides,* top = LO of *Globigerinoides obliquus* or LO of *G. woodi* as a proxy. Apart from *Globoconella inflata* and *G. ruber, G. crassaformis* and *Globigerina* spp. are also common.

BIOSTRATIGRAPHY OF LEG 182 SITES

Site 1126 (Holes 1126B, 1126C, and 1126D)

At Site 1126, Miocene sediments were recovered in Samples 182-1126D-7R-CC, 15–16 cm, through 182-1126B-8H-3, 76–78 cm, between 204.61 and 67.3 meters below seafloor (mbsf), and Pliocene sediments were recovered in Samples 182-1126B-8H-2, 76–78 cm, through 6H-6, 75–77 cm, between 65.8 and 52.8 mbsf (Fig. F3). Hiatuses were identified in the early Miocene through Pliocene, and several layers of slumped sediments are present in the upper Miocene and lower Pliocene sections.

The lower Miocene resides in Samples 182-1126D-7R-CC, 15–16 cm (204.61 mbsf), through 182-1126B-19H-5, 73–75 cm (154.53 mbsf), an interval with poor core recovery. Zone SAN3 cannot be positively identified, and Zones SAN4 to SAN6 are strongly condensed between 154.53 and 159.55 mbsf, indicating hiatuses at ~155 and between 170 and 180 mbsf. The planktonic foraminiferal assemblage consists mainly of *G. woodi, G. bulloides, Globorotaloides suteri,* and tenuitellids in the lower part and *G. trilobus, G. woodi, G. praescitula,* and *G. zealandica* in the upper part. Species typical of early Miocene to older ages occur sporadically, including *Paragloborotalia semivera* and *C. dissimilis* (Fig. F3).

Middle Miocene Zone SAN7 is recognized by the FO of *P. sicana* in Sample 182-1126B-19H-3, 74–76 cm (151.54 mbsf). It was overshadowed in abundance upward in Cores 182-1126B-18H and 19H by numerous *Globigerinoides mitra* and frequent *G. trilobus, G. quadrilobatus,* and *G. falconensis* (Fig. F4). A short interval between 131.04 and 136.82

F3. Site 1126 planktonic foraminiferal biostratigraphy, p. 31.

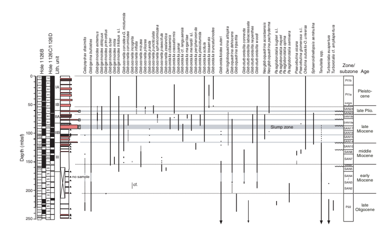

F4. Abundance variations of selected species, Hole 1126B, p. 32.

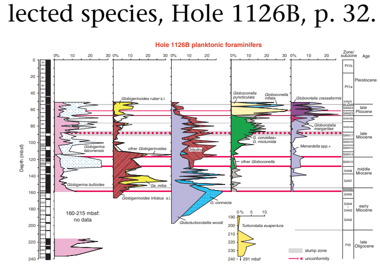

mbsf with *P. glomerosa* indicates that the 1-m.y. Zone SAN8 is probably hiatus-bound if not condensed between Samples 182-1126B-17H-2, 74–76 cm (131.04 mbsf), and 17H-CC, 13–16 cm (136.82 mbsf). An assemblage characterized by *F. peripheroronda* and *Orbulina* spp. denotes Zones SAN9–SAN10 in Samples 182-1126B-14H-6, 74–76 cm (117.74 mbsf), through 17H-1, 75–77 cm (129.76 mbsf). *P. mayeri* is rare or absent. The uppermost middle Miocene is not present at Site 1126, as the *F. peripheroronda* assemblage was overlain by upper Miocene sediments.

Zones SAN14–SAN19 of late Miocene age were identified in Samples 182-1126B-8H-3, 76–78 cm (67.26 mbsf), through 14H-4, 75–77 cm (114.75 mbsf). They contain *G. bulloides, G. falconensis, G. woodi, G. nepenthes, G. conoidea–G. miotumida, O. suturalis–Orbulina universa, G. dehiscens, Globorotalia scitula,* and, in the upper part, *Globorotalia cibaoensis, G. conomiozea,* and *G. pleisiotumida* (Fig. F3). A major reduction in the abundance of *Globigerinoides* and globorotaliids occurs from Zone SAN15 into Zone SAN16 in Hole 1126B (Fig. F4), probably indicating climatic cooling and low sea level. Slumped sediments fall in between Zones SAN17 and SAN18, and the contemporary assemblages were mixed with specimens of older species such as *P. glomerosa* s.l. in Sample 182-1126C-9H-5, 120–125 cm (82.2 mbsf). Many aggregates of the fairly to poorly preserved specimens from this and the underlying sample (Sample 182-1126C-9H-CC, 20–23 cm) at 84.59 mbsf are believed to have been cemented in a process of diagenesis. Frequent *Globoconella sphericomiozea, G. margaritae,* and *G. crassaformis* indicating Subzone SAN19b of the latest Miocene are present in Sample 182-1126B-8-CC, 13–16 cm (72.96 mbsf), but the latter taxon fails to present in other Miocene samples from above, Samples 182-1126B-8H-3, 76–78 cm, through 8H-6, 75–77 cm, between 67.26 and 71.75 mbsf.

The entire lower Pliocene is missing and the upper Pliocene is condensed between Samples 182-1126B-6H-CC, 0–5 cm (53.18 mbsf), and 8H-2, 76–78 cm (65.76 mbsf). A major biotic change across the Miocene/Pliocene boundary saw the extinction of many middle to late Miocene species including *G. conoidea* and *G. sphericomiozea* and the appearance of *Globoconella puncticulata* and *G. crassaformis,* as well an increased abundance of *G. ruber* and *G. falconensis* (Fig. F4). Zones SAN23 and SAN24 can be recognized based on the LO of *D. altispira* (3.09 Ma) in Sample 182-1126B-7H-6, 75–77 cm (62.25 mbsf), within a slump. Therefore, the slump at 60–63 mbsf likely bears an age of ~2.5–3.2 Ma.

Site 1128 (Holes 1128B and 1128C)

A 45-m-thick Neogene section recovered at this deepwater site is represented only by the upper Miocene and Pliocene (Fig. F5). Hiatuses were identified between the lower Oligocene and upper Miocene and between the lower and upper Pliocene. A slumped debrite overlying the lower Oligocene ooze contains species of various ages: *Subbotina angiporoides* and *Chiloguembelina cubensis* (early Oligocene), *G. suteri* and *P. semivera* (late Oligocene to early Miocene), *F. peripheroronda* and *P. mayeri* (middle Miocene), *G.* cf. *lenguaensis* and *G. juanai* (late Miocene), and *G. crassaformis* (Pliocene), suggesting a multiple slumping process (Fig. F5). A late Miocene age assemblage referable to Zones SAN17–SAN18 can be recognized in the upper part of the debrite. Although the youngest slumping episode appears to have taken place during the late Miocene–Pliocene, a conclusive age needs further studies (see Finn Surlyk et al., pers. comm., 2002).

F5. Site 1128 planktonic foraminiferal biostratigraphy, p. 33.

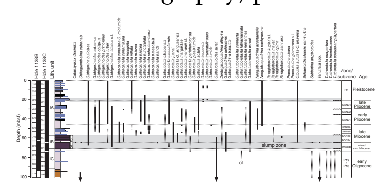

An undistorted Subzone SAN19a with *G. conomiozea, G. conoidea,* and rare *G. margaritae* is recorded overlying the debrite in Samples 182-1128B-6H-5, 78–80 cm (50.48 mbsf), through 182-1128C-7H-1, 75–77 cm (56.25 mbsf). Abundant *Globoconella sphericomiozea* (5%–70%) is present in Samples 182-1128B-6H-2, 74–76 cm (45.94 mbsf), through 6H-4, 74–76 cm (48.94 mbsf), indicating Subzone SAN19b of the uppermost Miocene (Fig. F5). Rare *G. conoidea* and *G. sphericomiozea* range into the lower Pliocene in Hole 1128B, although both are last found in the Miocene of Hole 1128C in Sample 182-1128C-6H-3, 75–77 cm (49.75 mbsf). Planktonic foraminifers decline to a minimum across the Miocene/Pliocene boundary between 44.4 and 46.75 mbsf in Samples 182-1128B-6H-1, 70–72 cm, and 182-1128C-6H-1, 75–77 cm, accompanied by an increase in benthic species, glauconite, and weathered grains.

The early Pliocene age assemblage with *Globoconella puncticulata, G. crassaformis,* and *G. margaritae* is present between 28.45 and 42.45 mbsf in Samples 182-1128B-4H-3, 75–77 cm, through 5H-6, 75–77 cm. Zone SAN20 tops at the LO of *G.* cf. *cibaoensis* at ~34 mbsf. As Zone SAN21 cannot be positively identified because of the rarity of the zonal marker *G. nepenthes,* a hiatus close to ~34 mbsf is then suggested. The LO of *G. margaritae* at 28.45 mbsf indicates the top of Zone SAN22. Another hiatus probably lies at this level, as it also coincides with the LOs of *Globorotalia menardii* and *N. acostaensis* and is only one sample below the LOs of *G. extremus* and *G. trilobus* s.l at 27 mbsf in Hole 1128B. Dissolution is also apparent, with up to 50% broken tests found in the assemblage from Samples 182-1128C-3H-3, 75–77 cm (21.25 mbsf), through 182-1128B-4H-1, 75–77 cm (25.45 mbsf). The coincidence of these events likely indicates the responses to the mid-Pliocene global cooling and a major ice-cap growth on Antarctica (e.g., Kennett, 1977). The overlying assemblage belongs in upper Pliocene Zones SAN23–SAN25, with abundant *Globoconella inflata, G. puncticulata, G. crassaformis,* and frequent *G. ruber* in Samples 182-1128B-3H-3, 76–78 cm (18.96 mbsf), through 4H-2, 75–77 cm (26.95 mbsf). The absence of *D. altispira* in samples above 28.45 mbsf also indicates that upper Pliocene sediments are mainly of Zone SAN24 age.

Site 1130 (Holes 1130A and 1130B)

The Neogene at Site 1130 is similar to that at Site 1128 in comprising mainly the upper Miocene and Pliocene, but the section is expanded between 225 and 328 mbsf in Holes 1130A and 1130B (Fig. F6). The upper Miocene ooze is mainly of Zones SAN17–SAN19 age, unconformably overlying the upper Oligocene chert-carbonate sequence. Zone SAN17 with *G. plesiotumida* and *G. extremus* extends from 327.05 to 309.15 mbsf in Samples 182-1130A-35X-4, 85–87 cm, to 33X-5, 75–77 cm. Upsection, Zone SAN18 is marked at base by the FO of *G. conomiozea* in Sample 182-1130A-33X-4, 85–87 cm (307.75 mbsf), Subzone SAN19a by the LO of *G. lenguaensis* in Sample 32X-1, 75–77 cm (293.55 mbsf), and Subzone SAN19b by the FCO of *Globoconella sphericomiozea* in Sample 31X-1, 75–77 cm (283.85 mbsf). It is noteworthy that *G. dehiscens* is not present in any upper Miocene samples from these two holes, although its LO has been recorded in Zone SAN18 at Site 1126 (Fig. F3) and in Subzone SAN19a at Site 1128 (Fig. F5). A steady decrease in the abundance of *G. woodi* from the upper Miocene to Pliocene was matched by an increase in globorotaliids (*Globorotalia, Globoconella,* and *Menardella*) and *Globigerinoides* (Fig. F7).

F6. Site 1130 planktonic foraminiferal biostratigraphy, p. 34.

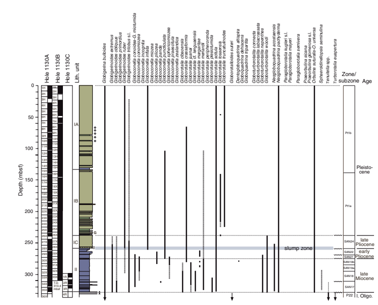

F7. Abundance variations of selected species, Hole 1130A, p. 35.

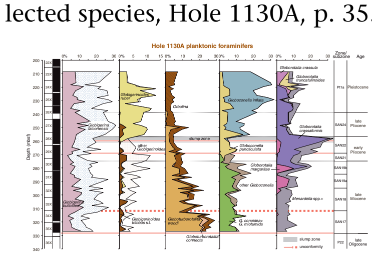

The Miocene/Pliocene boundary lies between the LCO of *Globoconella sphericomiozea* in Sample 182-1130A-29X-5, 75–77 cm (270.65 mbsf), and the FO of *G. puncticulata* in Sample 29X-CC, 36–39 cm (273.71 mbsf). Only in Holes 1130A and 1130B did we observe an overlap between these two datums. The FO of *G. crassaformis,* which was found coeval with the FO of *G. puncticulata* and both together indicating the Miocene/Pliocene boundary in other holes, is present within Subzone SAN19b in Sample 182-1130A-30X-5, 76–78 cm (280.26 mbsf). The concurrence of these species probably resulted from sediment mixing, and the lowermost Pliocene (Zone SAN20) is likely missing. Nevertheless, the population of *G. crassaformis* from Cores 182-1130B-29X and 30X is dominated by sinistrally coiled specimens, similar to those recorded in the lower Pliocene of New Zealand (Hornibrook et al., 1989, fig. 28). The LO of *G. nepenthes* in Sample 182-1130A-29X-4, 85–87 cm (269.25 mbsf), defines the upper limit of the undivided Zone SAN21. The lower/upper Pliocene boundary falls at the FO of *Globoconella inflata* in Sample 182-1130A-28X-3, 75–77 cm (258.05 mbsf), ~1 m below the slump zone between 256.5 and 257.3 mbsf.

As from other holes, the upper Pliocene in Hole 1130A contains a less diverse assemblage predominated by *G. inflata, G. puncticulata, G. crassaformis,* and *G. ruber,* and its upper boundary lies close to 240.25 mbsf with the LO of *G. extremus* in Sample 182-1130B-26X-5, 75–77 cm. The LO of *G. woodi* in Sample 182-1130A-26X-3, 75–77 cm (238.75 mbsf), can also be used as a proxy. The Zone SAN23 marker *D. altispira* was observed only in the uppermost Miocene (278.85mbsf) but not in any Pliocene samples from Holes 1130A or 1130B, suggesting that the upper Pliocene section could be mainly of Zones SAN24–SAN25 age. Consequently, the FO of *G. truncatulinoides* in Sample 182-1130A-25X-1, 75–77 cm (226.15 mbsf), is probably not a true FO record but represents a younger local occurrence of that species at ~1 Ma.

Site 1132 (Holes 1132B and 1132C)

Only ~3% of the cored Neogene section was recovered at this shallow-water site, with the core catcher samples the only material available. About 90% of this material is represented by middle Miocene chert-carbonates, which attain 190 m out of the 210-m Neogene section between 240 and 450 mbsf. The lower and upper Miocene are both thin and incomplete, and the Pliocene is missing (Fig. **F8**). Planktonic foraminifers are rare and poorly preserved. Hiatuses are suspected at the early/middle Miocene boundary, within the middle Miocene, at the middle/late Miocene boundary, and at the late Miocene/Pleistocene boundary.

F8. Site 1132 planktonic foraminiferal biostratigraphy, p. 36.

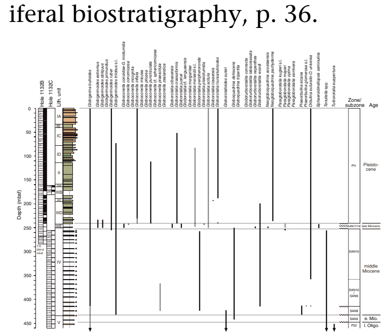

The lower Miocene is represented by a single sample, Sample 182-1132C-23R-CC, 18–21 cm (441.68 mbsf), with rare *G. suteri, G. dehiscens, Tenuitella* spp., and *G. bulloides*. The absence of *G. woodi, G. trilobus,* and other younger species suggests a Zone SAN1 assemblage. The contacts of this thin unit with the underlying upper Oligocene (mid to lower Zone P22) and overlying middle Miocene are therefore unconformable.

P. sicana, indicating middle Miocene Zone SAN7 is present in Samples 182-1132C-21R-CC, 23–26 cm (423.13 mbsf), and 22R-CC, 10–13 cm (432.3 mbsf). The latter sample also contains the FO of *F. peripheroronda*. In Sample 182-1132C-20R-CC, 22–25 cm (413.82 mbsf), the coexistence of *P. sicana, P. glomerosa,* and *O. suturalis–O. universa* indicates Zone SAN9. Farther upsection, however, core catchers from Cores 182-

1132C-15R to 19R are in such a poor state that neither *P. glomerosa* nor *O. universa* was observed. The undifferentiated Zones SAN9–SAN10 interval extends up to Sample 182-1132B-29X-CC, 23–26 cm (257.43 mbsf), because of the persistent occurrence of *F. peripheroronda* (LO ≈ 13.5 Ma). Sample 182-1132C-3R-CC, 7–8 cm (255.87 mbsf), contains *P. mayeri* but without *F. peripheroronda,* probably representing Zones SAN11 to SAN13.

The upper Miocene is represented only by Samples 182-1132B-27X-CC, 34–37 cm (241.8 mbsf), and 28X-CC, 32–35 cm (250.73 mbsf). *Globoconella cibaoensis, G. extremus,* and (in the latter sample) *G. conomiozea* indicate that these two samples fall, respectively, in Zones SAN17 and SAN18. Rare specimens similar to *P. mayeri* are likely representatives of *Paraglorotalitia challengeri* if they are not the reworked *P. mayeri*.

Site 1134 (Holes 1134A and 1134B)

A good recovery, especially in the upper parts of Holes 1134A and 1134B, allows a better biostratigraphic resolution by planktonic foraminifers. Neogene sediments comprise the interval between ~50 and 235 mbsf, including a relatively complete Miocene section (Fig. **F9**). Hiatuses occur mainly in the middle Miocene to Pliocene. The abundance variations of species in Hole 1134A (Fig. **F10**) are comparable with those in Hole 1126B (Fig. **F4**).

F9. Site 1134 planktonic foraminiferal biostratigraphy, p. 37.

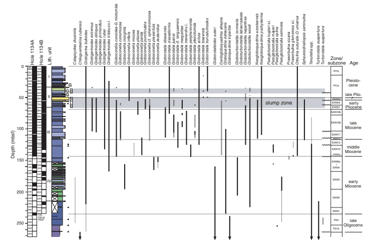

F10. Abundance variations of selected species, Hole 1134A, p. 38.

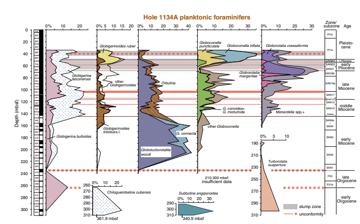

Lower Miocene Zone SAN2 with *G. dehiscens* and later with *G. woodi* and *G. connecta* is present between Samples 182-1134A-27X-1, 75–77 cm (234.35 mbsf), and 23X-CC, 32–35 cm (197.83 mbsf). The FO of *Globoconella incognita* in Sample 182-1134A-23X-1, 75–77 cm (195.85 mbsf), denotes Zone SAN3, in which *P. semivera* is also characteristic. *G. trilobus* first occurs in Sample 182-1134A-19X-CC, 29–32 cm (162.84 mbsf), whereas the FO of *G. praescitula* is observed ~5 m below, in Sample 20X-1, 75–77 cm (167.05 mbsf). Both datums are close to the base of Zone N6 (≈ SAN4), but unlike those previously reported from other southern Australian localities (e.g., Li and McGowran, 2000), they are here inverse in the order of distribution. This pattern suggests that *G. trilobus* was rare in its early transition from *G. connecta* and its FO could have been slightly diachronous between regions if they are not obscured by hiatuses. The boundary between Zones SAN5 and SAN6 cannot be defined without *C. dissimilis,* a species last observed below 189 mbsf in Zone SAN3. The upper Zone SAN6 appears to be missing, as the diagnostic species *Globoconella miozea* first occurs together with and above the Zone SAN7 marker *P. sicana* in Samples 182-1134B-16X-5, 75–77 cm (145.35 mbsf), and 17X-1, 75–77 cm (148.95 mbsf). *G. mitra* here is not as characteristic as in Zone SAN7 of Hole 1126B, although it ranges up to Zone SAN13 in Hole 1134A. Therefore, the mixing between the Zone SAN5–lower SAN6 species *G. praescitula* and *G. zealandica* and Subzone SAN7a *P. sicana* without significant *G. mitra* suggests that a hiatus is probably present at least in the upper Zone SAN6–SAN7 interval.

Farther upsection, a middle Miocene assemblage with *P. glomerosa* and *O. suturalis* indicating Zone SAN9 or younger is present in Samples 182-1134B-16X-3, 75–77 cm (142.35 mbsf), and 182-1134A-17X-CC, 31–34 cm (144.17 mbsf). Accordingly, Zone SAN8 (15.1–16.1 Ma) as a whole is likely hiatus-bound, if it is not condensed in the 1.2-m unsampled interval between 144.17 and 145.35 mbsf. Zone SAN10 with *O. universa* and *F. peripheroronda* extends up to Sample 182-1134A-14H-5, 75–77 cm (125.13 mbsf). *P. mayeri* is also present in this interval. An overlap in the ranges of *F. peripheroronda* and *G. lenguaensis* s.l. was recorded at 125.13–129.75 mbsf, and their transitional morphologies appear to support a predecessor-descendant relationship between them as implied by Kennett and Srinivasan (1983). However, many studies indicate that the FO of *G. lenguaensis* is in Zone N12 (= mid-SAN12) and the LO of *F. peripheroronda* in Zone N10 (= SAN10–SAN11) and there is even a gap within Zone N12 between the former and an advanced form of the latter, the LO of *F. peripheroacuta* (Chaisson and Leckie, 1993), a species rarely recorded from southern Australia. Therefore, the overlap between the ranges of *G. lenguaensis* and *F. peripheroronda* likely reflects a sediment disturbance resulting from events such as a hiatus or slump. Reworking also caused the presence of other older species such as *P. glomerosa* s.l. (Zones SAN8–SAN9). Sample 182-1134A-14H-5, 75–77 cm (125.13 mbsf), not only contains the LOs of *F. peripheroronda* and *P. mayeri* but also the FOs of *M. menardii* and *G. nepenthes,* indicating Zone SAN13. Therefore, Zone SAN12 is probably missing, representing a hiatus of at least 1 m.y.

The middle/late Miocene boundary is also unconformable, overlain by a Zones SAN17–SAN18 assemblage comprising *Globorotalia cibaoensis, G.* cf. *conomiozea, N. acostaensis,* and *Sphaeroidinellopsis seminulina* in Samples 182-1134A-13H-5, 75–77 cm (115.75 mbsf), through 14H-1, 75–77 cm (119.25 mbsf). Subzones SAN19a and SAN19b, respectively, are defined at the base by the FO of *G. margaritae* in Sample 182-1134A-12H-3, 75–77 cm (103.25 mbsf), and by the FCO of *Globoconella sphericomiozea* in Sample 11H-1, 75–77 cm (90.75 mbsf). The LO of *G. lenguaensis* is present in Sample 182-1134A-10H-5, 75–77 cm (87.28 mbsf), and the FO of *Globoconella pliozea* in Sample 9H-5, 78–80 cm (77.78 mbsf). As at Site 1130, *G. crassaformis* first occurs within Subzone SAN19b in Sample 182-1134A-9H-3, 77–79 cm (74.77 mbsf).

The lower Pliocene Zone SAN21 is defined by the coexistence of *Globoconella puncticulata* and *Globorotalia cibaoensis* in Samples 182-1134A-8H-3, 75–77 cm (65.25 mbsf), and 8H-5, 78–80 cm (68.28 mbsf). *G. crassaformis* and *G. falconensis* are most abundant (Fig. **F10**). Almost the entire Pliocene section is occupied by a slump between 49.25 and 62.25 mbsf with displaced specimens of such older species as *G. suteri, G. dehiscens,* and *G. conomiozea*. However, several diagnostic datums recognized are in the correct order for determining zones. Zones SAN21 and SAN22 were then justified at the top, respectively, by the consistent LO of *G. nepenthes* in Sample 182-1134A-8H-1, 75–77 cm (62.25 mbsf), and the FO of *Globoconella inflata* in Sample 7H-3, 75–77 cm (55.75 mbsf). The coexistence of the LO of *D. altispira* and the FO of *G. inflata* at 55.75 mbsf indicates that Zone SAN23 is likely missing. The LCO of *G. extremus* in Sample 182-1134A-7H-1, 77–79 cm (52.77 mbsf), denotes lower Zone SAN24. One sample above the latter datum contains the Zone SAN25 marker *G. truncatulinoides* in Sample 182-1134A-6H-5, 75–77 cm (49.25 mbsf). Another slumped assemblage with Pliocene and older species is present in the lower part of the Pleistocene, coinciding with the consistent occurrence of *G. truncatulinoides* (Fig. **F9**).

Summary of Neogene Biostratigraphy

Figure **F11** summarizes the planktonic foraminiferal results, emphasizing the new SAN zones and their correlated N zones. The following generalizations can be made.

F11. Biostratigraphic correlation of the Neogene, p. 39.

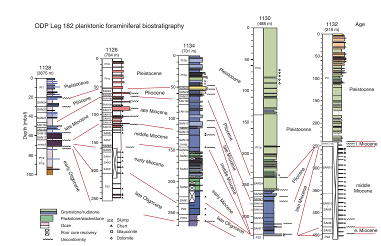

1. The most complete Neogene sections were recovered from intermediate depths at Sites 1126 and 1134.
2. Sediments are dated to planktonic foraminiferal zones and subzones, although uncertainties exist, especially for the lower Miocene at Sites 1126 and 1134 and middle Miocene at Site 1132, with low core recoveries.
3. Most Neogene units are bounded by hiatuses, numbered 1–11 for the Miocene and 12–15 for the Pliocene and basal Pleistocene (detailed below and in Figs. F12 and F13). The lower and middle Miocene are missing from Sites 1128 and 1130, and at least part of the middle and upper Miocene are absent from all sites studied.
4. The entire Pliocene is missing from Site 1132, and the section at Sites 1126, 1128, 1130 and 1134 is condensed.
5. Slumps occur mainly in the uppermost Miocene and Pliocene, largely concurring with hiatuses. A congestion of these events in this interval may reflect stronger fluctuations at generally lower sea levels, probably conjoined with tectonic activities in the region (Dickinson et al., 2001).
6. The abundance variations of planktonic foraminifers in Holes 1126B, 1130A, and 1134A (Figs. F4, F7, F10) reveal a cool-temperate regime in the early Miocene with abundant *G. woodi,* a warm-temperate middle Miocene with abundant *G. trilobus* s.l and *Orbulina,* a fluctuating cool- to warm-temperate late Miocene with abundant *G. conoidea* and *Menardella* spp., and a temperate Pliocene with abundant *G. crassaformis* and *Globoconella puncticulata.*
7. An influx of *Globoconella inflata* and *G. ruber* in the late Pliocene was probably related to a period of high productivity induced by cooling and northward expansion of the fertile Subantarctic Water (Hodell and Warnke, 1991).
8. Species diversity was low, ~20 species, in the Eocene–Oligocene, although the number could have been obscured by poor preservation (Li et al., this volume). Thirty or more species were present in two periods: the early middle Miocene and latest Miocene. Diversity gradually declined to ~20 species in the Pliocene, and only about 15 species were recorded in recent sediments (Li and McGowran, 1998).
9. Subtropical species are rare and are mainly present in the upper lower Miocene and younger intervals, indicating climatic warming and a stronger flow of the Leeuwin Current (McGowran et al., 1997a). They include *G. quadrilobatus, G. sacculifer, G. mitra, G. conglobatus, P. glomerosa* s.l., *G. lenguaensis, G. margaritae, G. plesiotumida, M. menardii, S. seminulina,* and *G. nepenthes.*
10. The local assemblages responded to global warmings and coolings with speciations and extinctions as well as changing abundances. There is also faunal evidence of other paleoceanographic events, such as the development of the circum-Antarctic Current (Kennett, 1977) and glaciations defined isotopically during the Miocene and Pliocene (Miller et al., 1991, 1998) (Fig. F12).

Hiatuses and Sequence Boundaries

A plot of planktonic foraminifer datum levels from Tables T2, T3, T4, T5, and T6 revealed the duration and position of hiatuses, as well as changes in sedimentation rates at these five sites (Fig. F12). The num-

F12. Time-depth diagram of planktonic foraminifer datums, p. 40.

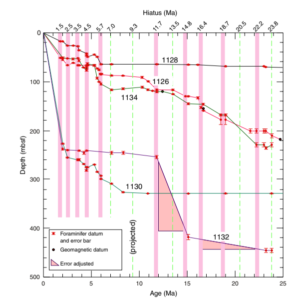

F13. Neogene carbonates from the Great Australian Bight, p. 41.

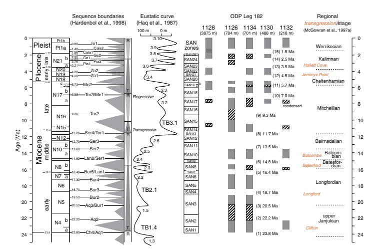

T2. Datum levels, Hole 1126B, p. 43.

T3. Datum levels, Hole 1128B, p. 44.

T4. Datum levels, Hole 1130A, p. 45.

T5. Datum levels, Holes 1132B and 1132C, p. 46.

T6. Datum levels, Hole 1134A, p. 47.

bered hiatuses 1–15 fall mostly at the major third-order boundaries recognized by Hardenbol et al. (1998) and correspond to major falls in sea level (Haq et al., 1987) (Fig. **F13**). Longer gaps in the sedimentary column indicate erosion and/or nondeposition for at least 3 m.y., probably related to repeated erosional events concurring with the hiatuses. The hiatuses are described below in ascending order.

1. Hiatus 1, between Zones P22 and SAN1 or SAN2, is equivalent to Oligocene/Miocene boundary Ch4/Aq1 at 23.8 Ma (Hardenbol et al., 1998). Upper Oligocene Zone P22 sediments unconformably underlie upper Miocene Zone SAN17 in Hole 1130A. At Site 1128, the hiatus is subsumed in a debrite representing a gap between the lower Oligocene and upper Miocene. Zone P22 in Holes 1126B, 1132C, and 1134A is condensed, although because of poor recovery planktonic foraminifers cannot resolve how much of it is missing. The estimated duration of hiatus 1 is ~0.5 m.y. Within the limit of our biostratigraphic resolution, sedimentary accumulation resumes coevally after the event at two slope sites and one shelf site.
2. Hiatus 2, between Zones SAN2 and SAN3, is equivalent to lower Miocene boundary Aq2 at 22.2 Ma. The coexistence of the FOs of *G. woodi* (~23 Ma) and *G. connecta* (~22.2 Ma) in Holes 1126B and 1134A indicates the upper part of Zone SAN2 is probably missing (Fig. **F12**), although poor core recovery hinders a firm conclusion. The hiatus is subsumed in the gap between Zones SAN2 and SAN7 in Hole 1132C, in the gap between Zones P22 and N17 in Hole 1130A, and in the debrite at Site 1128. Its duration is estimated to be <0.5 m.y.
3. Hiatus 3, within Zone SAN3, lower Miocene boundary Aq3/Bur1 at 20.5 Ma, is equivalent to the second-order TB1/TB2 boundary of Haq et al. (1987). This hiatus is subsumed in the gap between Zones SAN2 and SAN8 in Hole 1132C, in the gap between Zones P22 and SAN17 in Hole 1130A, and in the debrite at Site 1128. It is also suspected in Holes 1126B and 1134A, but the poor recovery hampers a proper resolution. At least 1 m.y. is estimated for its duration.
4. Hiatus 4, lower Zone SAN4, is equivalent to lower Miocene boundary Bur3 at 18.7 Ma. In Holes 1126B and 1134A, the coexistence of *G. trilobus* and *G. praescitula* indicates part of SAN4 is missing. The hiatus is subsumed in the gap between Zones SAN2 and SAN8 in Hole 1132C, in the gap between Zones P22 and SAN17 in Hole 1130A, and in the debrite at Site 1128. Its duration is estimated to be ~0.5 m.y.
5. Hiatus 5, between Zone SAN6 and SAN7, is equivalent to Bur5/Lan1 at the lower/middle Miocene boundary at 16.4 Ma. The absence of at least part of these two zones from Holes 1126B, 1132C, and 1134A best exemplifies this hiatus. It is subsumed in the gap between Zones P22 and SAN17 in Hole 1130A and in the debrite at Site 1128. The estimated duration is ~0.5 m.y.
6. Hiatus 6, between Zones SAN8 and SAN9, is equivalent to middle Miocene boundary Lan2/Ser1 at 14.8 Ma. It is documented in Holes 1126B, 1132C, and 1134A, where much of SAN8 is missing and SAN9 is highly condensed. It is subsumed in the gap between Zones P22 and SAN17 in Hole 1130A and in the debrite at Site 1128. The estimated duration is at least 0.5 m.y.

7. Hiatus 7, within Zone SAN11, is proximal to middle Miocene boundary Ser2 at 13.5 Ma. It is marked by *F. peripheroronda* with (in Hole 1134A) or without (in Hole 1126B) *P. mayeri*. The estimated duration is >0.5 m.y.
8. Hiatus 8, between Zones SAN12 and SAN13, is proximal to middle Miocene boundary Ser4/Tor1 at 11.7 Ma, the second-order TB2/TB3 boundary. It is represented in Holes 1126B, 1132C, and 1134A with Zones SAN13 or SAN14 overlying Zone SAN10, indicating that the hiatus may also incorporate middle Miocene sequence boundary Ser3 with >1 m.y. duration.
9. Hiatus 9, between Zones SAN15 and SAN16, is equivalent to upper Miocene boundary Tor2 at 9.3 Ma. Zone SAN17 sediments unconformably overlie, respectively, Zones SAN14 in Hole 1134A, Zone SAN10 in Hole 1132C, and Zone P22 in Hole 1130A. Contemporary sediment sections are highly condensed in Hole 1126B (Fig. **F12**), and a major reduction in warm-water species including *Menardella* spp. and *Globigerinoides* spp. in Zone SAN16 between 95 and 100 mbsf probably coincides with this event (Fig. **F4**). The hiatus is subsumed in the debrite at Site 1128. The estimated duration is ~2 m.y.
10. Hiatus 10, between Zones SAN17 and SAN18, is proximal to upper Miocene boundary Tor3/Me1 at ~7.0 Ma. It is represented by a slump in Holes 1126B and 1126C and by a highly condensed interval with these two zones in Holes 1134A and 1134B and 1128B and 1128C (upper part of the debrite). In Hole 1132C, undifferentiated Zones SAN16–SAN17 unconformably underlie Pleistocene sediments. The estimated duration is at least 0.5 m.y.
11. Hiatus 11, between Subzones SAN19a and SAN19b, is proximal to the uppermost Miocene boundary Me2 at 5.7 Ma. It is subsumed in the gaps between Subzone SAN19b and Zone SAN18 in Holes 1126B and 1126C (coeval with a slump) and between Zone SAN17 and the Pleistocene in Hole 1132C. However, it cannot be recognized at Sites 1130 and 1134. Its duration is estimated to be <0.5 m.y.
12. Hiatus 12, between Zones SAN20 and SAN21, is equivalent to lower Pliocene boundary Za1 close to 4.5 Ma. In Holes 1130A and 1130B, Zone SAN22 overlies a condensed SAN21 sediment, with SAN20 likely missing. In Holes 1134A and 1134B, Zone SAN21 is not only similarly condensed but is also deluged by slumps. The entire Zone SAN20 appears to be missing from all sites, including the deepest Site 1128 (Fig. **F11**). Its estimated duration is ~0.5 m.y.
13. Hiatus 13, between Zones SAN22 and SAN23, is proximal to the lower/upper Pliocene boundary at ~3.5 Ma. In Holes 1126B and 1126C, Zone SAN23 unconformably overlies Subzone SAN19b, whereas at Sites 1128, 1130, and 1134, Zone SAN24 overlies Zone SAN22. Slumps are also observed in Holes 1126B, 1126C, 1130A, and 1130B. The hiatus is subsumed in the gap between upper Miocene Zones SAN17 and the lower Pleistocene in Hole 1132C. Its duration is estimated to be ~0.5 m.y.
14. Hiatus 14, lower Zone SAN24, is equivalent to upper Pliocene boundaries Ge1 and Pia2 between 2.5 and 2.8 Ma. A slump at ~51 mbsf in Holes 1126B and 1126C and another one between 50 and 56 mbsf in Holes 1134A and 1134B coincide with this event. The hiatus is subsumed in the gaps between Zones SAN22 and SAN24 at Sites 1128, 1130, and 1134 and between upper

Miocene Zones N16–N17 and the lower Pleistocene in Hole 1132C. Its duration is estimated to be ~0.5 m.y.

15. Hiatus 15, within the lower Pleistocene, is probably equivalent to boundaries Cala1 and Cala2 between 1.56 and 1.40 Ma. This judgment is based on the condensed sections between the onset of the Jaramillo (1.07 Ma) and termination of the Olduvai (1.77 Ma) in Holes 1130B (respectively, at 212 and 215 mbsf) and Hole 1132B (respectively, at 193 and 222 mbsf), as well as in holes from the eastern transect (Feary, Hine, Malone, et al., 2000). Soon after its FO at ~2 Ma, *G. truncatulinoides* disappeared from all sites and reappeared just prior to or during the Jaramillo (0.99–1.07 Ma). The duration of hiatus 15 is estimated to be at least 0.5 Ma.

Regional Correlation

Although the unconformable Oligocene/Miocene contact cannot be positively decided, the absence or rarity of such markers as *P. kugleri* and *T. euapertura* indicate there is a possibility. The basal Miocene from the Gambier Basin (western Otway Basin) (Fig. **F1**), a more temperate locality from the east of the Great Australian Bight, contains many specimens of *P. kugleri,* indicating warm-water influence after glaciation Mi-1 of Miller et al. (1991, 1998) (see Li et al., 2000). The subsequent occurrence of *G. dehiscens* and *G. woodi* signifies the biotic response to an early stage of the Miocene climatic oscillations (McGowran, 1979; McGowran and Li, 1994). McGowran and Li (1996, 1997) quantified changes in Miocene planktonic and benthic foraminiferal assemblages through the Lakes Entrance section from the Gippsland Basin, finding parallel trends with sea level and isotope climatic curves at both the 10^7 (second-order) and 10^6 (third-order) years scales. Regional transgressions, each defining a regional stage, reflect major third-order changes in global sea level, although the uplift of the southern Australian margin in the later Miocene obscured part of the record (McGowran et al., 1997b). This neritic record is confirmed and strengthened by the results of Leg 182, as summarized in Fig. **F13.**

Clifton Transgression (Upper Janjukian Regional Stage)

Deposited during the Clifton Transgression are the Clifton Formation and upper Gambier Limestone (both Otway Basin), upper Abrakurrie Limestone (Eucla Basin), upper Port Willunga Formation (St. Vincent Basin), lower Mannum Formation (Murray Basin), and Puebla Clay (Torquay Basin). The planktonic foraminiferal assemblage is characterized by *G. dehiscens, G. woodi,* and *G. connecta.*

Longford Transgression (Longfordian Stage)

The presence of the larger benthic foraminifers *Operculina* and *Amphistegina* is the most distinctive biofacies feature of this transgression in many neritic localities along the southern Australian margin. Planktonic species include *G. trilobus, G. praescitula,* and *G. zealandica.*

Batesford and Balcombe Transgressions (Batesfordian and Balcombian Stages)

Although distinguishable with or without the larger benthic *Lepidocyclina howchini* and the Balcombe also by the planktonic *O. suturalis,* the foraminiferal assemblage in these two transgressions comprises a similarly high diversity with many keeled globorotaliid forms. The larger benthic species found in these and previous transgressions are inferred to have immigrated from the tropics probably by way of the Leeuwin Current (McGowran et al., 1997a). Shallow-water limestones of these transgressions reach their maximum inland limit in several basins, including the Eucla Basin to the north of the Great Australian Bight (Lowry, 1970). They accumulated in a warm and oligotrophic environment at the zenith of the Miocene climatic maximum (McGowran, 1986; McGowran and Li, 1994; McGowran et al., 1997b).

Later Middle Miocene to Late Miocene Transgressions (Bairnsdalian and Mitchellian Stages)

Although the two local stages, Bairnsdalian and Mitchellian, characterize these regional events, only in the Otway and Gippsland Basin can any onshore upper middle to upper Miocene sediments be observed. Records of other basins were eroded because of a structural uplift of the southern Australian margin in the late Miocene (McGowran et al., 1997b; Dickinson et al., 2001). In the Gippsland Basin, planktonic foraminiferal assemblages shifted from dominance by *Globigerinoides* and *Globorotalia* to dominance by *Neogloboquadrina* and *Globigerina* (Li and McGowran, 2000). The later middle Miocene instability surely also reflects major growth of the East Antarctic ice sheet and associated Antarctic cooling and a major drop in global sea level (Flower and Kennett, 1994).

Pliocene Transgressions

Packages of calcareous sandstones formed in several basins during Pliocene transgressions contain shallow-water foraminiferal assemblages with few age-diagnostic species. Planktonic foraminifers are represented mainly by *G. woodi*. The Jemmys Point Formation from the eastern Gippsland Basin and Hallet Cove Sandstone in the St. Vincent Basin, respectively, signify these regional events in the early to mid-Pliocene. The unconformable contacts between the Pliocene and the underlying Miocene (mostly middle Miocene) and overlying Quaternary have been well documented (Ludbrook, 1961; Lowry, 1970; McGowran et al., 1997b; Li et al., 2000). Together with those found in the later middle to late Miocene, they indicate periods of regional uplift and erosion probably resulting from collision to the north between Australia and Indonesia (Veevers, 2000).

CONCLUSIONS

1. Neogene planktonic foraminifers in sediments from the Great Australian Bight are dominated by southern temperate species, with abundant *G. woodi* in the early Miocene, *G. trilobus* and *G. conoidea* in the middle and late Miocene, and *G. crassaformis* and *Globoconella puncticulata* in the Pliocene.

2. Warm subtropical species are rare, and they are mainly confined to the later early Miocene and younger intervals; their high abundance especially during the latest early to early middle Miocene indicates climatic warming and a vigorous flow of the Leeuwin Current from the northwest during the Miocene climatic optimum.
3. New planktonic foraminiferal Zones SAN1 to SAN25 were proposed for refining the southern Australian Neogene. They can be recognized on first or last occurrence datum levels of marker species that have been widely used in the region. These datums also provide the base for correlating the SAN zones with other zonation schemes, especially the standard N zones from the tropics and subtropics (Fig. F2).
4. All Neogene sections in Holes 1126B and 1126C, 1128B and 1128C, 1130A and 1130B, 1132B, and 1134A and 1134B are bounded by hiatuses of ~0.5 to >3 m.y. in duration. The longer gaps in Holes 1128B and 1128C and 1130A and 1130B eradicated a record of >20 and ~16 m.y., respectively.
5. Most slumps coincide with hiatuses, and their concentration in the late Miocene and Pliocene indicates region-wide slope failure at times of low sea level and/or intense tectonic activities.
6. Fifteen hiatuses represent 15 synchronous erosional events from the base of the Miocene to the lower part of the Pleistocene. These are local manifestations of major third-order boundaries at about (1) 23.8, (2) 22.3, (3) 20.5, (4) 18.7, (5) 16.4, (6) 14.8, (7) 13.5, (8) 11.5, (9) 9.3, (10) 7.0, (11) 6.0, (12) 4.5, (13) 3.5, (14) 2.5, and (15) 1.5 Ma, respectively (Fig. F12).
7. The Neogene succession from the Great Australian Bight samples the regional transgressions and stages that were defined previously on the neritic record. An onshore and offshore correlation helps understand better the evolution of southern Australian margin during the Neogene.

SPECIES LIST AND TAXONOMIC NOTES

Planktonic foraminifers described in the species list below are illustrated in Plates P1, P2, P3, P4, P5, and P6.

Cassigerinella chipolensis (Cushman and Ponton); Kennett and Srinivasan, 1983, p. 18, Pl. 1, figs. 3–5.

Catapsydrax dissimilis (Cushman and Bermudez); (Pl. P1, figs. 5, 6); Kennett and Srinivasan, 1983, p. 22, pl. 2, figs. 1, 3–8.

Catapsydrax parvulus Bolli, Loeblich, and Tappan; (Pl. P5, fig. 25); Kennett and Srinivasan, 1983, p. 26, pl. 3, figs. 7–9.

Catapsydrax unicavus Bolli, Loeblich, and Tappan; Kennett and Srinivasan, p. 26, pl. 3, figs. 1–3.

Dentoglobigerina altispira (Cushman and Jarvis); (Pl. P6, fig. 20); Kennett and Srinivasan, 1983, p. 188, pl. 46, figs. 4–6.

Dentoglobigerina baroemoenensis LeRoy; Kennett and Srinivasan, 1983, p. 186, pl. 46, figs. 1–3.

Fohsella peripheroronda (Blow and Banner); (Pl. P2, figs. 24–26); Kennett and Srinivasan, 1983, p. 96, pl. 22, figs. 1–3.

P1. Early Miocene planktonic foraminifers, p. 48.

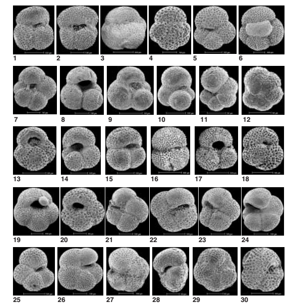

P2. Early–middle Miocene planktonic foraminifers, p. 49.

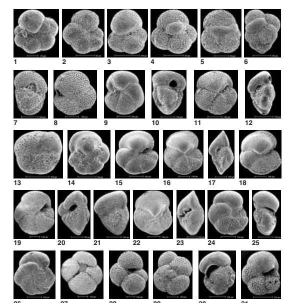

P3. Middle Miocene planktonic foraminifers, p. 50.

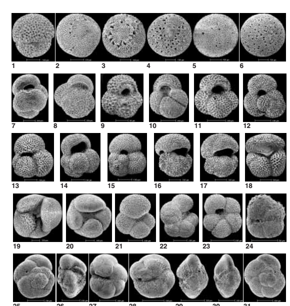

P4. Middle–late Miocene planktonic foraminifers, p. 51.

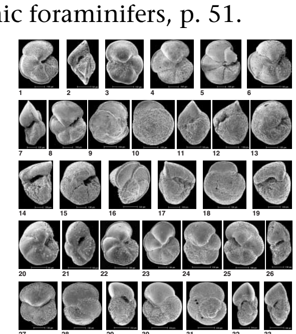

Globigerina bulloides d'Orbigny; (Pl. **P1,** fig. 8; Pl. **P6,** figs. 21, 22); Kennett and Srinivasan, 1983, p. 36, pl. 6, figs. 4–6.

Globigerina ciperoensis Bolli; (Pl. **P1,** fig. 7; Pl. **P3,** fig. 23); Kennett and Srinivasan, 1983, p. 28, pl. 4, figs. 6–8.

Globigerina eamesi Blow; Kennett and Srinivasan, 1983, p. 34, pl. 5, figs. 7–9.

Globigerina falconensis Blow; (Pl. **P1,** figs. 9, 10; Pl. **P6,** fig. 23); Kennett and Srinivasan, 1983, p. 40, pl. 7, figs. 1–3.

Globigerina praebulloides Blow; Kennett and Srinivasan, 1983, p. 36, pl. 6, figs. 1–3.

Globigerina quinqueloba Natland; (Pl. **P1,** figs. 11, 12; Pl. **P3,** fig. 24; Pl. **P6,** fig. 24); Kennett and Srinivasan, 1983, p. 32, pl. 75, figs. 4–6.

Globigerinella obese (Bolli); (Pl. **P3,** fig. 21; Pl. **P6,** fig. 25); Kennett and Srinivasan, 1983, p. 234, pl. 59, figs. 2–5.

Globigerinella siphonifera (Brady); (Pl. **P6,** figs. 26, 27); Kennett and Srinivasan, 1983, p. 238, pl. 60, figs. 4–6.

Globigerinita glutinata (Egger); (Pl. **P2,** figs. 4, 5; Pl. **P6,** fig. 30); Kennett and Srinivasan, 1983, p. 224, pl. 56, figs. 1, 3–5.

Globigerinita boweni Brönnimann and Resig, 1971, p. 1271, pl. 26, figs. 1–4.

Globigerinita naparimaensis Brönnimann; (Pl. **P6,** fig. 29); Li et al., 1992, p. 581, pl. 2, fig. 8.

Globigerinita praestainforthi Blow; Li et al., 1992, p. 581, pl. 3, fig. 1.

Globigerinita uvula (Ehrenberg); (Pl. **P2,** fig. 6); Li et al., 1992, p. 579, pl. 3, figs. 10, 11.

Globigerinoides bollii Blow; Kennett and Srinivasan, 1983, p. 70, pl. 15, figs. 4–6.

Globigerinoides bulloideus Crescenti; Kennett and Srinivasan, 1983, p. 60, pl. 12, figs. 7–9.

Globigerinoides conglobatus (Brady); Kennett and Srinivasan, 1983, p. 58, pl. 12, figs. 4–6.

Globigerinoides extremus Bolli; (Pl. **P6,** figs. 10, 11); Kennett and Srinivasan, 1983, p. 58, pl. 12, figs. 1–3.

Globigerinoides kennetti Keller and Poore; (Pl. **P6,** figs. 14, 15); Kennett and Srinivasan, 1983, p. 72, pl. 15, figs. 7–9.

Globigerinoides mitra Todd; (Pl. **P3,** figs. 16, 17); Kennett and Srinivasan, 1983, p. 76, pl. 16, figs. 7–9.

Remarks: This species occurs abundantly in Zones N7–N8 of Hole 1126B. The late Miocene record probably belongs in a morphologically very similar species, *Globigerinoides seigliei* Bermudez and Bolli with a range of Zones N16–N18 according to Kennett and Srinivasan (1983).

Globigerinoides obliquus Bolli; (Pl. **P3,** figs. 14, 15; Pl. **P6,** fig. 9); Kennett and Srinivasan, 1983, p. 56, pl. 11, figs. 7–9.

Globigerinoides parawoodi Keller; (Pl. **P3,** figs. 11, 12); Kennett and Srinivasan, 1983, p. 70, pl. 15, figs. 1–3.

Globigerinoides primordius Blow and Banner; Kennett and Srinivasan, 1983, p. 54, pl. 11, figs. 1–3.

Globigerinoides quadrilobatus (d'Orbigny); (Pl. **P3,** fig. 13; Pl. **P6,** figs. 16, 17); Kennett and Srinivasan, 1983, p. 66, pl. 14, figs. 1–3.

Globigerinoides ruber (d'Orbigny); (Pl. **P6,** figs. 12, 13); Kennett and Srinivasan, 1983, p. 78, pl. 17, figs. 1–3.

P5. Late Miocene–early Pliocene planktonic foraminifers, p. 52.

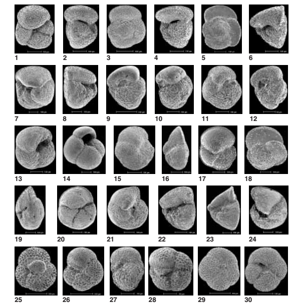

P6. Late Miocene–late Pliocene planktonic foraminifers, p. 53.

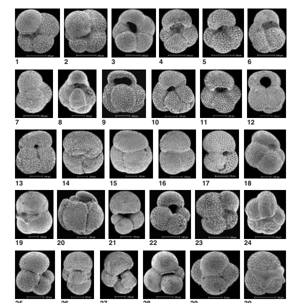

Globigerinoides sacculifer (Brady); (Pl. **P6,** fig. 18); Kennett and Srinivasan, 1983, p. 66, pl. 14, figs. 4–6.

Globigerinoides subquadratus Brönnimann; (Pl. **P1,** figs. 17, 18); Kennett and Srinivasan, 1983, p. 74, pl. 16, figs. 1–3.

Remarks: This species is very similar to *G. ruber* but occurs mainly between Zones upper N6–N8.

Globigerinoides tenellus Parker; Kennett and Srinivasan, 1983, p. 80, pl. 17, figs. 7–9.

Remarks: Occurs sporadically in the late Pliocene.

Globigerinoides trilobum (Reuss); (Pl. **P1,** fig. 16); Kennett and Srinivasan, 1983, p. 62, pl. 13, figs. 1–3.

Globoconella conica (Jenkins); (Pl. **P2,** figs. 19–21); Jenkins, 1985 p. 276, pl. 2, figs. 7, 8a–8c, 9a–9c.

Globoconella conoidea Walters; (Pl. **P2,** figs. 22, 23; Pl. **P4,** figs. 10, 11); Kennett and Srinivasan, 1983, p. 112, pl. 26, figs. 4–6.

Globoconella conomiozea (Kennett); (Pl. **P4,** figs. 14–16); Kennett and Srinivasan, 1983, p. 114, pl. 26, figs. 7–9.

Globoconella miotumida (Jenkins); (Pl. **P4,** figs. 1, 2); Jenkins, 1960, p. 362, *Globorotalia menardii miotumida,* pl. 4, figs. 9a–9c.

Globoconella inflata d'Orbigny; (Pl. **P5,** figs. 12–14); Kennett and Srinivasan, 1983, p. 118, pl. 27, figs. 7–9.

Globoconella miozea (Finlay); (Pl. **P2,** fig. 13); Kennett and Srinivasan, 1983, p. 112, pl. 26, figs. 1–3.

Globoconella pliozea Hornibrook; (Pl. **P5,** figs. 17–20); Hornibrook et al., 1989, p. 133, fig. 29, no. 6.

Globoconella puncticulata (Deshayes); (Pl. **P5,** figs. 9–11); Kennett and Srinivasan, 1983, p. 116, pl. 27, figs. 4–6.

Globoconella sphericomiozea (Walters); (Pl. **P4,** figs. 17–19); Kennett and Srinivasan, 1983, p. 116, pl. 27, figs. 1–3.

Remarks: Although rare, some middle to late Miocene specimens of *Globoconella* (Pl. **P4,** figs. 12, 13) are as thickly walled as *G. sphericomiozea,* which has been reported as restricted to the latest Miocene. We refer these forms to *G.* cf. *sphericomiozea,* pending further studies of their affinity with typical *G. sphericomiozea.*

Globoconella zealandica (Hornibrook); (Pl. **P2,** figs. 7–10); Kennett and Srinivasan, 1983, p. 108, pl. 25, figs. 1–3.

Globoquadrina dehiscens (Chapman, Parr and Collins); (Pl. **P1,** figs. 1, 2; Pl. **P3,** fig. 18); Kennett and Srinivasan, 1983, p. 184, pl. 44, fig. 2; pl. 45, figs. 7–9.

Globoquadrina praedehiscens Blow and Banner; Kennett and Srinivasan, 1983, p. 182, pl. 45, figs. 4–6.

Globoquadrina venezuelana Hedberg; (Pl. **P1,** fig. 3; Pl. **P3,** figs. 19, 20); Kennett and Srinivasan, 1983, p. 180, pl. 44, figs. 5–7.

Globorotalia cibaoensis Bermudez; (Pl. **P4,** figs. 32, 33); Kennett and Srinivasan, 1983, as *Globorotalia (Hirsutella) cibaoensis,* p. 136, pl. 32, figs. 1–3.

Globorotalia crassaconica Hornibrook; (Pl. **P5,** fig. 28); Hornibrook et al., 1989, p. 129, fig. 29, no. 11.

Globorotalia crassaformis (Galloway and Wissler); (Pl. **P5,** figs. 1–6); Kennett and Srinivasan, 1983, p. 146, pl. 34, figs. 6–8.

Globorotalia crassula Cushman and Stewart; (Pl. **P5,** figs. 15, 16); Kennett and Srinivasan, 1983, p. 144, pl. 34, figs. 3–5.

Globorotalia explicationis (Jenkins); (Pl. **P4,** fig. 6); Jenkins, 1985, as *Globorotalia explicationis,* p. 278, fig. 7, no. 16.

Globorotalia juanai Bermudez and Bolli; (Pl. **P4,** figs. 29–31); Kennett and Srinivasan, 1983, as *Globorotalia (Hirsutella) juanai,* p. 134, pl. 31, figs. 6–8.

Globorotalia lenguaensis Bolli; (Pl. **P3,** figs. 25–31); Kennett and Srinivasan, 1983, p. 152, pl. 36, figs. 5–7.

Globorotalia margaritae Bolli; (Pl. **P4,** figs. 26–28); Kennett and Srinivasan, 1983, as *Globorotalia (Hirsutella) margaritae,* p. 136, pl. 32, figs. 4–6.

Globorotalia merotumida Blow and Banner; (Pl. **P4,** fig. 23); Kennett and Srinivasan, 1983, p. 154, pl. 37, figs. 4–5.

Globorotalia panda (Jenkins); Kennett and Srinivasan, 1983, as *Globorotalia (Globoconella) panda,* p. 110, pl. 25, figs. 7–9.

Globorotalia plesiotumida Blow and Banner; (Pl. **P4,** figs. 20–22); Kennett and Srinivasan, 1983, p. 156, pl. 37, figs. 7–9.

Globorotalia praescitula Blow; (Pl. **P2,** figs. 11, 12); Kennett and Srinivasan, 1983, as *Globorotalia (Globoconella) praescitula,* p. 108, pl. 25, figs. 4–6.

Globorotalia scitula (Brady); (Pl. **P4,** fig. 25); Kennett and Srinivasan, as *Globorotalia (Hirsutella) scitula* 1983, p. 134, pl. 31, figs. 1, 3–5.

Globorotalia tosaensis Takayanagi and Saito; (Pl. **P5,** figs. 21, 22); Kennett and Srinivasan, 1983, p. 148, pl. 35, figs. 1–3.

Globorotalia truncatulinoides (d'Orbigny); (Pl. **P5,** figs. 23, 24); Kennett and Srinivasan, 1983, p. 148, pl. 35, figs. 4–6.

Globorotaloides suteri Bolli; (Pl. **P1,** fig. 4); Kennett and Srinivasan, 1983, p. 214, pl. 53, figs. 1, 3–5.

Globorotaloides variavilis Bolli; Kennett and Srinivasan, 1983, p. 214, pl. 53, figs. 2, 6–8.

Globoturborotalita apertura (Cushman); Kennett and Srinivasan, 1983, as *Globigerina (Zeaglobigerina) apertura,* p. 44, pl. 8, figs. 4–6.

Globoturborotalita brazieri (Jenkins); Jenkins, 1985, as *Globigerina brazieri,* p. 274, fig. 6.20.

Globoturborotalita connecta (Jenkins); (Pl. **P1,** fig. 15); Kennett and Srinivasan, 1983, as *Globigerina (Zeaglobigerina) connecta,* p. 44, pl. 8, figs. 1–3.

Globoturborotalita decoraperta (Takayanagi and Saito); (Pl. **P3,** figs. 7, 8); Kennett and Srinivasan, 1983, as *Globigerina (Zeaglobigerina) decoraperta,* p. 48, pl. 9, figs. 4–6.

Globoturborotalita druryi (Akers); (Pl. **P3,** fig. 10); Kennett and Srinivasan, 1983, as *Globigerina (Zeaglobigerina) druryi,* p. 46, pl. 8, figs. 7–9.

Globoturborotalita nepenthes (Todd); (Pl. **P6,** figs. 6–8); Kennett and Srinivasan, 1983, as *Globigerina (Zeaglobigerina) nepenthes,* p. 48, pl. 9, figs. 1–3.

Globoturborotalita rubescens (Hofker); (Pl. **P3,** fig. 9; Pl. **P6,** fig. 5); Kennett and Srinivasan, 1983, as *Globigerina (Zeaglobigerina) rubescens,* p. 50, pl. 9, figs. 7–9.

Globoturborotalita woodi (Jenkins); (Pl. **P1,** figs. 13, 14; Pl. **P6,** fig. 4); Kennett and Srinivasan, 1983, as *Globigerina (Zeaglobigerina) woodi,* p. 43, pl. 7, figs. 4–6.
Remarks: Chaproniere (1992) discussed the FO of *G. woodi* in the early Miocene.

Menardella archeomenardii (Bolli); (Pl. **P2,** figs. 14, 15); Kennett and Srinivasan, 1983, p. 122, pl. 28, figs. 3–5.

Menardella menardii (Parker, Jones, and Brady); (Pl. **P4,** figs. 4, 5); Kennett and Srinivasan, 1983, as *Globorotalia* (*Menardella*) *menardii,* p. 124, pl. 29, figs. 1–3.

Menardella praemenardii (Cushman and Stainforth); (Pl. **P2,** figs. 16, 17; Pl. **P4,** fig. 3); Kennett and Srinivasan, 1983, p. 122, pl. 28, figs. 6–8.

Neogloboquadrina acostaensis (Blow); (Pl. **P6,** fig. 2); Kennett and Srinivasan, 1983, p. 196, pl. 48, figs. 1–3.

Neogloboquadrina continuosa (Blow); (Pl. **P5,** fig. 26); Kennett and Srinivasan, 1983, p. 192, pl. 47, figs. 3–5.

Neogloboquadrina dutertrei (d'Orbigny); (Pl. **P6,** fig. 3); Kennett and Srinivasan, 1983, p. 198, pl. 48, figs. 7–9.

Neogloboquadrina humerosa (Takayanagi and Saito); Kennett and Srinivasan, 1983, p. 196, pl. 48, figs. 4–6.

Neogloboquadrina nympha (Jenkins); (Pl. **P5,** figs. 27, 28); Hornibrook et al., 1989, p. 132, as *Globorotalia mayeri nympha,* pl. 48, figs. 4–6.

Remarks: This later middle Miocene form is morphologically similar to smaller individuals of *N. acostaensis* from the late Miocene.

Neogloboquadrina pachyderma (Ehrenberg); (Pl. **P5,** figs. 29–30; Pl. **P6,** fig. 1); Kennett and Srinivasan, 1983, p. 192, pl. 47, figs. 6–8.

Orbulina bilobata (d'Orbigny); Kennett and Srinivasan, 1983, p. 88, pl. 20, figs. 7–9.

Orbulina suturalis Brönnimann; (Pl. **P3,** fig. 4); Kennett and Srinivasan, 1983, p. 86, pl. 20, figs. 1–3.

Orbulina universa d'Orbigny; (Pl. **P3,** figs. 5, 6); Kennett and Srinivasan, 1983, p. 86, pl. 20, figs. 4–6.

Paragloborotalia bella (Jenkins); (Pl. **P1,** figs. 27, 28); Kennett and Srinivasan, 1983, as *Globorotalia (Jenkinsella) bella,* p. 174, pl. 43, figs. 1–3.

Paragloborotalia incognita (Walters); (Pl. **P1,** fig. 30); Kennett and Srinivasan, 1983, as *Globoconella* p. 106, pl. 24, figs. 6–8.

Paragloborotalia mayeri (Cushman and Ellisor); (Pl. **P2,** figs. 30, 31); Kennett and Srinivasan, 1983, as *Globorotalia (Jenkinsella) mayeri,* p. 174, pl. 43, figs. 4–6.

Paragloborotalia nana (Bolli); (Pl. **P1,** figs. 21, 22); Bolli and Saunders, 1985, as *Globorotalia opima nana,* p. 202, fig. 26, nos. 15–23.

Paragloborotalia semivera (Hornibrook); (Pl. **P1,** figs. 23, 24); Kennett and Srinivasan, 1983, as *Globorotalia (Jenkinsella) semivera,* p. 172, pl. 42, figs. 3–5.

Paragloborotalia siakensis (LeRoy); (Pl. **P1,** figs. 25, 26); Kennett and Srinivasan, 1983, as *Globorotalia (Jenkinsella) siakensis,* p. 172, pl. 42, figs. 6–8.

Praeorbulina glomerosa (Blow) s.l.; (Pl. **P3,** figs. 2, 3); Kennett and Srinivasan, 1983, as *Praeorbulina glomerosa* subspp. *curva, glomerosa, circularis,* pp. 82–84, pl. 18, figs. 3–7; pl. 19, figs. 1–5.

Praeorbulina sicana (De Stefani); (Pl. **P3,** fig. 1); Kennett and Srinivasan, 1983, as *Globigerinoides sicanus,* p. 62, pl. 13, figs. 4–6.

Praeorbulina transitoria (Blow); Kennett and Srinivasan, 1983, p. 84, pl. 19, figs. 6–8.

Sphaeroidinellopsis disjuncta (Finlay); Kennett and Srinivasan, 1983, p. 206, pl. 51, figs. 3–5.

Sphaeroidinellopsis kochi Caudri; (Pl. **P2,** figs. 28, 29); Kennett and Srinivasan, 1983, p. 210, pl. 52, figs. 1–3.

Sphaeroidinellopsis seminulina (Schwager); (Pl. **P2,** fig. 27; Pl. **P6,** fig. 19); Kennett and Srinivasan, 1983, p. 206, pl. 51, figs. 6–8.

Tenuitella clemenciae (Bermúdez); Li et al., 1992, p. 579, pl. 3, figs. 8, 9.

Tenuitella minutissima (Bolli); (Pl. **P2,** fig. 2); Li et al., 1992, p. 579, pl. 3, figs. 4–6.

Tenuitellinata angustiumbilicata (Bolli); (Pl. **P2,** fig. 1); Li et al., 1992, p. 579, pl. 1, figs. 9, 10; Li and McGowran, 2000, p. 48, fig. 23P.

Tenuitellinata juveniles (Bolli); (Pl. **P2,** Fig. 3; Pl. **P6,** fig. 28); Li et al., 1992, p. 579, pl. 2, figs. 3–6.

Turborotalia cf. *T. ampliapertura* (Pl. **P1,** figs. 19, 20); Bolli and Saunders, 1985, p. 182, fig. 14, nos. 1–3.

Remarks: These forms probably reworked from the Oligocene, although some appear to represent variations of *Globoturborotalita woodi.*

Turborotalia euapertura (Jenkins); Jenkins, 1960, as *Globigerina euapertura,* p. 351, pl. 1, figs. 8a, 8b, 8c.

Remarks: Common in the Oligocene, rare to sporadic in the earliest Miocene.

ACKNOWLEDGMENTS

This research used samples provided by the Ocean Drilling Program (ODP). ODP is sponsored by the U.S. National Science Foundation (NSF) and participating countries under management of Joint Oceanographic Institutions (JOI), Inc. Funding for this research was provided by the Australian Research Council and ODP Australia Secretariat. The manuscript benefited greatly from two ODP reviewers' comments. The Centre for Electron Microscopy and Microanalysis of Adelaide University provided the electronic scanning facility.

REFERENCES

Berggren, W.A., 1992. Paleogene planktonic foraminifer magnetobiostratigraphy of the Southern Kerguelen Plateau (Sites 747–749). *In* Wise, S.W., Jr., Schlich, R., et al., *Proc. ODP, Sci. Results,* 120 (Pt. 2): College Station, TX (Ocean Drilling Program), 551–568.

Berggren, W.A., Kent, D.V., Swisher, C.C., III, and Aubry, M.-P., 1995. A revised Cenozoic geochronology and chronostratigraphy. *In* Berggren, W.A., Kent, D.V., Aubry, M.-P., and Hardenbol, J. (Eds.), *Geochronology, Time Scales and Global Stratigraphic Correlation.* Spec. Publ.—SEPM (Soc. Sediment. Geol.), 54:129–212.

Blow, W.H., 1979. *The Cainozoic Globigerinida:* Leiden (E.J. Brill).

Bolli, H.M., and Saunders, J.B., 1985. Oligocene to Holocene low latitude planktic foraminifera. *In* Bolli, H.M., Saunders, J.B., and Perch-Nielsen, K. (Eds.), *Plankton Stratigraphy:* Cambridge (Cambridge Univ. Press), 155–262.

Brönnimann, P., and Resig, J., 1971. A Neogene globigerinacean biochronologic timescale of the Southwestern Pacific. *In* Winterer, E.L., Riedel, W.R., et al., *Init. Repts. DSDP,* 7 (Pt. 2): Washington (U.S. Govt. Printing Office), 1235–1469.

Carter, R.M., McCave, I.N., Richter, C., Carter, L., et al., 1999. *Proc. ODP, Init. Repts.,* 181 [CD-ROM]. Available from: Ocean Drilling Program, Texas A&M University, College Station, TX 77845-9547, U.S.A.

Chaisson, W.P., and Leckie, R.M., 1993. High-resolution Neogene planktonic foraminifer biostratigraphy of Site 806, Ontong Java Plateau (western equatorial Pacific). *In* Berger, W.H., Kroenke, L.W., Mayer, L.A., et al., *Proc. ODP, Sci. Results,* 130: College Station, TX (Ocean Drilling Program), 137–178.

Chaproniere, G.C.H., 1992. The distribution and development of late Oligocene and early Miocene reticulate globigerines in Australia. *Mar. Micropaleontol.,* 18:279–305.

Chaproniere, G.C.H., Shafik, S., Truswell, E.M., Macphail, M.K., and Partridge, A.D., 1996. Cainozoic. *In* Young, C.G., and Laurie, J. (Eds.), *Australian Phanerozoic Timescale:* Melbourne (Oxford Univ. Press), 175–186.

Dickinson, J.A., Wallace, M.W., Holdgate, G.R., Daniels, J., Gallagher, S.J., and Thomas, L., 2001. Neogene tectonics in SE Australia: implications for petroleum systems. *APEA J.,* 22–38.

Feary, D.A., Hine, A.C., Malone, M.J., et al., 2000. *Proc. ODP, Init. Repts.,* 182 [CD-ROM]. Available from: Ocean Drilling Program, Texas A&M University, College Station, TX 77845-9547, U.S.A.

Flower, B.P., and Kennett, J.P., 1994. The middle Miocene climatic transition: East Antarctic ice sheet development, deep ocean circulation, and global carbon cycling. *Palaeogeogr., Palaeoclimatol., Palaeoecol.,* 108:537–555.

Haq, B.U., Hardenbol, J., and Vail, P.R., 1987. Chronology of fluctuating sea levels since the Triassic. *Science,* 235:1156–1167.

Hardenbol, J., Thierry, J., Farley, M.B., Jacquin, Th., de Graciansky, P.-C., and Vail, P.R. (with numerous contributors), 1998. Mesozoic and Cenozoic sequence chronostratigraphic framework of European basins. *In* Graciansky, P.-C., Hardenbol, J., Jacquin, T., and Vail, P.R. (Eds.), *Mesozoic-Cenozoic Sequence Stratigraphy of European Basins.* Spec. Publ.—SEPM, 60:3–13, 763–781, and chart supplements.

Hodell, D.A., and Warnke, D.A., 1991. Climatic evolution of the Southern Ocean during the Pliocene epoch from 4.8 to 2.6 million years ago. *Quat. Sci. Rev.,* 10:205–214.

Hornibrook, N. de B., Brazier, R.C., and Strong, C.P., 1989. Manual of New Zealand Permian to Pleistocene foraminiferal biostratigraphy. *N. Z. Geol. Surv. Paleontol. Bull.,* 56:1–175.

Huber, B.T., 1991. Paleogene and early Neogene planktonic foraminifer biostratigraphy of Sites 738 and 744, Kerguelen Plateau (southern Indian Ocean). *In* Barron, J., Larsen, B., et al., *Proc. ODP, Sci. Results,* 119: College Station, TX (Ocean Drilling Program), 427–449.

Jenkins, D.G., 1960. Planktonic foraminifera from the Lakes Entrance oil shaft, Victoria, Australia. *Micropaleontology,* 6:345–371.

———, 1971. New Zealand Cenozoic planktonic foraminifera. *N. Z. Geol. Surv. Paleontol. Bull.,* 42:1–278.

———, 1985. Southern mid-latitude Paleocene to Holocene planktic foraminifera. *In* Bolli, H.M., Saunders, J.B., and Perch-Nielsen, K. (Eds.), *Plankton Stratigraphy:* Cambridge (Cambridge Univ. Press), 263–282.

———, 1993. Cenozoic southern mid- and high-latitude biostratigraphy and chronostratigraphy based on planktonic foraminifera. *In* Kennett, J.P., and Warnke, D.A. (Eds.), *The Antarctic Paleoenvironment: A Perspective on Global Change.* Antarct. Res. Ser., 60:125–144.

Jenkins, D.G., and Srinivasan, M.S., 1986. Cenozoic planktonic foraminifers from the equator to the sub-Antarctic of the southwest Pacific. *In* Kennett, J.P., von der Borch, C.C., et al., *Init. Repts. DSDP,* 90: Washington (U.S. Govt. Printing Office), 795–834.

Kennett, J.P., 1977. Cenozoic evolution of Antarctic glaciation, the circum-Antarctic Ocean, and their impact on global paleoceanography. *J. Geophys. Res.,* 82:3843–3860.

Kennett, J.P., Keller, G., and Srinivasan, M.S., 1985. Miocene planktonic foraminiferal biogeography and paleoceanographic development of the Indo-Pacific region. *In* Kennett, J.P. (Ed.), *The Miocene Ocean: Paleoceanography and Biogeography.* Mem.—Geol. Soc. Am., 163:197–236.

Kennett, J.P., and Srinivasan, M.S., 1983. *Neogene Planktonic Foraminifera: A Phylogenetic Atlas:* Stroudsburg, PA (Hutchinson Ross).

Li, Q., Davies, P.J., and McGowran, B., 1999. Foraminiferal sequence biostratigraphy of the Oligo-Miocene Janjukian strata from Torquay, southeastern Australia. *Aust. J. Earth Sci.,* 46:261–273.

Li, Q., and McGowran, B., 1998. Oceanographic implications of recent planktonic foraminifera along the southern Australian margin. *Mar. Freshwater Res.,* 49:439–445.

———, 2000. Miocene foraminifera from Lakes Entrance oil shaft, southeastern Australia. *Assoc. Australas. Paleontol. Mem. Ser.*, 22:1–142.

Li, Q., McGowran, B., and White, M.R., 2000. Sequences and biofacies packages in the mid-Cenozoic Gambier Limestone, South Australia: reappraisal of foraminiferal evidence. *Aust. J. Earth Sci.,* 47:955–970.

Li, Q., Radford, S.S., and Banner, F.T., 1992. Distribution of microperforate tenuitellid planktonic foraminifers in Holes 747A and 749B, Kerguelen Plateau. *In* Wise, S.W. Jr., Schlich, R., et al., *Proc. ODP, Sci. Results,* 120: College Station, TX (Ocean Drilling Program), 569–594.

Lowry, D.C., 1970. Geology of the Western Australian part of the Eucla Basin. *Bull.—Geol. Surv. West. Aust.,* 122.

Ludbrook, N.H., 1961. Stratigraphy of the Murray Basin in South Australia. *Bull.—Geol. Surv. S. Aust.,* 36:1–96.

McGowran, B., 1979. The Tertiary of Australia: foraminiferal overview. *Mar. Micropaleontol.,* 4:235–264.

———, 1986. Cainozoic oceanic and climatic events: the Indo-Pacific foraminiferal biostratigraphic records. *Palaeogeogr., Palaeoclimatol., Palaeoecol.,* 55:247–265.

McGowran, B., and Li, Q., 1994. The Miocene oscillation in southern Australia. *Rec. S. Aust. Mus.,* 27:197–212.

———, 1996. Ecostratigraphy and sequence biostratigraphy, with a neritic foraminiferal example from the Miocene in southern Australia. *Hist. Biol.,* 11:137–169.

———, 1997. Miocene climatic oscillation recorded in the Lakes Entrance oil shaft, southern Australia: reappraisal of the planktonic foraminiferal record. *Micropaleontology,* 43:129–148.

McGowran, B., Li, Q., Cann, J., Padley, D., McKirdy, D.M., and Shafik, S., 1997a. Biogeographic impact of the Leeuwin Current in southern Australia since the late middle Eocene. *Palaeogeogr., Palaeoclimatol., Palaeoecol.,* 136:19–40.

McGowran, B., Li, Q., and Moss, G., 1997b. The Cenozoic neritic record in southern Australia: the biogeohistorical framework. *In* James, N.P., and Clarke, J., *Cool-Water Carbonates.* Spec. Publ.— SEPM, 56:185–203.

McGowran, B., Lindsay, J.M., and Harris, W.K., 1971. Attempted reconciliation of Tertiary biostratigraphic systems, Otway Basin. *In* Wopfner, H., and Douglas, J.G. (Eds.), *The Otway Basin in Southeastern Australia.* Spec. Bull. S. Aust., Geol. Surv.—Victoria, Geol. Surv., 273–281.

Miller, K.G., Mountain, G.S., Browning, J.V., Kominz, M., Sugarman, P.J., Christie-Blick, N., Katz, M.B., and Wright, J.D., 1998. Cenozoic global sea level, sequences, and the New Jersey transect: results from coastal plain and continental slope drilling. *Rev. Geophys.,* 36:569–601.

Miller, K.G., Wright, J.D., and Fairbanks, R.G., 1991. Unlocking the Ice House: Oligocene–Miocene oxygen isotopes, eustasy, and margin erosion. *J. Geophys. Res.,* 96:6829–6848.

Morgans, H.E.G., Scott, G.H., Beu, A.G., Graham, I.J., Mumme, T.C., George, W.St., and Strong, C.P., 1996. New Zealand Cenozoic Time Scale (version 11/96). *Rep.—Inst. Geol. Nucl. Sci.,* 96/38:1–12.

Scott, G.H., Bishop, S., and Burt, B.J., 1990. Guide to some Neogene Globotalids (foraminiferida) from New Zealand. *N. Z. Geol. Surv. Paleontol. Bull.,* 61:1–135.

Srinivasan, M.S., and Kennett, J.P., 1981. Neogene planktonic foraminiferal biostratigraphy and evolution: equatorial to subantarctic, South Pacific. *Mar. Micropaleontol.,* 6:499–533.

Swart, P.K., Wortmann, U.G., Mitterer, R.M., Malone, M.J., Smart, P.L., Feary, D.A., Hine, A.C., 2000. Hydrogen sulfide-rich hydrates and saline fluids in the continental margin of South Australia. *Geology,* 28:1039–1042.

Veevers, J.J. (Ed.), 2000. *Billion-Year Earth History of Australia and Neighbours in Gondwanaland:* Sydney (GEMOC Press, Macquarie Univ.), 400.

Wright, J.D., and Thunell, R.C., 1988. Neogene planktonic foraminiferal biogeography and paleoceanography of the Indian Ocean. *Micropaleontology,* 34:193–216.

APPENDIX

Counts of planktonic foraminifers from Holes 1126B, 1126C, 1128B, 1128C, 1130A, 1130B, 1132B, 1134A, and 1134B are found in Tables AT1, AT2, AT3, AT4, AT5, AT6, AT7, AT8, and AT9, respectively.

Figure F1. A. Map showing the modern circulation around southern Australia and location of Cenozoic basins. 1 = Bremer Basin, 2 = Eucla Basin, 3 = St. Vincent Basin, 4 = Murray Basin, 5 = Otway Basin, 6 = Bass Basin, 7 = Gippsland Basin. **B.** Location of ODP Leg 182 sites and oil exploration drill hole Jerboa-1. Contours are shown in meters.

A

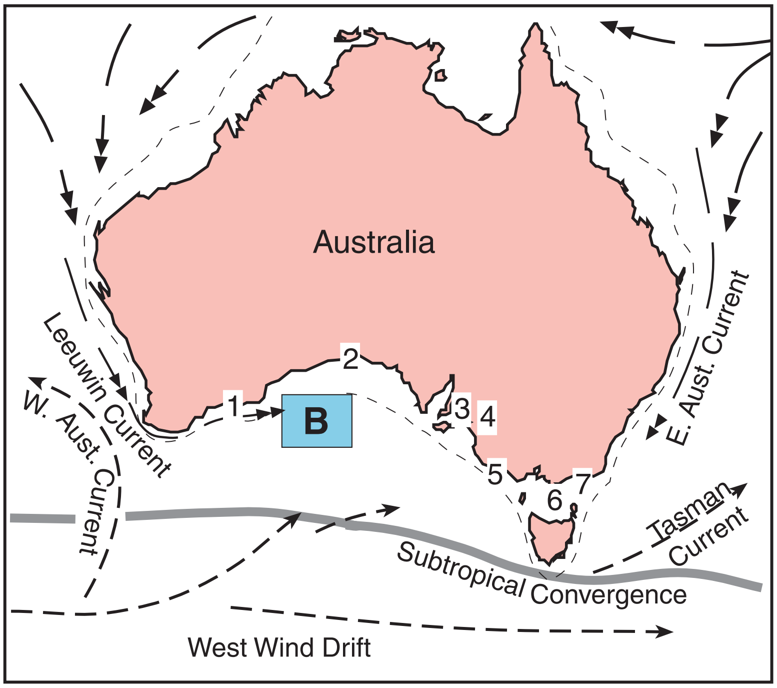

B

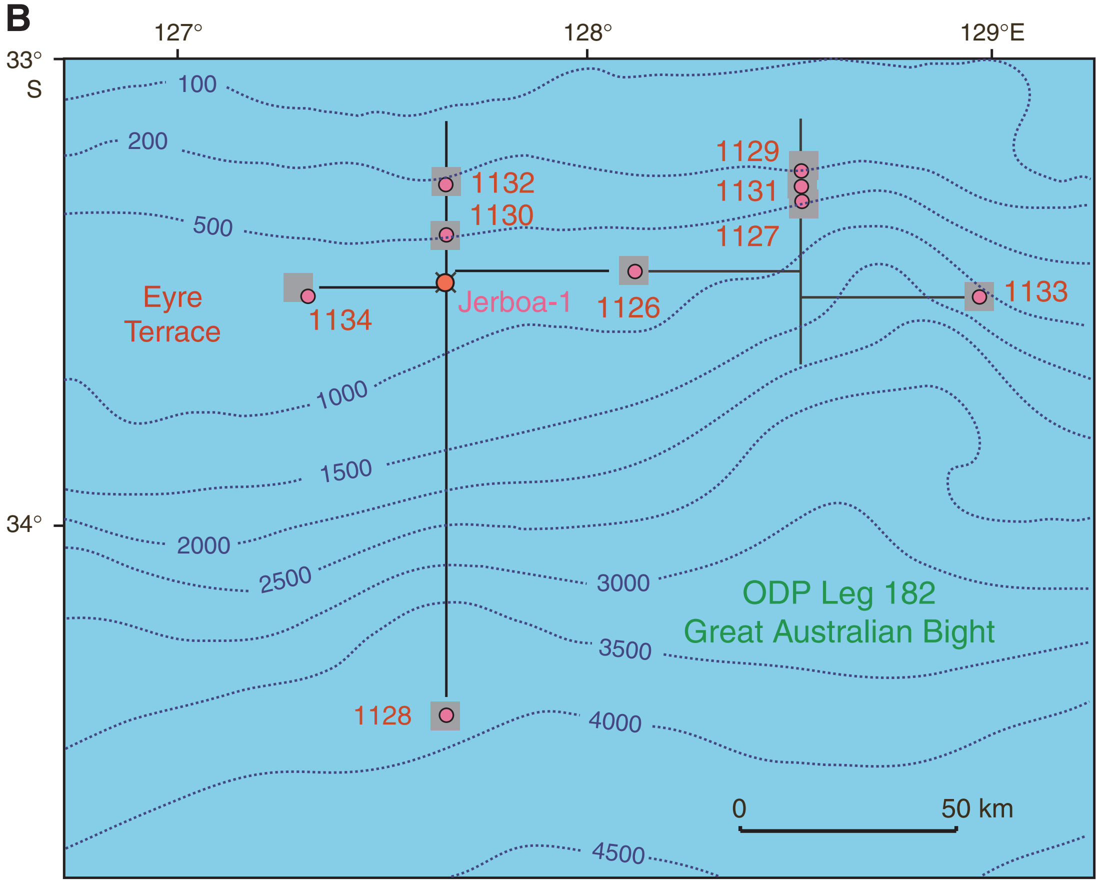

Figure F2. Neogene and Quaternary geochronostratigraphy of Berggren et al. (1995), showing the standard Neogene N zones, Miocene M zones, temperate Miocene Mt zones, and Pliocene Pl zones, as well as datum levels of diagnostic planktonic foraminifers. The southern Neogene SN zones of Jenkins (1993) are correlated with datums recalculated by Scott et al. (1990), Morgans et al. (1996), and Carter, McCave, Richter, Carter, et al. (1999). The new southern Australian Neogene SAN zonation scheme was based on datum levels widely found in the region (McGowran, 1989; McGowran et al., 1997a). Numbers are estimated ages in millions of years, mainly by Berggren et al. (1995) (see also Feary, Hine, Malone, et al., 2000 and Table T3, p. 44). FO = first occurrence, FCO = first common occurrence, LO = last occurrence, LCO = last common occurrence.

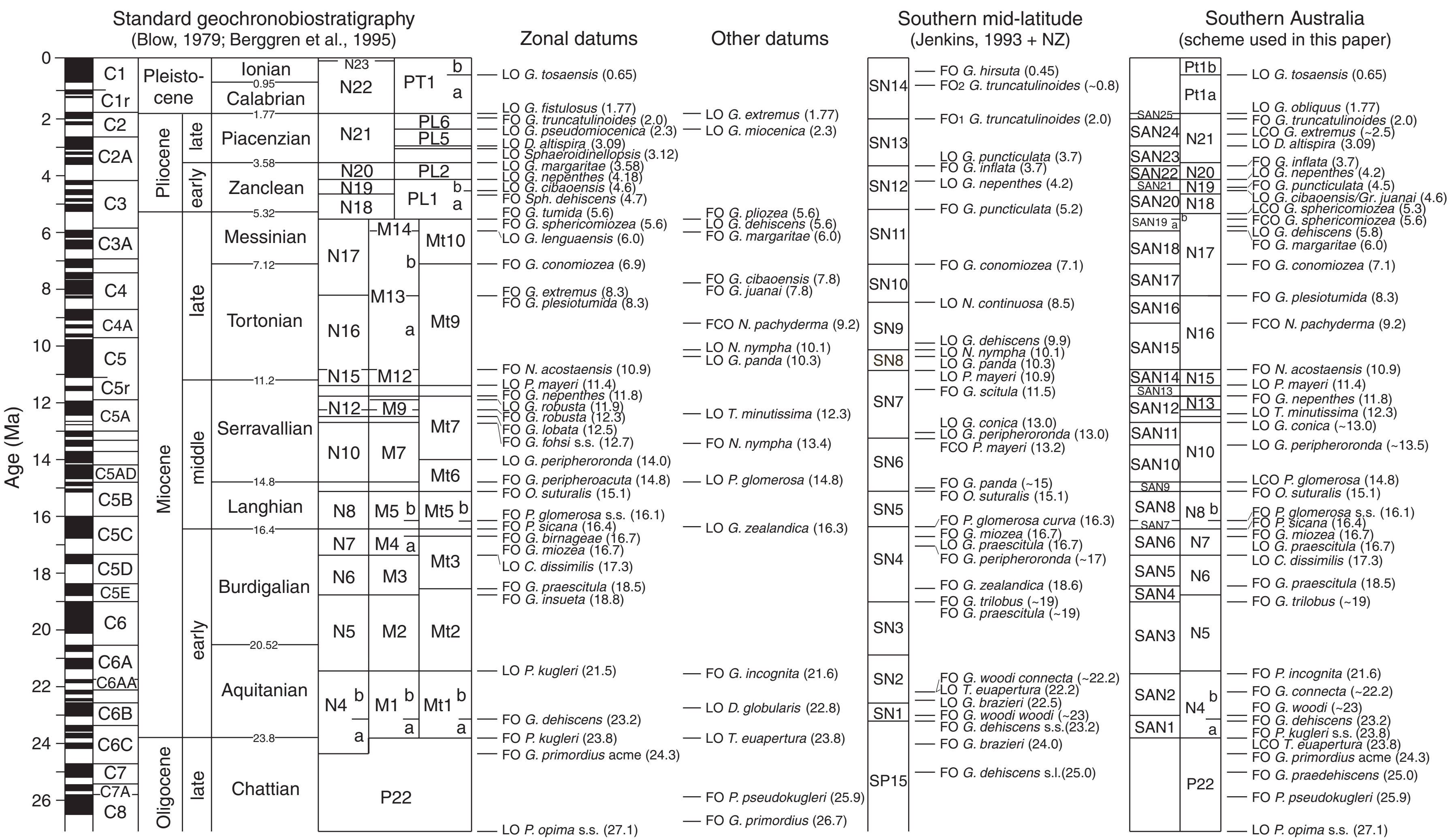

Figure F3. Planktonic foraminiferal biostratigraphy of the Neogene and Quaternary in Holes 1126B, 1126C, and 1126D. Ranges of common species and relevant zones are shown, together with slumped intervals and unconformities (wavy lines). Plio. = Pliocene.

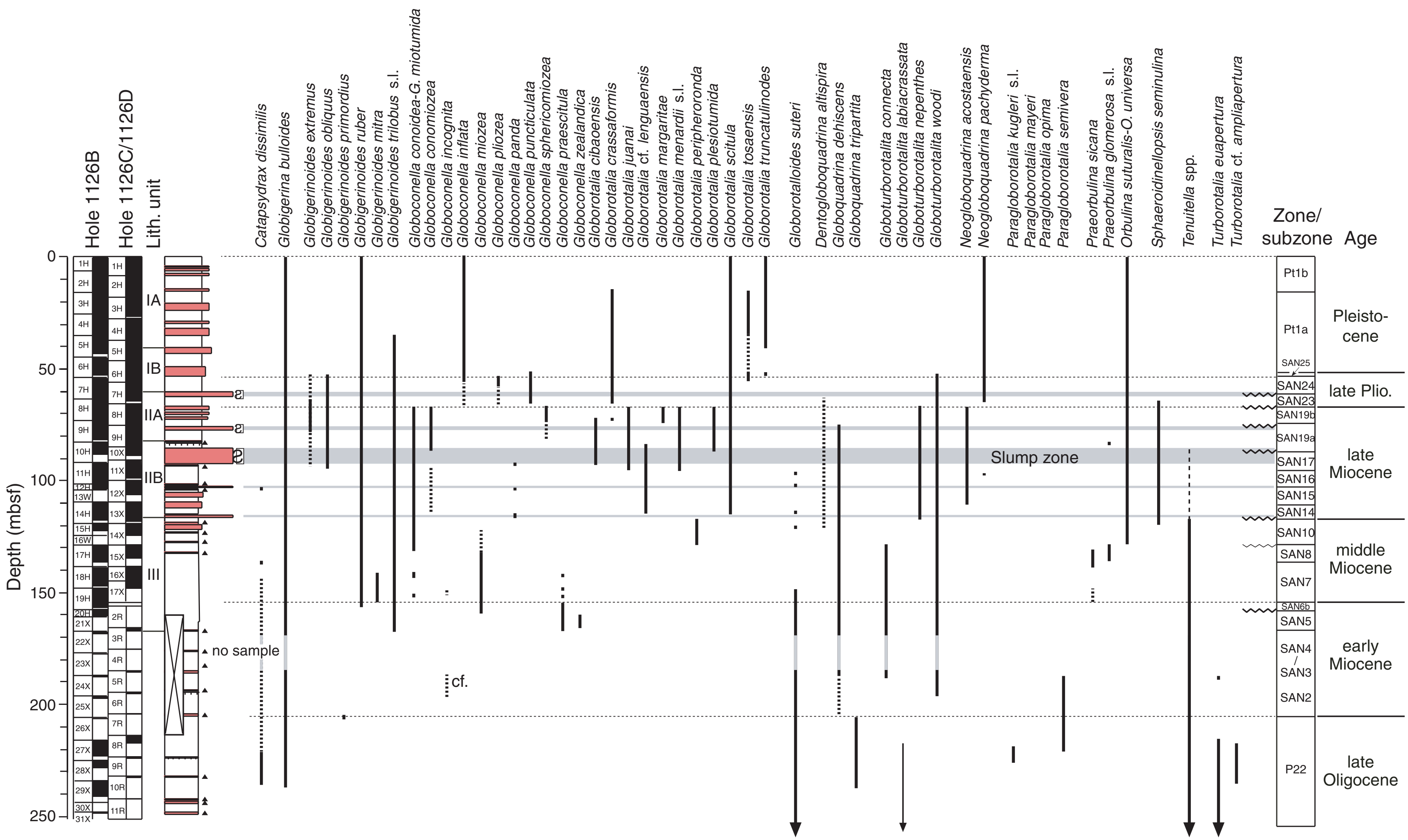

Figure F4. Abundance variations of selected species in the late Oligocene to Pliocene from Hole 1126B. *Globoturborotalita woodi* is dominant in the early Miocene and *Globigerinoides* in the middle Miocene, whereas *Globoconella* and *Orbulina* are more abundant in the late Miocene. The Pliocene contains abundant such newly evolved species as *Globoconella puncticulata, G. inflata,* and *Globorotalia crassaformis.*

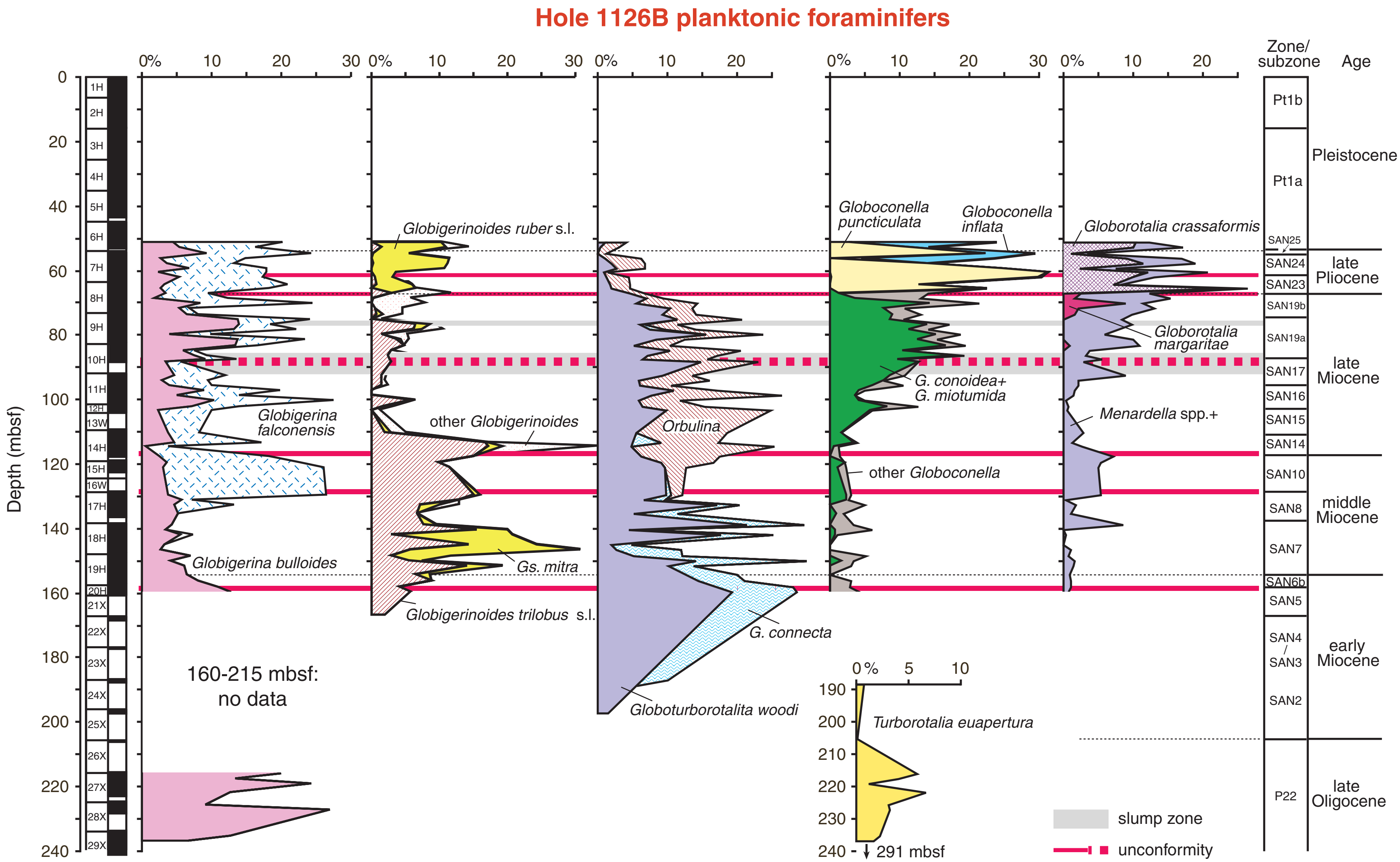

Figure F5. Planktonic foraminiferal biostratigraphy of the Neogene in Holes 1128B and 1128C. Ranges of common species and relevant zones are shown, together with slumped intervals and unconformities (wavy lines).

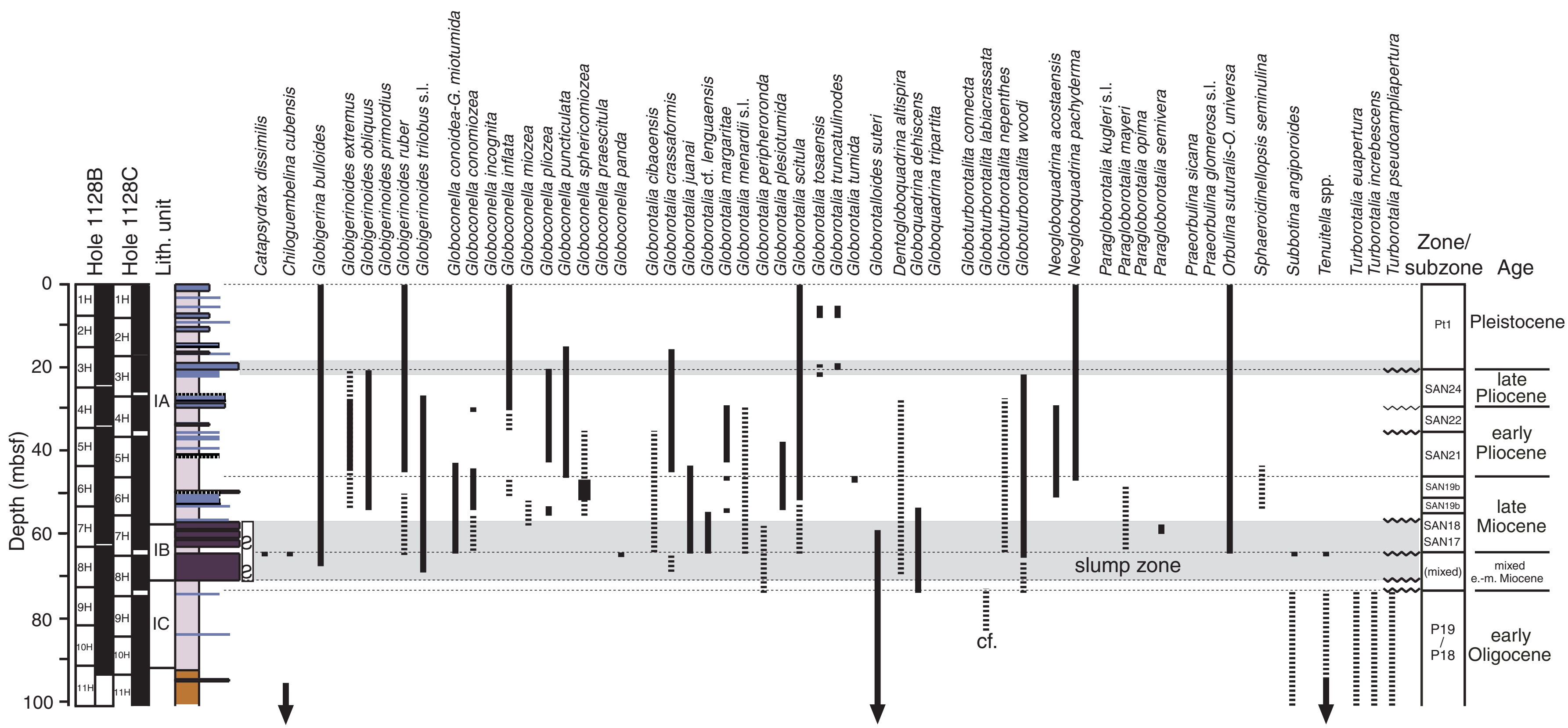

Figure F6. Planktonic foraminiferal biostratigraphy of the Neogene and Quaternary in Holes 1130A, 1130B, and1130C. Ranges of common species and relevant zones are shown, together with slumped intervals and unconformities (wavy lines).

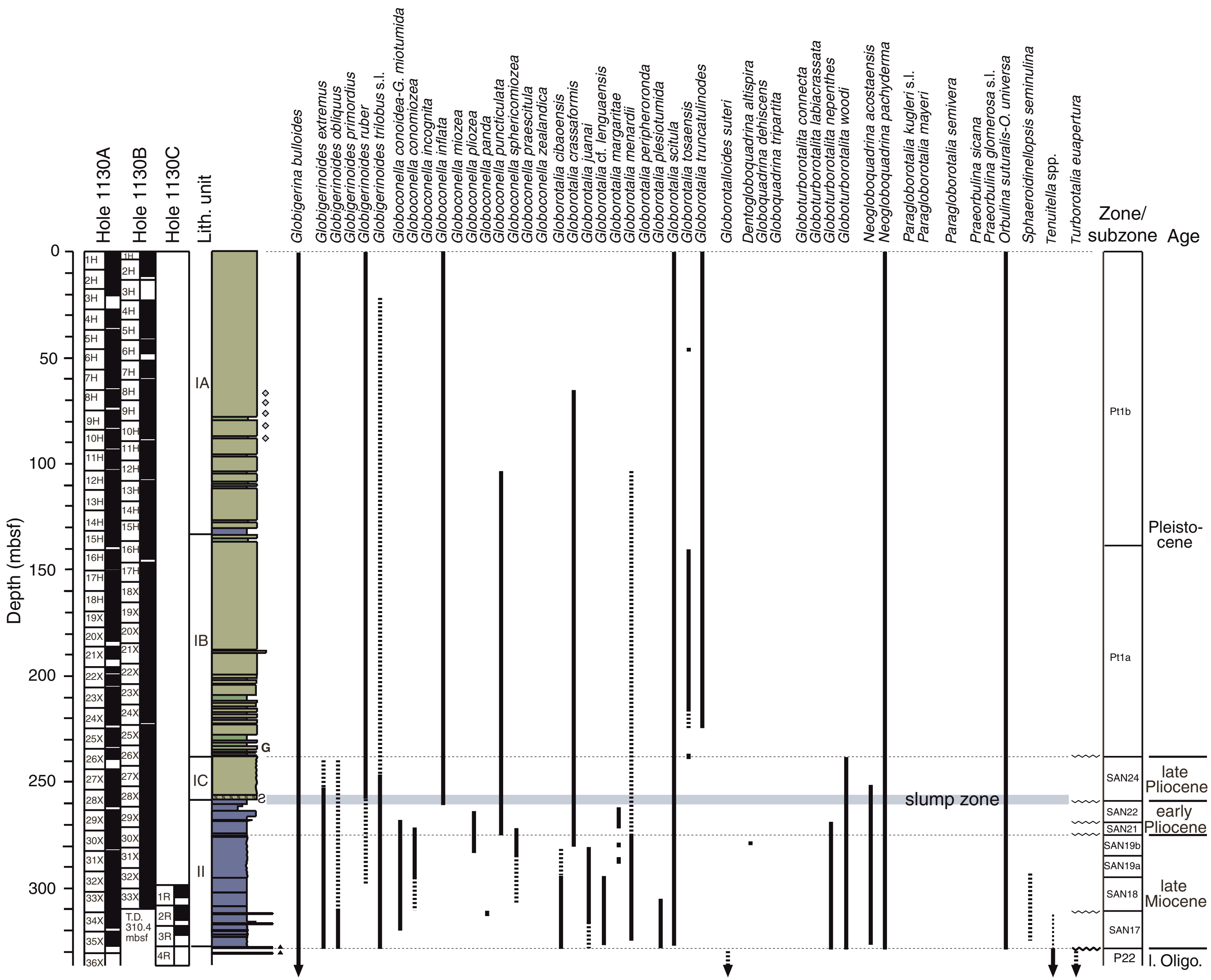

Figure F7. Abundance variations of selected species in the late Miocene to basal Pleistocene from Hole 1130A. A generalized late Miocene trend is that *Globoturborotalita woodi* dominated the Zone SAN17 assemblage, *Globigerina bulloides* and *G. falconensis* both increased their abundance in Zone SAN18 and Subzone SAN19a, and a steady increase in *Globigerinoides* (*Gs. extremus*), *Globorotalia margaritae,* and *Globoconella* (*G. sphericomiozea*) characterized Subzones SAN19a and SAN19b. *Globorotalia crassaformis* was abundant in the early Pliocene, reaching a maximum of ~30% in the slump close to the early/late Pliocene boundary probably due to the robustness of its tests. In the late Pliocene, *Globigerinoides ruber, Globoconella inflata,* and *Globigerina falconensis* increased to become dominant but *Globigerinoides trilobus* and *Menardella* spp. declined to a minimum.

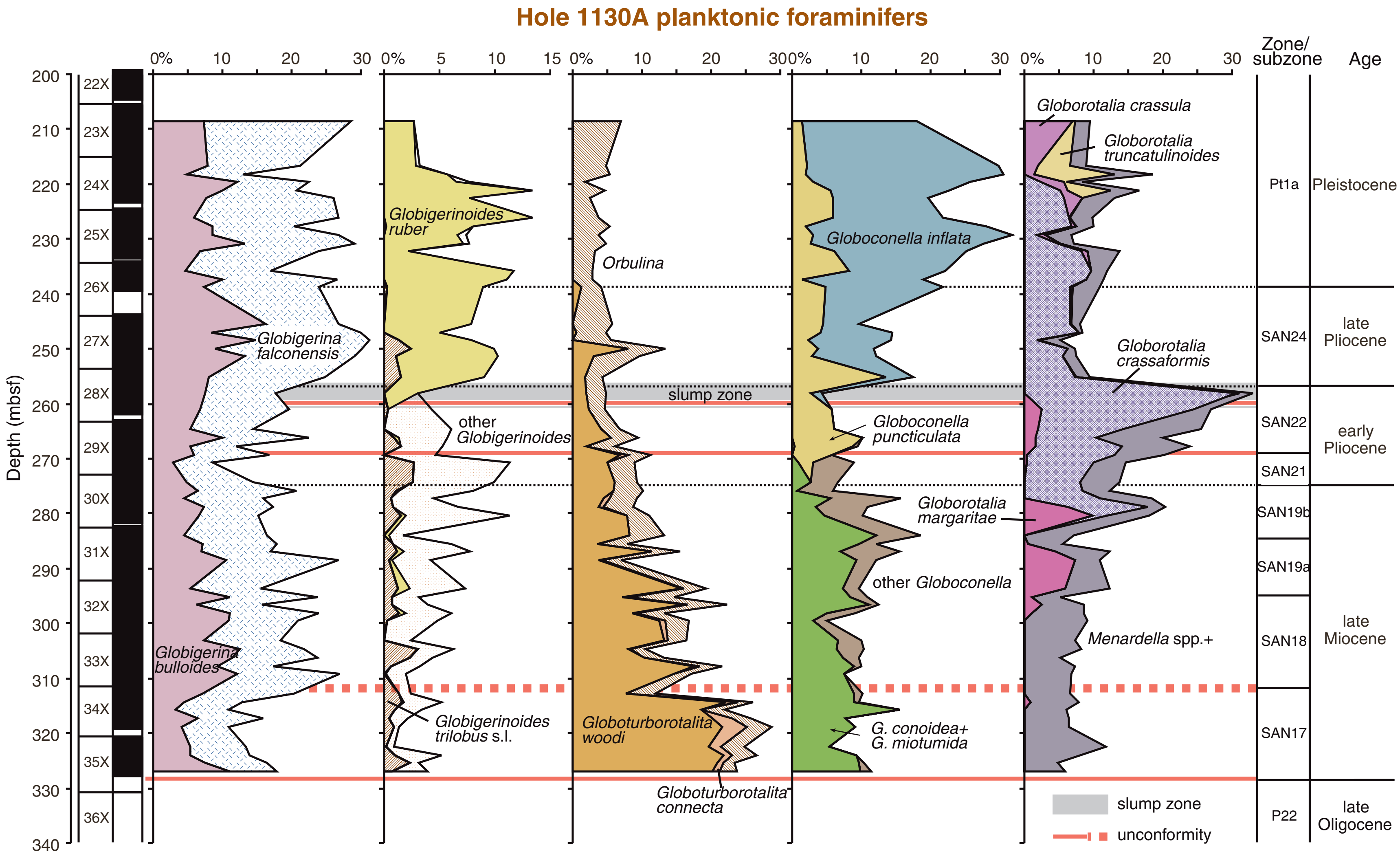

Figure F8. Planktonic foraminiferal biostratigraphy of the Neogene and Quaternary in Holes 1132B and 1132C. Ranges of common species and relevant zones are shown. Unconformities are indicated by wavy lines. The poor recovery of the Miocene section hampered a proper resolution. T.D. = total depth.

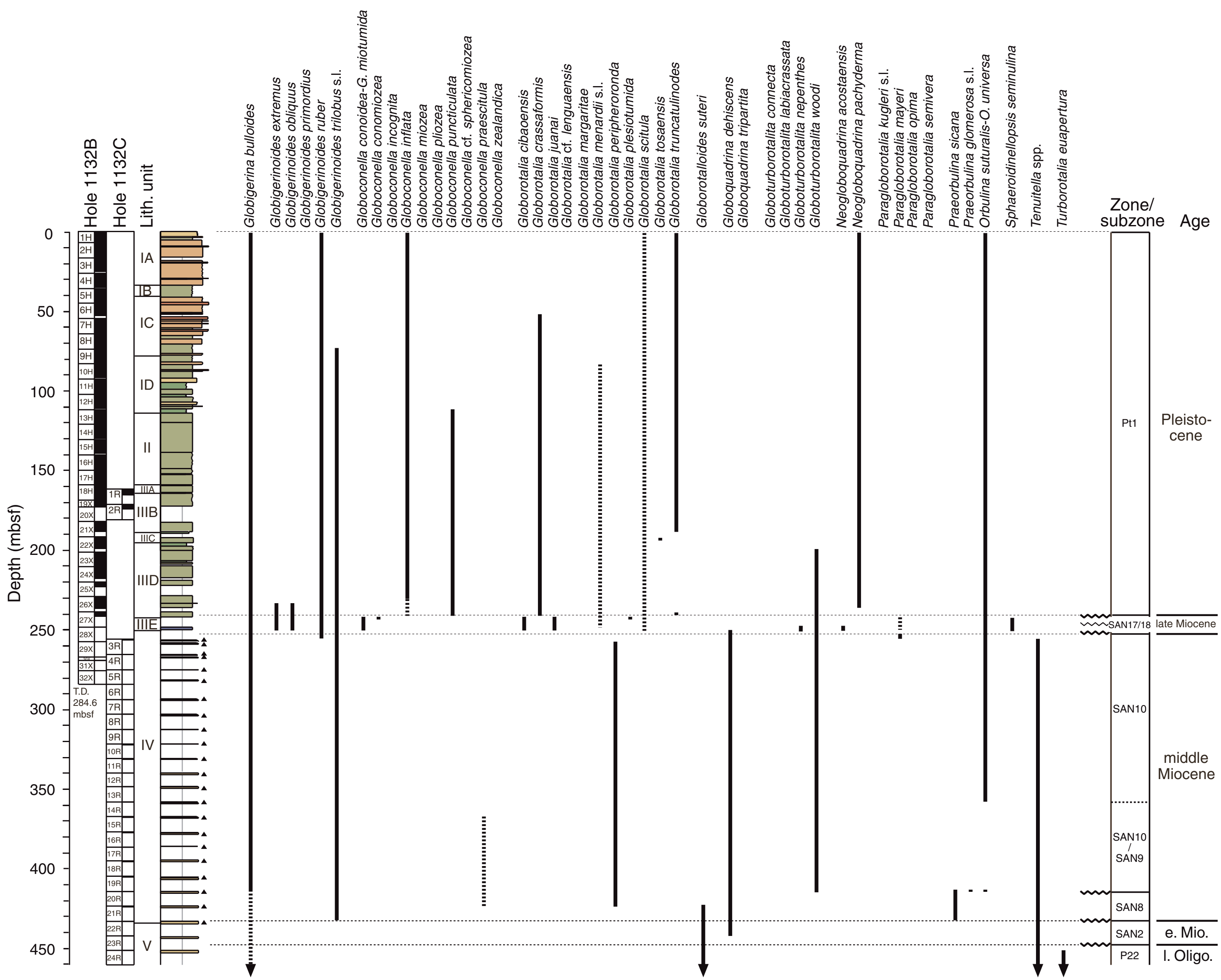

Figure F9. Planktonic foraminiferal biostratigraphy of the Neogene and Quaternary in Holes 1134AB and 1134B. Ranges of common species and relevant zones are shown, together with slumped intervals and unconformities (wavy lines).

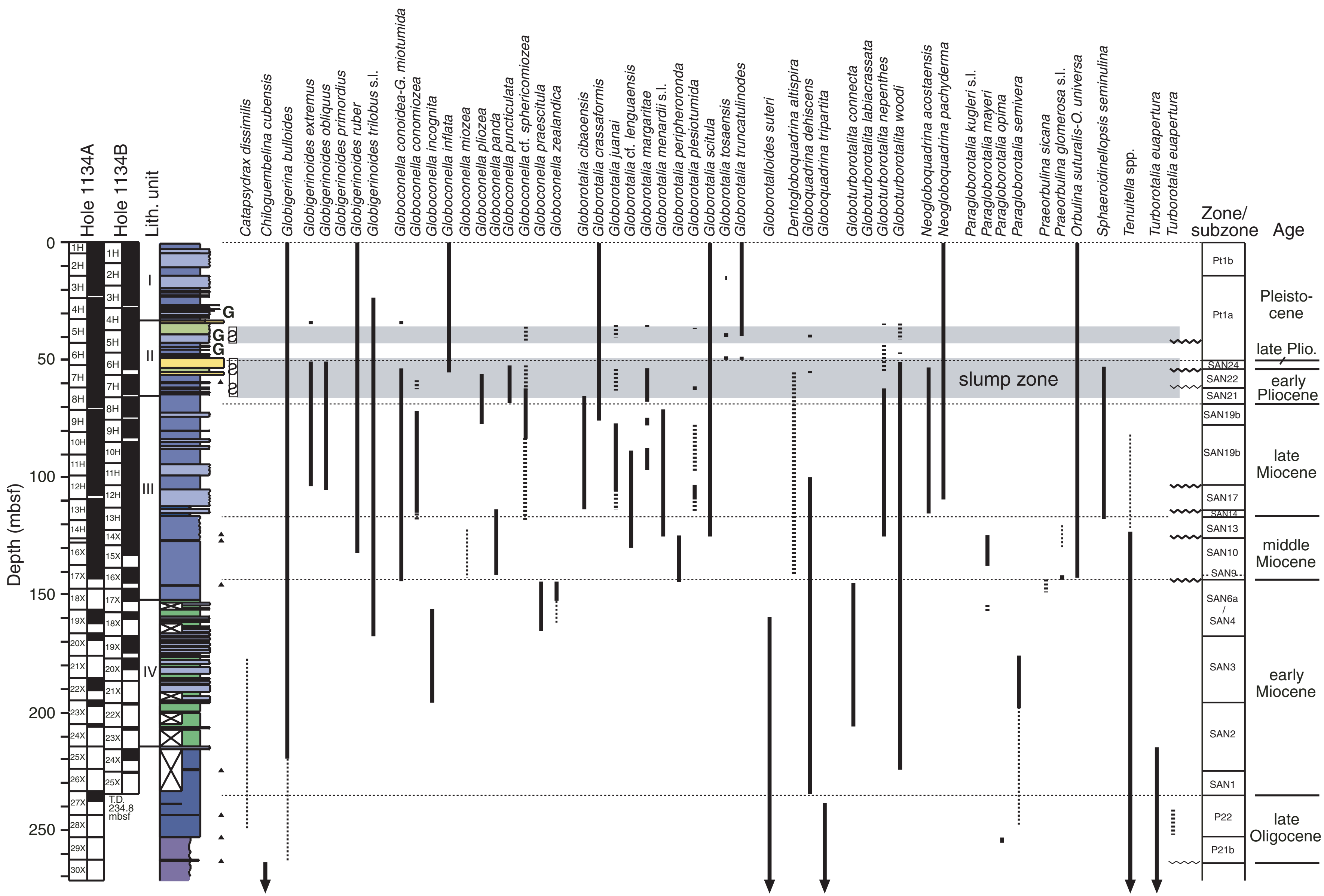

Figure F10. Abundance variations of selected species in the Oligocene to basal Pleistocene from Hole 1134A. Assemblage characteristics are similar to those from Holes 1126B (Fig. F4, p. 32) and 1130A (Fig. F7, p. 35).

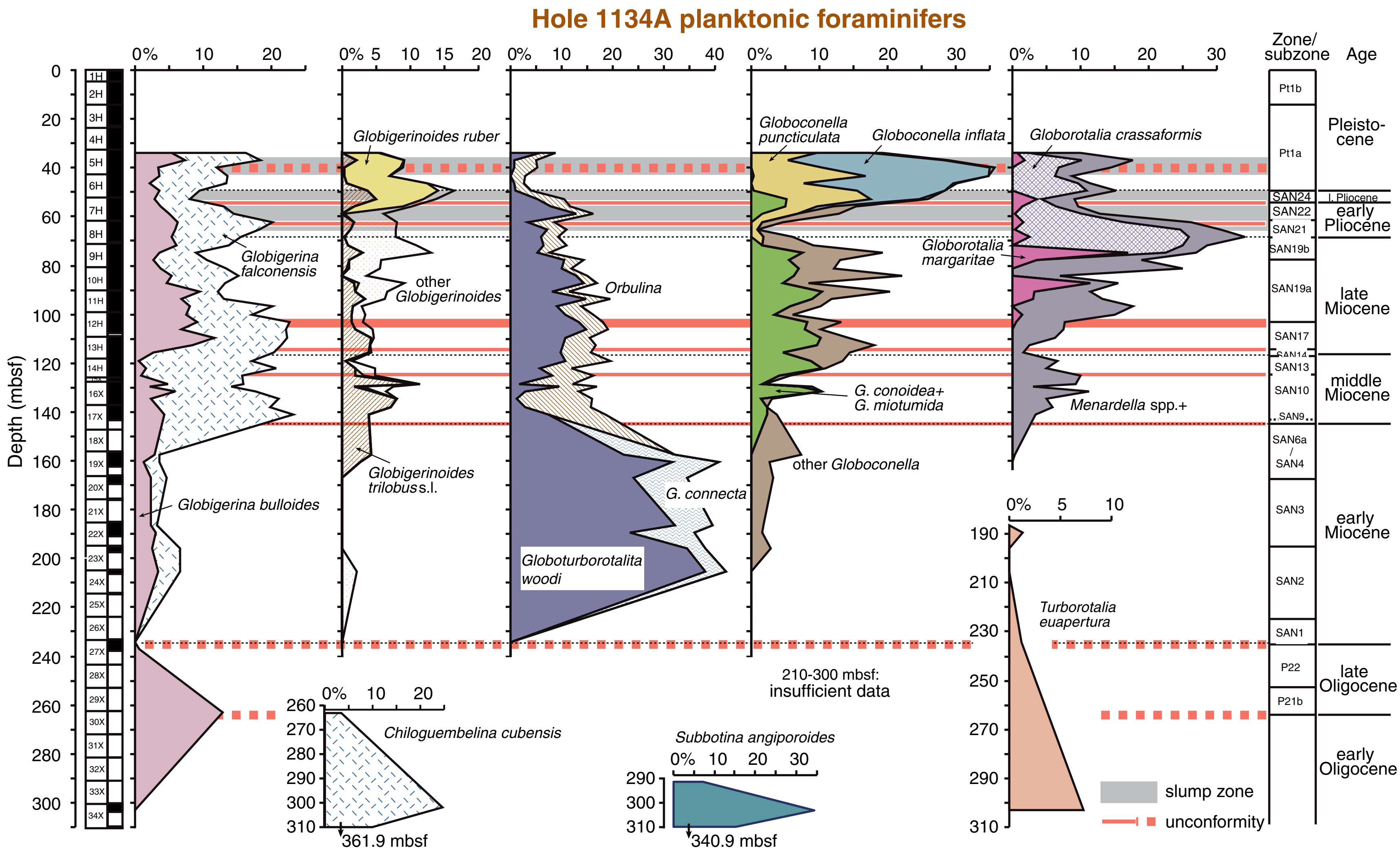

Figure F11. Biostratigraphic correlation of the Neogene from ODP Leg 182 sites studied. Most units are hiatus-bounded. Relative complete sections are from Sites 1126 and 1134. Note the different scales.

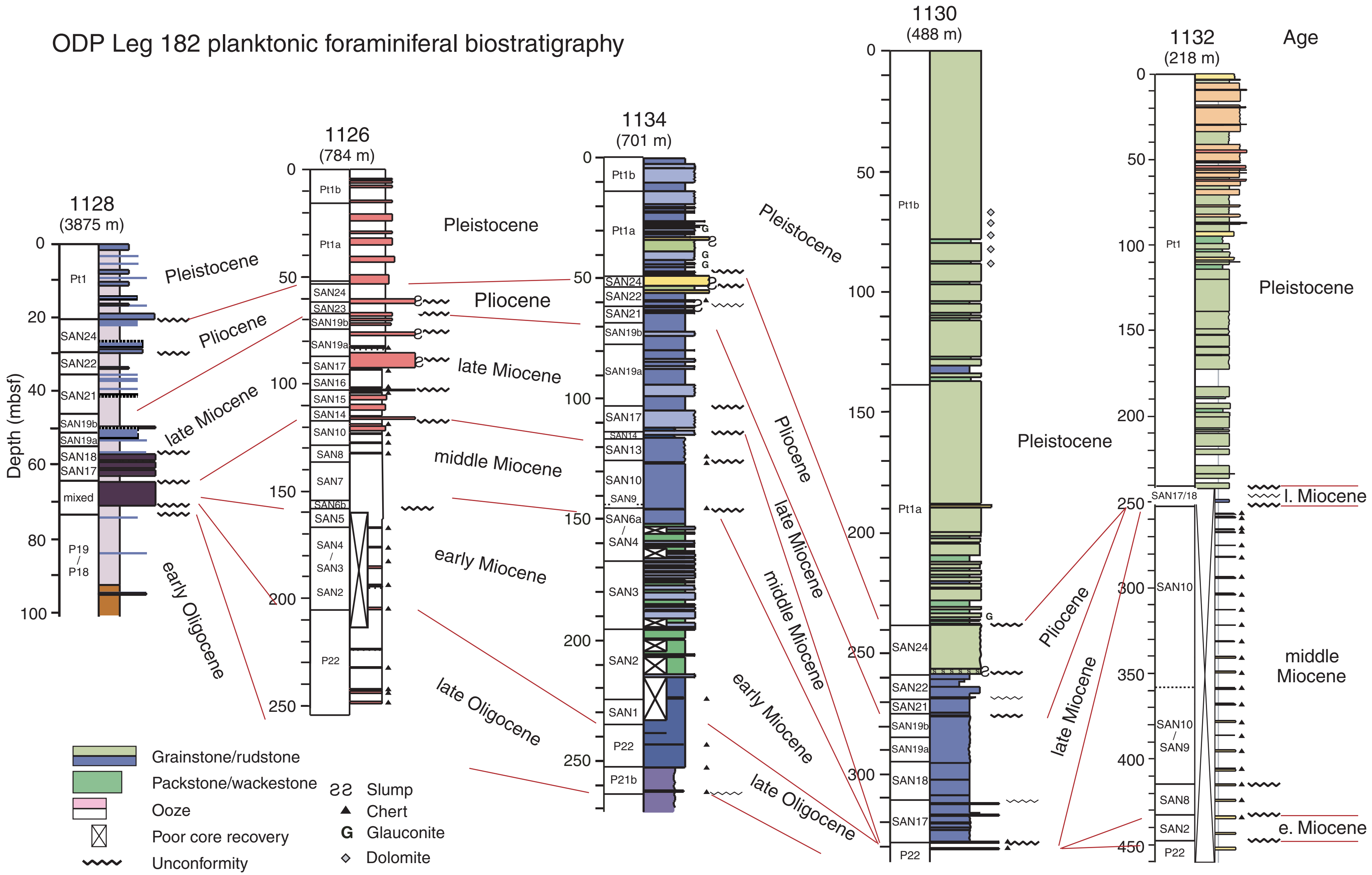

Figure F12. Time-depth diagram for important planktonic foraminifer datums (as listed in Tables T2, p. 43, T3, p. 44, T4, p. 45, T5, p. 46, and T6, p. 47), showing position of unconformities and variations of sedimentation rates between sites. The labeled 15 hiatuses are inferred mainly from this data set and partly from changes in the characteristics of related assemblages.

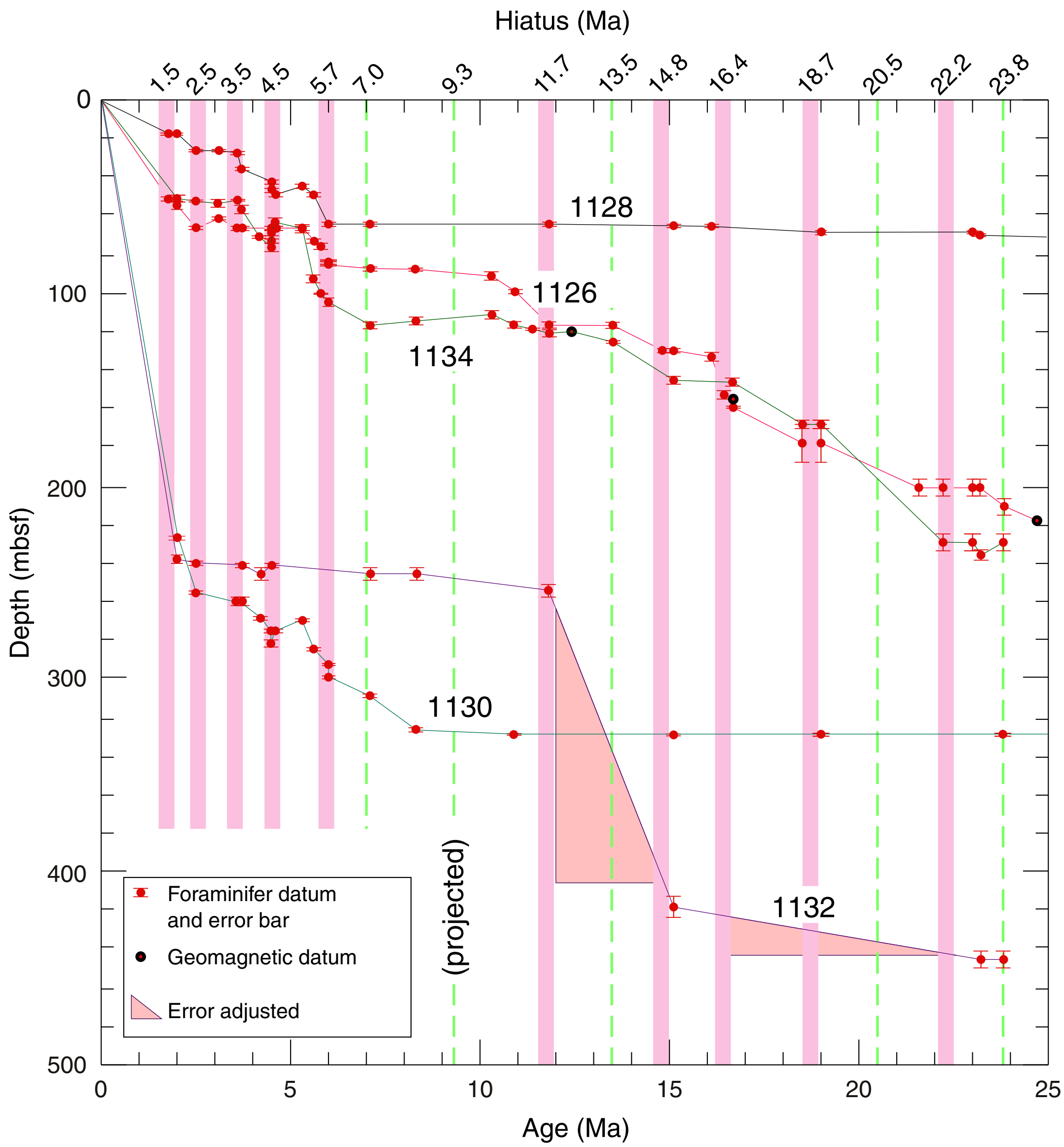

Figure F13. Positioning of the Neogene carbonates from the Great Australian Bight in the global sequence-stratigraphical hierarchy of Haq et al. (1988) and Hardenbol et al. (1998). Regional transgressions and stages after McGowran (1979, 1986, 1989) and McGowran et al. (1997). The 15 hiatuses identified coincide with major third-order boundaries (see text).

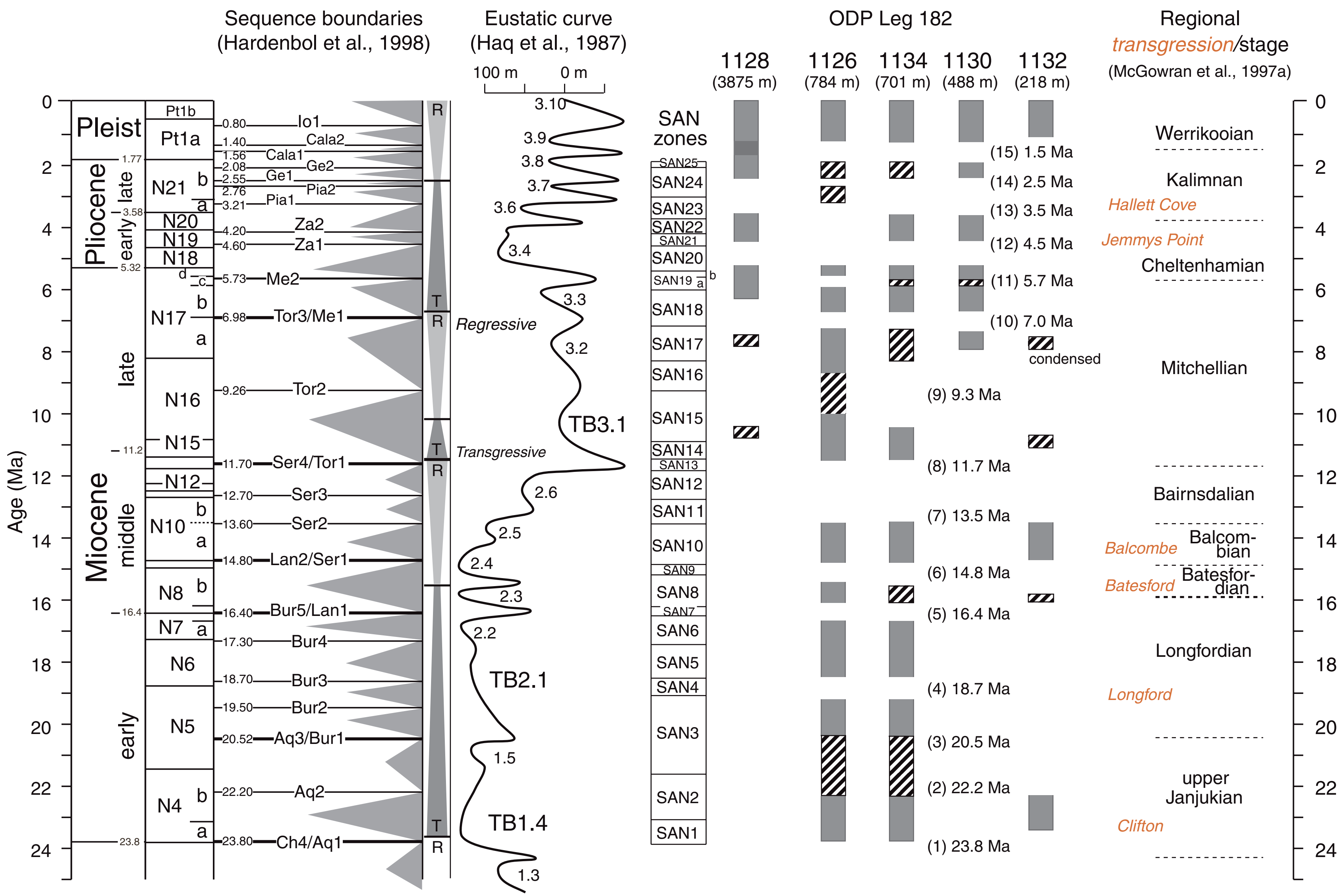

Table T1. Site parameters and Neogene samples used in this study.

Hole	Water depth (m)	Penetration (m)	Studied interval (mbsf)	Core catcher	Core samples
1126B	783.8	463.3	51–237	23	63
1126C				12	7
1126D				10	0
1128B	3874.2	452.6	16–84	9	33
1128C				9	12
1130A	487.8	395.2	209–327	13	55
1130B				11	12
1130C				3	0
1132B	218.3	603.2	230–452	5	7
1132C				22	0
1134A	701.0	397.1	33–250	25	44
1134B				22	9
	Totals:	164	242		

Table T2. Listing of datum levels, Hole 1126B.

Datum	Age (Ma)	Midpoint (mbsf)	Stratigraphic error (m)	Shallow sample: Core, section, interval (cm)	Shallow sample: Depth (mbsf)	Deep sample: Core, section, interval (cm)	Deep sample: Depth (mbsf)
				182-1126B-		182-1126B-	
LO *Globigerinoides obliquus*	1.77	52.00	0.75	6H-5, 75–77	51.25	6H-6, 75–77	52.75
FO *Globorotalia truncatulinoides*	2.00	54.39	1.635	6H-6, 75–77	52.75	6H-CC, 26–29	56.02
LCO *Globigerinoides extremus/G. obliquus*	2.50	66.51	0.75	8H-2, 76–78	65.76	8H-3, 76–78	67.26
LO *Dentoglobigerina altispira*	3.09	61.50	0.75	7H-5, 75–77	60.75	7H-6, 75–77	62.25
LO *Globorotalia margaritae*	3.58	66.51	0.75	8H-2, 76–78	65.76	8H-3, 76–78	67.26
FO *Globorotalia inflata*	3.70	66.51	0.75	8H-2, 76–78	65.76	8H-3, 76–78	67.26
FO *Globorotalia puncticulata*	4.50	66.51	0.75	8H-2, 76–78	65.76	8H-3, 76–78	67.26
FO *Globorotalia crassaformis*	4.50	73.36	0.395	8H-CC, 13–16	72.96	9H-1, 75–77	73.75
LO *Globorotalia cibaoensis/G. juanai*	4.60	66.51	0.75	8H-2, 76–78	65.76	8H-3, 76–78	67.26
LCO *Globorotalia sphericomiozea*	5.30	66.51	0.75	8H-2, 76–78	65.76	8H-3, 76–78	67.26
FCO *Globorotalia sphericomiozea*	5.60	73.36	0.395	8H-CC, 13–16	72.96	9H-1, 75–77	73.75
LO *Globoquadrina dehiscens*	5.80	76.00	0.75	9H-2, 75–77	75.25	9H-3, 75–77	76.75
FO *Globorotalia margaritae*	6.00	84.00	0.745	10H-1, 75–77	83.25	10H-2, 74–76	84.74
LO *Globorotalia lenguaensis*	6.00	82.64	0.615	9H-CC, 15–18	82.02	10H-1, 75–77	83.25
FO *Globorotalia conomiozea*	7.10	86.89	0.635	10H-3, 75–77	86.25	10H-4, 52–54	87.52
FO *Globorotalia plesiotumida*	8.30	87.94	0.415	10H-4, 52–54	87.52	10H-5, 75–77	88.35
LO *Globorotalia panda*	10.30	90.55	2.2	10H-5, 75–77	88.35	11H-1, 75–77	92.75
FO *Neogloboquadrina acostaensis*	10.90	99.49	0.74	11H-5, 75–77	98.75	11H-6, 73–75	100.23
FO *Globoturborotalita nepenthes*	11.80	116.25	1.495	14H-4, 75–77	114.75	14H-6, 74–76	117.74
LO *Globorotalia peripheroronda*	13.50	116.25	1.495	14H-4, 75–77	114.75	14H-6, 74–76	117.74
LO *Praeorbulina glomerosa*	14.80	130.30	0.745	17H-1 75–77	129.55	17H-2, 74–76	131.04
FO *Orbulina suturalis*	15.10	130.30	0.745	17H-1, 75–77	129.55	17H-2, 74–76	131.04
FO *Praeorbulina glomerosa*	16.10	134.05	1.48	17H-3, 77–79	132.57	17H-5, 73–75	135.53
FO *Praeorbulina sicana*	16.40	153.04	1.495	19H-3, 74–76	151.54	19H-5, 73–76	154.53
Top of C5Cn	16.70	155.70					
FO *Globorotalia miozea*	16.70	159.92	0.365	20H-2, 75–77	159.55	20H-CC, 6–9	160.28
FO *Globorotalia praescitula*	18.50	178.18	9.825	22X-CC, 17–20	168.35	24X-CC, 23–26	188.00
FO *Globigerinoides trilobus*	19.00	178.18	9.825	22X-CC, 17–20	168.35	24X-CC, 23–26	188.00
FO *Globorotalia incognita*	21.60	201.57	4.285	25X-CC, 15–18	197.28	26X-CC, 15–18	205.85
FO *Globoturborotalita connecta*	22.20	201.57	4.285	25X-CC, 15–18	197.28	26X-CC, 15–18	205.85
FO *Globoturborotalita woodi*	23.00	201.57	4.285	25X-CC, 15–18	197.28	26X-CC, 15–18	205.85
FO *Globoquadrina dehiscens*	23.20	201.57	4.285	25X-CC, 15–18	197.28	26X-CC, 15–18	205.85
LCO *Turborotalia euapertura*	23.80	210.95	5.1	26X-CC, 15–18	205.85	27X-1, 75–77	216.05
Top of C7n	24.70	217.80					

Notes: Datum levels listed here were used to generate Figure **F12**, p. 40. FO = first occurrence of taxon, FCO = first common occurrence of taxon, LO = last occurrence of taxon, LCO = last common occurrence of taxon. Midpoint = the middle depth between the sample where the taxon occurs and the adjacent sample where it does not occur. Stratigraphic error = one-half the distance between the sample where the taxon occurs and the adjacent sample where it does not occur.

Table T3. Listing of datum levels, Hole 1128B.

Datum	Age (Ma)	Midpoint (mbsf)	Stratigraphic error (m)	Shallow sample: Core, section, interval (cm)	Shallow sample: Depth (mbsf)	Deep sample: Core, section, interval (cm)	Deep sample: Depth (mbsf)
				182-1128B-		182-1128B-	
LO *Globigerinoides obliquus*	1.77	18.21	0.76	3H-2, 75–77	17.45	3H-3, 76–78	18.96
FO *Globorotalia truncatulinoides*	2	18.21	0.76	3H-2, 75–77	17.45	3H-3, 76–78	18.96
LCO *Globigerinoides extremus/G. obliquus*	2.5	26.20	0.75	4H-1, 75–77	25.45	4H-2, 75–77	26.95
LO *Dentoglobigerina altispira*	3.09	26.20	0.75	4H-1, 75–77	25.45	4H-2, 75–77	26.95
LO *Globorotalia margaritae*	3.58	27.70	0.75	4H-2, 75–77	26.95	4H-3, 75–77	28.45
FO *Globorotalia inflata*	3.7	35.71	0.75	5H-1, 76–78	34.96	5H-2, 75–77	36.45
FO *Globorotalia puncticulata*	4.5	46.67	0.73	6H-2, 74–76	45.94	6H-3, 70–72	47.40
FO *Globorotalia crassaformis*	4.5	43.08	0.63	5H-6, 75–77	42.45	5H-CC, 11–13	43.70
LO *Globorotalia cibaoensis/G. juanai*	4.6	49.71	0.77	6H-4, 74–76	48.94	6H-5, 78–80	50.48
LCO *Globorotalia sphericomiozea*	5.3	45.17	0.77	6H-1, 70–72	44.4	6H-2, 74–76	45.94
FCO *Globorotalia sphericomiozea*	5.6	49.71	0.77	6H-4, 74–76	48.94	6H-5, 78–80	50.48
LO *Globoquadrina dehiscens*	5.8	49.71	0.77	6H-4, 74–76	48.94	6H-5, 78–80	50.48
FO *Globorotalia margaritae*	6	64.20	0.75	8H-1, 75–77	63.45	8H-2, 75–77	64.95
LO *Globorotalia lenguaensis*	6	64.20	0.75	8H-1, 75–77	63.45	8H-2, 75–77	64.95
FO *Globorotalia conomiozea*	7.1	64.20	0.75	8H-1, 75–77	63.45	8H-2, 75–77	64.95
FO *Globoturborotalita nepenthes*	11.8	64.20	0.75	8H-1, 75–77	63.45	8H-2, 75–77	64.95
FO *Orbulina suturalis*	15.1	65.70	0.75	8H-2, 75–77	64.95	8H-3, 75–77	66.45
FO *Praeorbulina glomerosa*	16.1	65.70	0.75	8H-2, 75–77	64.95	8H-3, 75–77	66.45
FO *Globigerinoides trilobus*	19	68.70	0.75	8H-4, 75–77	67.95	8H-5, 75–77	69.45
FO *Globoturborotalita woodi*	23	68.70	0.75	8H-4, 75–77	67.95	8H-5, 75–77	69.45
FO *Globoquadrina dehiscens*	23.2	70.22	0.77	8H-5, 75–77	69.45	8H-6, 79–83	70.99
Top C10n	28.3	75.20		9H-2, 150–	75.2		

Notes: Datum levels listed here were used to generate Figure **F12**, p. 40. FO = first occurrence of taxon, FCO = first common occurrence of taxon, LO = last occurrence of taxon, LCO = last common occurrence of taxon. Midpoint = the middle depth between the sample where the taxon occurs and the adjacent sample where it does not occur. Stratigraphic error = one-half the distance between the sample where the taxon occurs and the adjacent sample where it does not occur.

Table T4. Listing of datum levels, Hole 1130A.

Datum	Age (Ma)	Midpoint (mbsf)	Stratigraphic error (m)	Shallow sample: Core, section, interval (cm)	Shallow sample: Depth (mbsf)	Deep sample: Core, section, interval (cm)	Deep sample: Depth (mbsf)
				182-1130A-		182-1130A-	
FO *Globorotalia truncatulinoides*	2.00	226.95	0.8	25X-1, 75–77	226.15	25X-2, 85–87	227.75
LCO *Globigerinoides extremus/G. obliquus*	2.50	255.71	0.66	28X-1, 75–77	255.05	28X-2, 58–62	256.38
LO *Globorotalia margaritae*	3.58	259.55	1.5	28X-3, 75–77	258.05	28X-5, 75–77	261.05
FO *Globorotalia inflata*	3.70	259.55	1.5	28X-3, 75–77	258.05	28X-5, 75–77	261.05
LO *Globoturborotalita nepenthes*	4.20	268.45	0.8	29X-3, 75–77	267.65	29X-4 85–87	269.25
FO *Globorotalia puncticulata*	4.50	275.06	0.8	30X-1, 76–78	274.26	30X-2, 85–87	275.85
FO *Globorotalia crassaformis*	4.50	281.56	1.3	30X-5, 76–78	280.26	30X-CC, 31–34	282.85
LO *Globorotalia cibaoensis/G. juanai*	4.60	275.06	0.8	30X-1, 76–78	274.26	30X-2, 85–87	275.85
LCO *Globorotalia sphericomiozea*	5.30	269.95	0.7	29X-4, 85–87	269.25	29X-5, 75–77	270.65
FCO *Globorotalia sphericomiozea*	5.60	284.65	0.8	31X-1, 75–77	283.85	31X-2, 85–87	285.45
FO *Globorotalia margaritae*	6.00	298.86	0.71	32X-4, 85–87	298.15	32X-5, 76–78	299.56
LO *Globorotalia lenguaensis*	6.00	293.15	0.4	31X-CC, 31–34	292.75	32X-1, 75–77	293.55
FO *Globorotalia conomiozea*	7.10	308.45	0.7	33X-4, 85–87	307.75	33X-5, 75–77	309.15
FO *Globorotalia plesiotumida*	8.30	326.25	0.8	35X-3, 75–77	325.45	35X-4, 85–87	327.05
FO *Neogloboquadrina acostaensis*	10.90	328.73	0.16	35X-5, 87–92	328.57	35X-CC, 27–30	328.89
FO *Orbulina suturalis*	15.10	328.73	0.16	35X-5, 87–92	328.57	35X-CC, 27–30	328.89
FO *Globigerinoides trilobus*	19.00	328.73	0.16	35X-5, 87–92	328.57	35X-CC, 27–30	328.89
LCO *Turborotalia euapertura*	23.80	328.73	0.16	35X-5, 87–92	328.57	35X-CC, 27–30	328.89

Notes: Datum levels listed here were used to generate Figure **F12,** p. 40. FO = first occurrence of taxon, FCO = first common occurrence of taxon, LO = last occurrence of taxon, LCO = last common occurrence of taxon. Midpoint = the middle depth between the sample where the taxon occurs and the adjacent sample where it does not occur. Stratigraphic error = one-half the distance between the sample where the taxon occurs and the adjacent sample where it does not occur.

Table T5. Listing of datum levels, Holes 1132B and 1132C.

Datum	Age (Ma)	Midpoint (mbsf)	Stratigraphic error (m)	Shallow sample: Core, section, interval (cm)	Shallow sample: Depth (mbsf)	Deep sample: Core, section, interval (cm)	Deep sample: Depth (mbsf)
				182-1132B-		182-1132B-	
FO *Globorotalia truncatulinoides*	2.00	237.90	1.35	26X-CC, 25–28	236.55	27X-1, 75–77	239.25
LCO *Globigerinoides extremus/G. obliquus*	2.50	240.00	0.75	27X-1, 75–77	239.25	27X-2, 75–77	240.75
FO *Globorotalia inflata*	3.70	241.28	0.525	27X-2, 75–77	240.75	27X-CC, 34–37	241.80
LO *Globoturborotalita nepenthes*	4.20	245.23	3.43	27X-CC, 34–37	241.80	28X-1, 76–78	248.66
FO *Globorotalia puncticulata*	4.50	241.28	0.525	27X-2, 75–77	240.75	27X-CC, 34–37	241.80
FO *Globorotalia crassaformis*	4.50	241.28	0.525	27X-2, 75–77	240.75	27X-CC, 34–37	241.80
FO *Globorotalia conomiozea*	7.10	245.23	3.43	27X-CC, 34–37	241.80	28X-1, 76–78	248.66
FO *Globorotalia plesiotumida*	8.30	245.23	3.43	27X-CC, 34–37	241.80	28X-1, 76–78	248.66
FO *Globoturborotalita nepenthes*	11.80	254.08	3.35	28X-CC, 32–35	250.73	29X-CC, 23–26	257.43
				182-1132C-		182-1132C-	
FO *Orbulina suturalis*	15.10	418.48	4.655	20R-CC, 22–25	413.82	21R-CC, 23–26	423.13
FO *Globoquadrina dehiscens*	23.20	446.31	4.63	23R-CC, 18–21	441.68	24R-CC, 14–17	450.94
LCO *Turborotalia euapertura*	23.80	446.31	4.63	23R-CC, 18–21	441.68	24R-CC, 14–17	450.94

Notes: Datum levels listed here were used to generate Figure **F12,** p. 40. FO = first occurrence of taxon, FCO = first common occurrence of taxon, LO = last occurrence of taxon, LCO = last common occurrence of taxon. Midpoint = the middle depth between the sample where the taxon occurs and the adjacent sample where it does not occur. Stratigraphic error = one-half the distance between the sample where the taxon occurs and the adjacent sample where it does not occur.

Table T6. Listing of datum levels, Hole 1134A.

Datum	Age (Ma)	Midpoint (mbsf)	Stratigraphic error (m)	Shallow sample: Core, section, interval (cm)	Shallow sample: Depth (mbsf)	Deep sample: Core, section, interval (cm)	Deep sample: Depth (mbsf)
				182-1134A-		182-1134A-	
FO *Globorotalia truncatulinoides*	2.00	50.63	1.38	6H-5, 75–77	49.25	6H-CC, 0–4	52.01
LCO *Globigerinoides extremus*	2.50	52.39	0.38	6H-CC, 0–4	52.01	7H-1, 77–79	52.77
LO *Dentoglobigerina altispira*	3.09	54.26	1.49	7H-1, 77–79	52.77	7H-3, 75–77	55.75
LO *Globorotalia margaritae*	3.58	52.39	0.38	6H-CC, 0–4	52.01	7H-1, 77–79	52.77
FO *Globorotalia inflata*	3.70	57.27	1.515	7H-3, 75–77	55.75	7H-5, 78–80	58.78
LO *Globoturborotalita nepenthes*	4.20	71.29	0.46	8H-CC, 19–23	70.83	9H-1, 75–77	71.75
FO *Globorotalia puncticulata*	4.50	69.56	1.275	8H-5, 78–80	68.28	8H-CC, 19–23	70.83
FO *Globorotalia crassaformis*	4.50	76.28	1.505	9H-3, 77–79	74.77	9H-5, 78–80	77.78
LO *Globorotalia cibaoensis/G. juanai*	4.60	63.75	1.5	8H-1, 75–77	62.25	8H-3, 75–77	65.25
LCO *Globorotalia sphericomiozea*	5.30	66.77	1.515	8H-3, 75–77	65.25	8H-5, 78–80	68.28
FCO *Globorotalia sphericomiozea*	5.60	92.25	1.5	11H-1, 75–77	90.75	11H-3, 75–77	93.75
LO *Globoquadrina dehiscens*	5.80	100.11	0.145	11H-CC, 16–19	99.96	12H-1, 75–77	100.25
FO *Globorotalia margaritae*	6.00	104.75	1.5	12H-3, 75–77	103.25	12H-5, 75–77	106.25
FO *Globorotalia conomiozea*	7.10	117.15	1.395	13H-5, 75–77	115.75	13H-CC, 10–13	118.54
FO *Globorotalia plesiotumida*	8.30	114.25	1.5	13H-3, 75–77	112.75	13H-5, 75–77	115.75
LO *Globorotalia panda*	10.30	111.25	1.5	13H-1, 75–77	109.75	13H-3, 75–77	112.75
FO *Neogloboquadrina acostaensis*	10.90	117.15	1.395	13H-5 75–77	115.75	13H-CC, 10–13	118.54
LO *Paragloborotalia mayeri*	11.40	118.90	0.355	13H-CC, 10–13	118.54	14H-1, 75–77	119.25
Base of C5An	12.40	119.80					
FO *Globoturborotalita nepenthes*	11.80	120.69	1.44	14H-1, 75–77	119.25	14H-3, 75–77	122.13
LO *Globorotalia peripheroronda*	13.50	125.64	0.51	14H-5, 75–77	125.13	14H-CC, 16–18	126.15
FO *Orbulina suturalis*	15.10	145.64	1.465	17X-CC, 31–34	144.17	18X-CC, 0–3	147.10
FO *Globorotalia miozea*	16.70	145.64	1.465	17X-CC, 31–34	144.17	18X-CC, 0–3	147.10
FO *Globorotalia praescitula*	18.50	168.59	1.54	20X-1, 75–77	167.05	20X-CC, 27–30	170.13
FO *Globigerinoides trilobus*	19.00	164.95	2.105	19X-CC, 29–32	162.84	20X-1, 75–77	167.05
FO *Globoturborotalita connecta*	22.20	229.20	5.15	26X-CC, 15–18	224.05	27X-1, 75–77	234.35
FO *Globoturborotalita woodi*	23.00	229.20	5.15	26X-CC, 15–18	224.05	27X-1, 75–77	234.35
FO *Globoquadrina dehiscens*	23.20	236.50	2.145	27X-1, 75–77	234.35	27X-CC, 34–37	238.64
LCO *Turborotalia euapertura*	23.80	229.20	5.15	26X-CC, 15–18	224.05	27X-1, 75–77	234.35

Notes: Datum levels listed here were used to generate Figure **F12**, p. 40. FO = first occurrence of taxon, FCO = first common occurrence of taxon, LO = last occurrence of taxon, LCO = last common occurrence of taxon. Midpoint = the middle depth between the sample where the taxon occurs and the adjacent sample where it does not occur. Stratigraphic error = one-half the distance between the sample where the taxon occurs and the adjacent sample where it does not occur.

Plate P1. **1, 2.** *Globoquadrina dehiscens;* (1) Sample 182-1134B-24X-3, 75–77 cm; (2) Sample 1134B-24X-1, 75–77 cm. **3.** *Globoquadrina venezuelana* (Sample 182-1134B-17X-3, 75–77 cm). **4.** *Globorotaloides suteri* (Sample 182-1134A-20X-1, 75–77 cm). **5, 6.** *Catapsydrax dissimilis;* (5) specimen without a bulla (Sample 182-1134B-23X-1, 75–77 cm); (6) Sample 182-1134B-24X-1, 75–77 cm. **7.** *Globigerina ciperoensis* (Sample 182-1134B-24X-3, 75–77 cm). **8.** *Globigerina praebulloides* (Sample 182-1134B-24X-1, 75–77 cm). **9, 10.** *Globigerina cf. falconensis;* (9) Sample 182-1134B-24X-3, 75–77 cm; (10) Sample 182-1134A-22X-3, 75–77 cm. **11, 12.** *Globigerina quinqueloba;* (11) Sample 182-1134A-19X-1, 75–77 cm; (12) Sample 182-1134B-17X-3, 75–77 cm. **13, 14.** *Globoturborotalita woodi* (Sample 182-1134B-24X-3, 75–77 cm). **15.** *Globoturborotalita connecta* (Sample 182-1134B-24X-3, 75–77 cm). **16.** *Globigerinoides trilobus* s.l. (Sample 182-1134A-19X-3, 75–77 cm). **17, 18.** *Globigerinoides subquadratus* (Sample 182-1134A-20X-1, 75–77 cm). **19, 20.** *Turborotalia* cf. *ampliapertura;* (19) Sample 182-1134A-22X-3, 75–77 cm; (20) Sample 182-1134A-20X-1, 75–77 cm. **21.** *Paragloborotalia nana* (Sample 182-1134B-24X-1, 75–77 cm). **22.** *Paragloborotalia nana–P. semivera* transition (Sample 182-1134B-23X-1, 75–77 cm). **23, 24.** *Paragloborotalia semivera;* (23) Sample 182-1134B-24X-1, 75–77 cm; (24) Sample 182-1134A-22X-3, 75–77 cm. **25, 26.** *Paragloborotalia siakensis* (Sample 182-1134A-22X-3, 75–77 cm). **27, 28.** *Paragloborotalia bella* (Sample 182-1134A-19X-3, 75–77 cm). **29.** *Paragloborotalia* sp. (Sample 182-1134B-24X-3, 75–77 cm). **30.** *Paragloborotalia incognita* (Sample 182-1134B-23X-1, 75–77 cm).

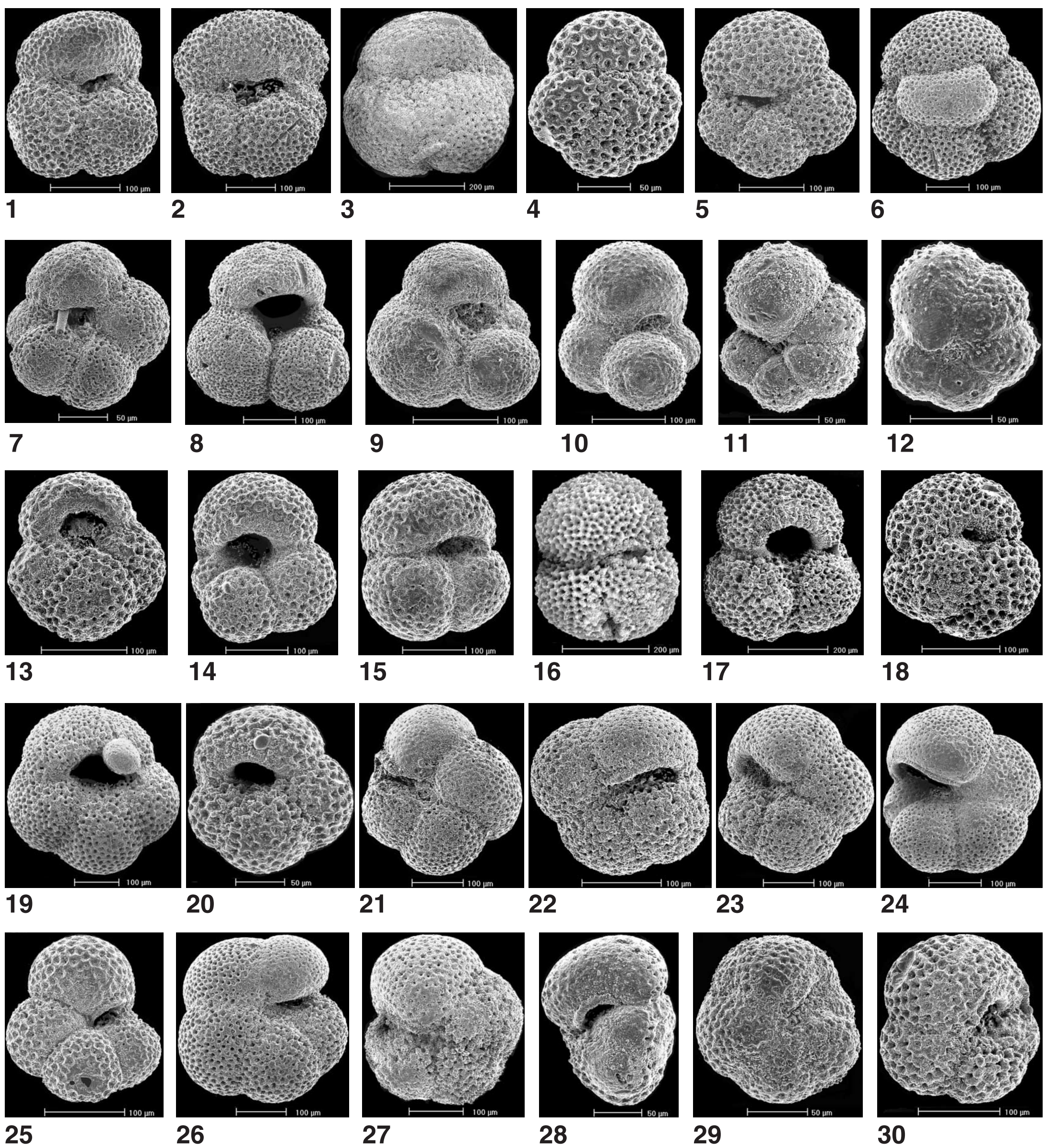

Plate P2. **1.** *Tenuitellinata angustiumbilicata* (Sample 182-1134A-19X-1, 75–77 cm). **2.** *Tenuitella minutissima* (Sample 182-1134A-24X-3, 75–77 cm). **3.** *Tenuitellinata juvenilis* (Sample 182-1134A-19X-1, 75–77 cm). **4.** *Globigerinita glutinata* s.l. (Sample 182-1134A-19X-1, 75–77 cm). **5.** *Globigerinita glutinata* (Sample 182-1134A-19X-1, 75–77 cm). **6.** *Globigerinita uvula* (Sample 182-1134A-24X-3, 75–77 cm). **7–10.** *Globoconella zealandica;* (7, 8) Sample 182-1134A-19X-1, 75–77 cm; (9, 10) Sample 182-1134B-16X-5, 75–77 cm. **11, 12.** *Globorotalia praescitula* (Sample 182-1134B-17X-3, 75–77 cm). **13.** *Globoconella* cf. *miozea* (Sample 182-1134A-19X-3, 75–77 cm). **14, 15.** *Globorotalia archeomenardii;* (14) a small specimen (Sample 182-1134A-20X-1, 75–77 cm); (15) a large specimen (Sample 182-1134B-16X-3, 75–77 cm). **16, 17.** *Menardella praemenardii* (Sample 182-1134A-17X-3, 75–77 cm). **18.** *Menardella praemenardii–M. panda* transition (Sample 182-1134B-16X-3, 75–77 cm). **19–21.** *Globoconella conica;* (19, 20) Sample 182-1134B-16X-3, 75–77 cm; (21) Sample 182-1134A-16X-5, 75–77 cm. **22, 23.** *Globoconella conoidea;* (22) Sample 182-1134A-17X-3, 75–77 cm; (23) Sample 182-1134A-17X-1, 75–77 cm. **24–26.** *Fohsella peripheroronda* (Sample 182-1134B-16X-3, 75–77 cm). **27.** *Sphaeroidinellopsis seminulina* (Sample 182-1134A-17X-1, 75–77 cm). **28, 29.** *Sphaeroidinellopsis kochi* (Sample 182-1134A-16X-5, 75–77 cm). **30, 31.** *Paragloborotalia mayeri* (Sample 182-1134A-16X-1, 75–77 cm).

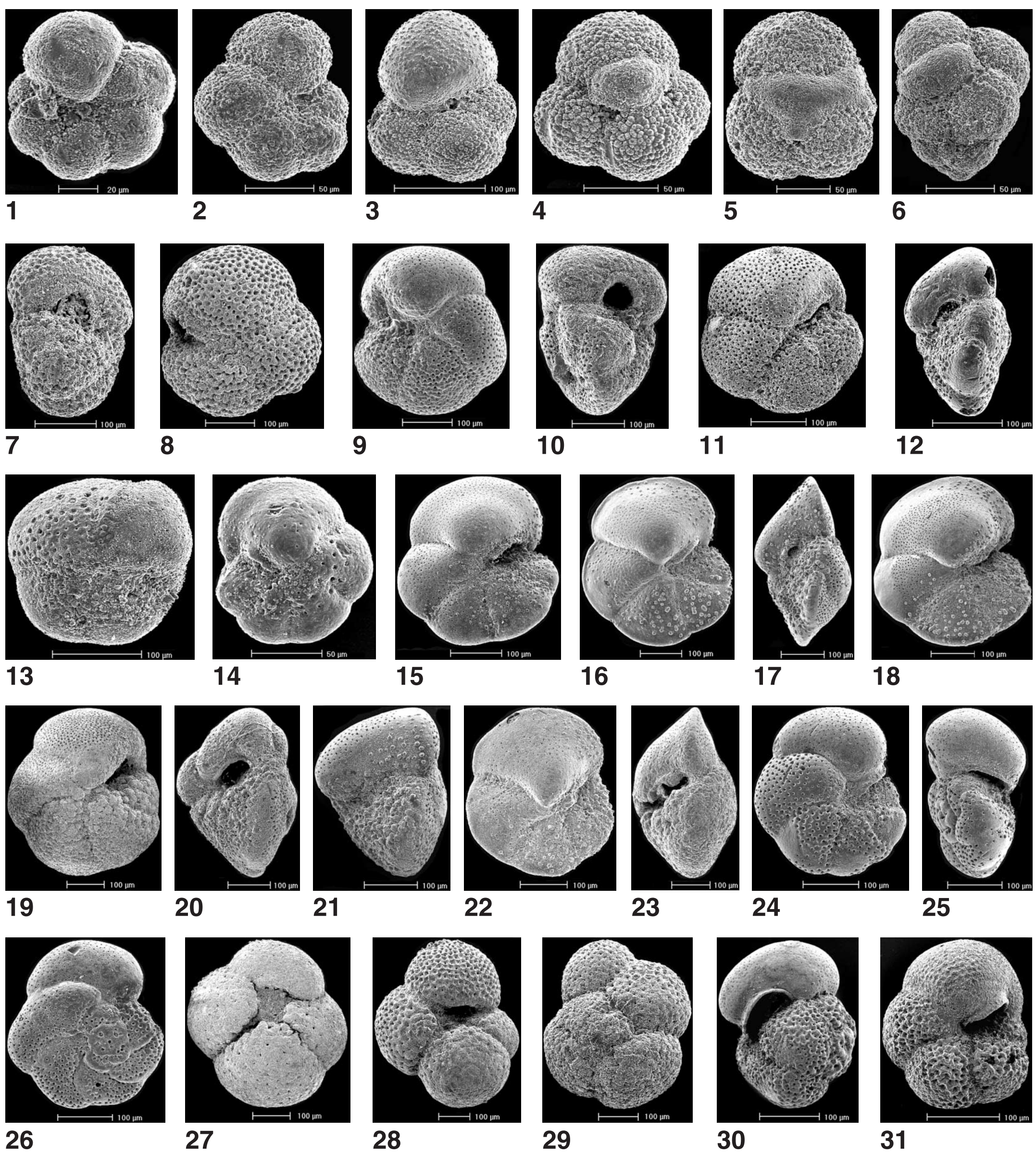

Plate P3. **1.** *Praeorbulina sicana* (Sample 182-1134B-16X-5, 75–77 cm). **2, 3.** *Praeorbulina glomerosa* s.l. (Sample 182-1134B-16X-3, 75–77 cm). **4.** *Orbulina suturalis* (Sample 182-1134B-16X-3, 75–77 cm). **5, 6.** *Orbulina universa;* (5) Sample 182-1134A-17X-1, 77–79 cm; (6) Sample 182-1134A-16X-3, 75–77 cm. **7.** *Globoturborotalita* cf. *decoraperta* (Sample 182-1134B-16X-5, 75–77 cm). **8.** *Globoturborotalita decoraperta* (Sample 182-1134B-16X-1, 75–77 cm). **9.** *Globoturborotalita rubescens* (Sample 182-1134A-16X-1, 75–77 cm). **10.** *Globoturborotalita druryi* (Sample 182-1134A-14H-1, 75–77 cm). **11, 12.** *Globigerinoides parawoodi* (Sample 182-1134A-15X-3, 75–77 cm). **13.** *Globigerinoides quadrilobatus* (Sample 182-1134A-16X-3, 75–77 cm). **14, 15.** *Globigerinoides obliquus* (Sample 182-1134A-16X-3, 75–77 cm). **16, 17.** *Globigerinoides mitra* (Sample 182-1134A-15X-3, 75–77 cm). **18.** *Globoquadrina dehiscens* (Sample 182-1134A-16X-3, 75–77 cm). **19, 20.** *Globoquadrina venezuelana;* (19) Sample 182-1134A-17X-1, 77–79 cm; (20) Sample 182-1134B-16X-3, 75–77 cm. **21.** *Globigerinella obesa* (Sample 182-1134B-16X-3, 75–77 cm). **22.** *Globigerinella obesa–G. siphonifera* transition (Sample 182-1134A-16X-5, 75–77 cm). **23.** *Globigerina ciperoensis* (Sample 182-1134A-16X-1, 75–77 cm). **24.** *Globigerina quinqueloba* (Sample 182-1134A-16X-1, 75–77 cm). **25–31.** *Globorotalia lenguaensis;* (25–27) Sample 182-1134A-16X-3, 75–77 cm; (28–31) Sample 182-1134A-14H-5, 75–77 cm.

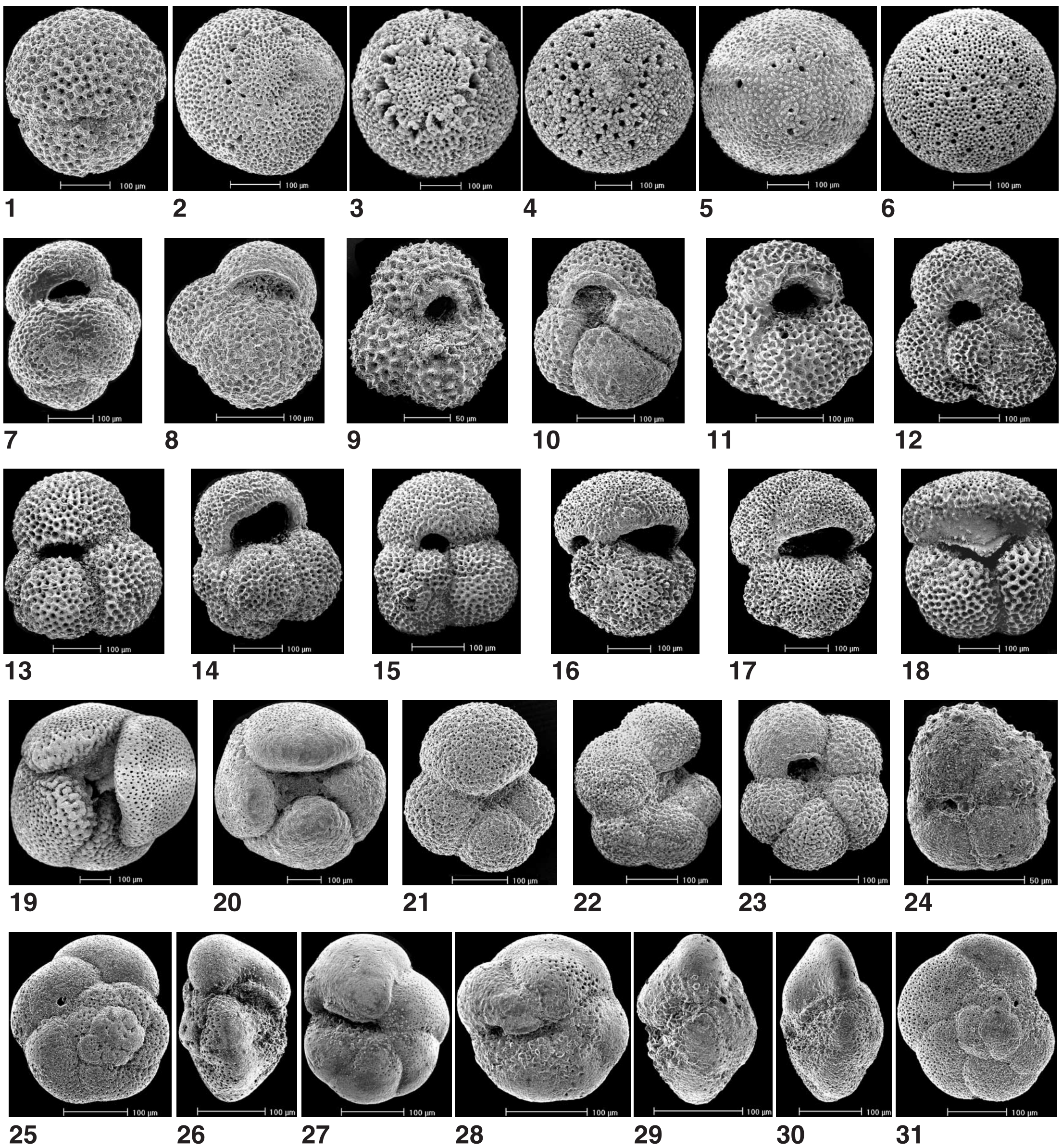

Plate P4. 1, 2. *Globorotalia miotumida* (Sample 182-1134A-15X-3, 75–77 cm). **3.** *Menardella praemenardii* (Sample 182-1134A-14H-5, 75–77 cm). **4, 5.** *Menardella menardii;* (4) Sample 182-1134A-14H-5, 75–77 cm; (5) Sample 182-1134A-14H-1, 75–77 cm. **6.** *Globorotalia explicationis* (Sample 182-1134A-14H-1, 75–77 cm). **7–9.** *Globorotalia panda;* (7–8) Sample 182-1134A-14H-1, 75–77 cm; (9) Sample 182-1134A-13H-3, 75–77 cm. **10, 11.** *Globoconella conoidea* (Sample 182-1134A-14H-3, 75–77 cm). **12, 13.** *Globoconella* cf. *G. sphaericomiozea* (Sample 182-1134A-13H-5, 75–77 cm). **14–16.** *Globoconella conomiozea;* (14, 15) Sample 182-1134A-13H-5, 75–77 cm; (16) Sample 182-1134A-12H-3, 75–77 cm. **17–19.** *Globoconella* cf. *G. sphaericomiozea* (Sample 182-1134A-13H-5, 75–77 cm). **20–22.** *Globorotalia plesiotumida;* (20–21) small specimens (Sample 182-1134A-14H-1, 75–77 cm); (22) Sample 182-1126C-9H-5, 45–50 cm. **23.** *Globorotalia* cf. *G. merotumida* (Sample 182-1134A-10H-3, 75–77 cm). **24.** *Globorotalia* cf. *G. margaritae primitiva (*Sample 182-1134A-13H-1, 75–77 cm). **25.** *Globorotalia scitula* (Sample 182-1126B-5H-2, 75–77 cm). **26–28.** *Globorotalia margaritae* (Sample 182-1134A-9H-3, 77–79 cm). **29–31.** *Globorotalia juanai* (Sample 182-1134A-11H-5, 75–77 cm). **32, 33.** *Globorotalia cibaoensis* (Sample 182-1134A-10H-3, 75–77 cm).

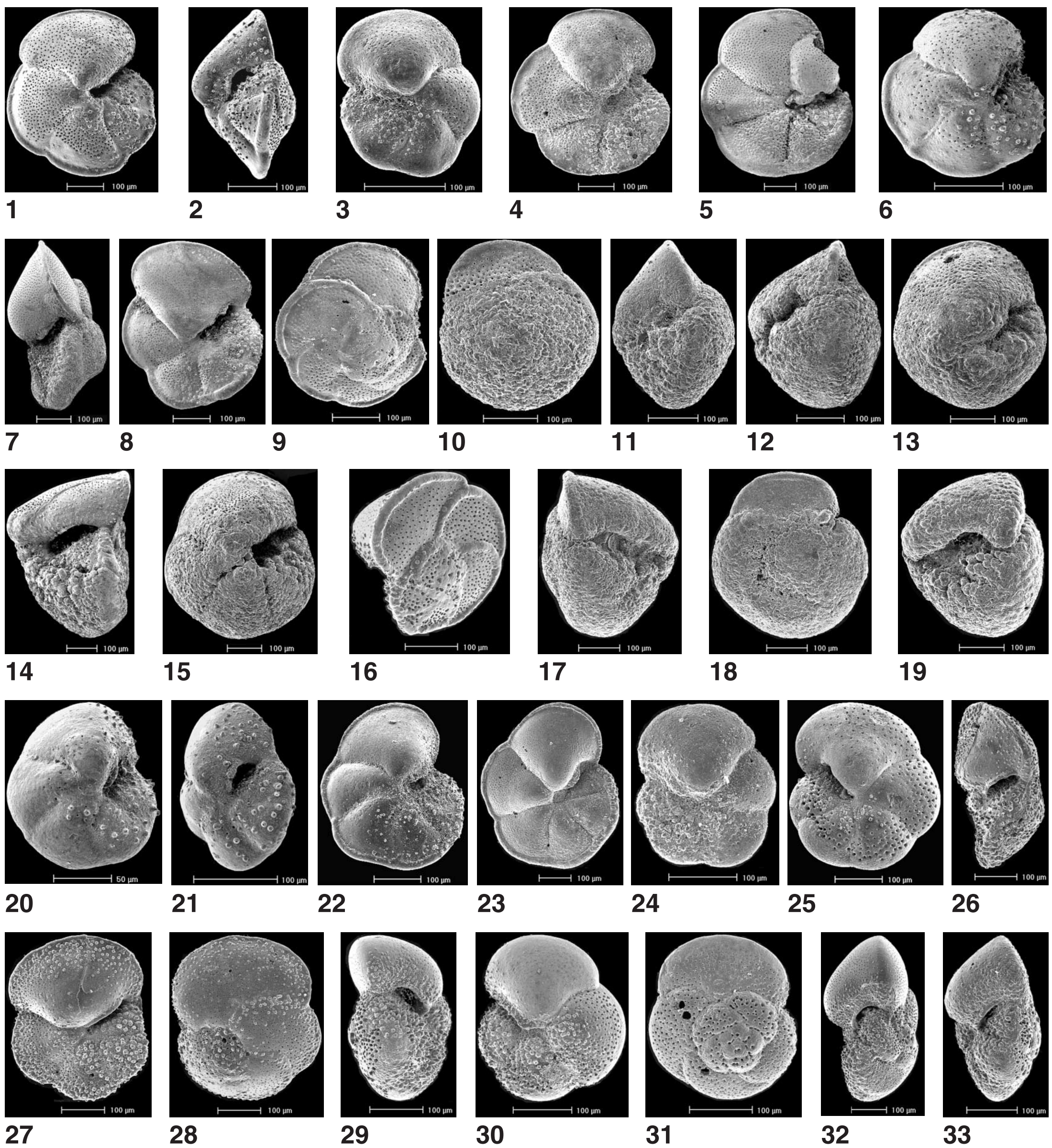

Plate P5. 1–6. *Globorotalia crassaformis;* (1–3) Sample 182-1134A-9H-1, 75–77 cm; (4) Sample 182-1134A-8H-3, 75–77 cm; (5) Sample 182-1134A-6H-1, 75–77 cm; (6) Sample 182-1134A-8H-1, 75–77 cm. **7, 8.** *Globorotalia crassaconica* (Sample 182-1134A-6H-5, 75–77 cm). **9–11.** *Globoconella puncticulata;* (9) Sample 182-1134A-8H-5, 78–80 cm; (10) Sample 182-1134A-8H-3, 75–77 cm; (11) Sample 182-1134A-8H-1, 75–77 cm. **12.** *Globoconella puncticulata–G. inflata* transition; small specimen (Sample 182-1134A-6H-5, 75–77 cm). **13, 14.** *Globoconella inflata;* (13) Sample 182-1134A-6H-5, 75–77 cm; (14) Sample 182-1134A-6H-1, 77–79 cm. **15, 16.** *Globorotalia crassula* (Sample 182-1134A-5H-3, 76–78 cm). **17–20.** *Globoconella pliozea;* (17) thin-walled specimen (Sample 182-1134A-9H-3, 77–79 cm); (18) thin-walled specimen (Sample 182-1134A-8H-5, 75–77 cm); (19–20) thick-walled specimen (Sample 182-1134A-8H-5, 75–77 cm). **21, 22.** *Globorotalia tosaensis* (Sample 182-1134A-6H-5, 75–77 cm). **23, 24.** *Globorotalia truncatulinoides* (Sample 182-1126C-3H-CC, 13–15 cm). **25.** *Catapsydrax parvulus* (Sample 182-1134A-14H-5, 75–77 cm). **26.** *Neogloboquadrina continuosa* (Sample 182-1134A-14H-5, 75–77 cm). **27, 28.** *Neogloboquadrina nympha* (Sample 182-1134A-14H-1, 77–79 cm). **29, 30.** *Neogloboquadrina pachyderma* (Sample 182-1134A-6H-1, 77–79 cm).

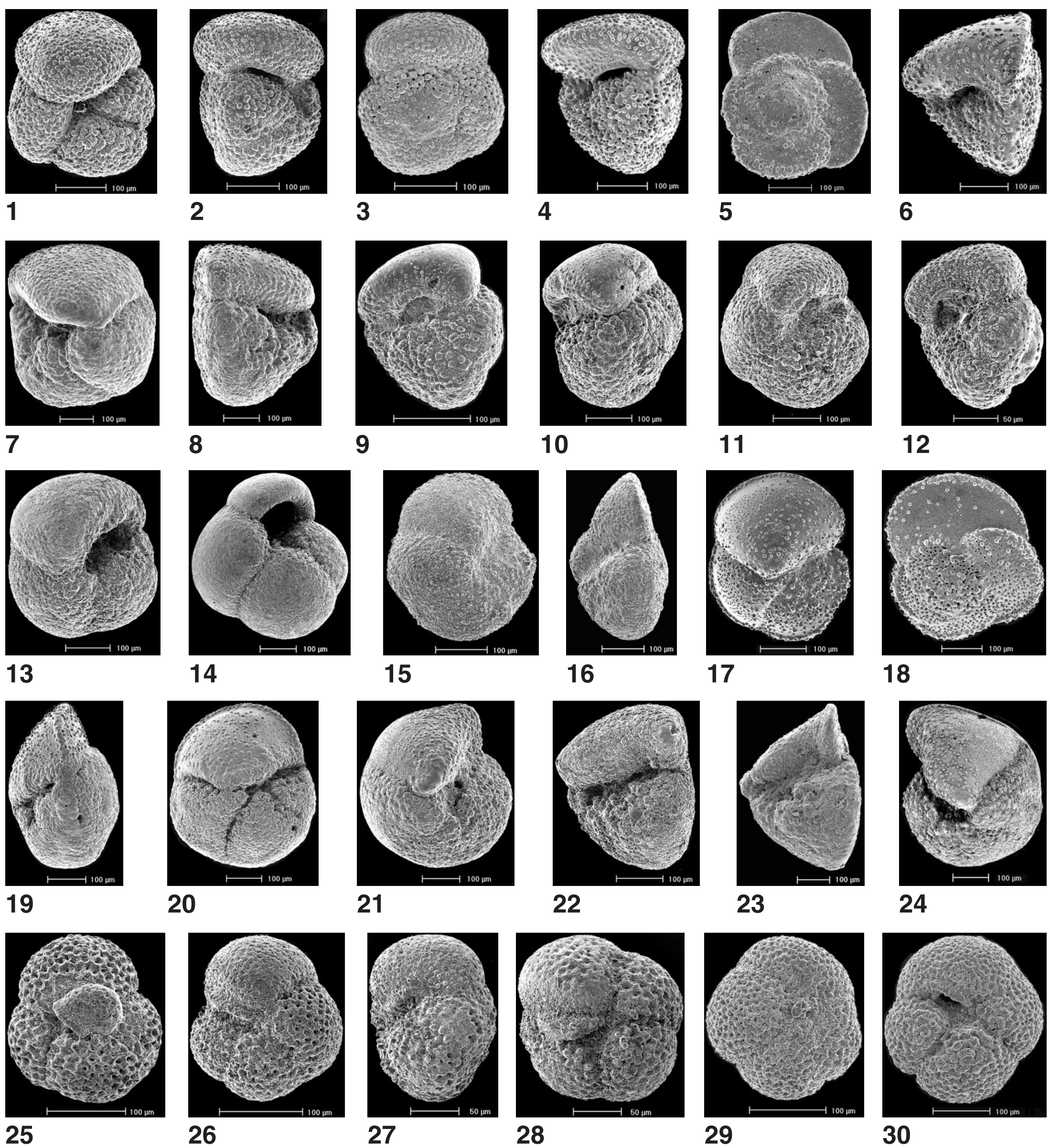

Plate P6. **1.** *Neogloboquadrina pachyderma* (Sample 182-1126B-5H-2, 75–77 cm). **2.** *Neogloboquadrina acostaensis* (Sample 182-1126B-5H-2, 75–77 cm). **3.** *Neogloboquadrina* cf. *N. dutertrei* (Sample 182-1134A-6H-1, 77–79 cm). **4.** *Globoturborotalita woodi;* thick-rimmed variant (Sample 182-1134A-8H-3, 75–77 cm). **5.** *Globoturborotalita rubescens* (Sample 182-1134A-13H-3, 75–77 cm). **6–8.** *Globoturborotalita nepenthes;* (6, 7) Sample 182-1134A-13H-1, 75–77 cm; (8) Sample 182-1134A-9H-1, 75–77 cm. **9.** *Globigerinoides obliquus* (Sample 182-1126B-5H-2, 75–77 cm). **10, 11.** *Globigerinoides extremus* (Sample 182-1134A-8H-3, 75–77 cm). **12, 13.** *Globigerinoides ruber* (Sample 182-1134A-6H-1, 77–79 cm). **14, 15.** *Globigerinoides kennetti;* (14) Sample 182-1134A-9H-3, 77–79 cm; (15) Sample 182-1134A-9H-1, 75–77 cm. **16, 17.** *Globigerinoides quadrilobatus* (Sample 182-1134A-13H-1, 75–77 cm). **18.** *Globigerinoides sacculifer* (Sample 182-1126C-9H-5, 45–50 cm). **19.** *Sphaeroidinelopsis seminulina* (Sample 182-1134A-8H-3, 75–77 cm). **20.** *Dentoglobigerina altispira* (Sample 182-1126C-8H-CC, 43–46 cm). **21, 22.** *Globigerina bulloides;* (21) Sample 182-1134A-8H-3, 75–77 cm; (22) Sample 182-1126B-5H-2, 75–77 cm. **23.** *Globigerina falconensis* (Sample 182-1126B-5H-2, 75–77 cm). **24.** *Globigerina quinqueloba* (Sample 182-1134A-8H-5, 78–80 cm). **25.** *Globigerinella obesa* (Sample 182-1126C-8H-CC, 43–46 cm). **26, 27.** *Globigerinella siphonifera;* (26) Sample 182-1134A-8H-3, 75–77 cm; (27) Sample 182-1134A-6H-5, 75–77 cm. **28.** *Tenuitellinata juvenilis* (Sample 182-1134A-15X-3, 75–77 cm). **29.** *Globigerinita naparimaensis* (Sample 182-1134A-6H-1, 77–79 cm). **30.** *Globigerinita glutinata* (Sample 182-1126B-5H-2, 75–77 cm).

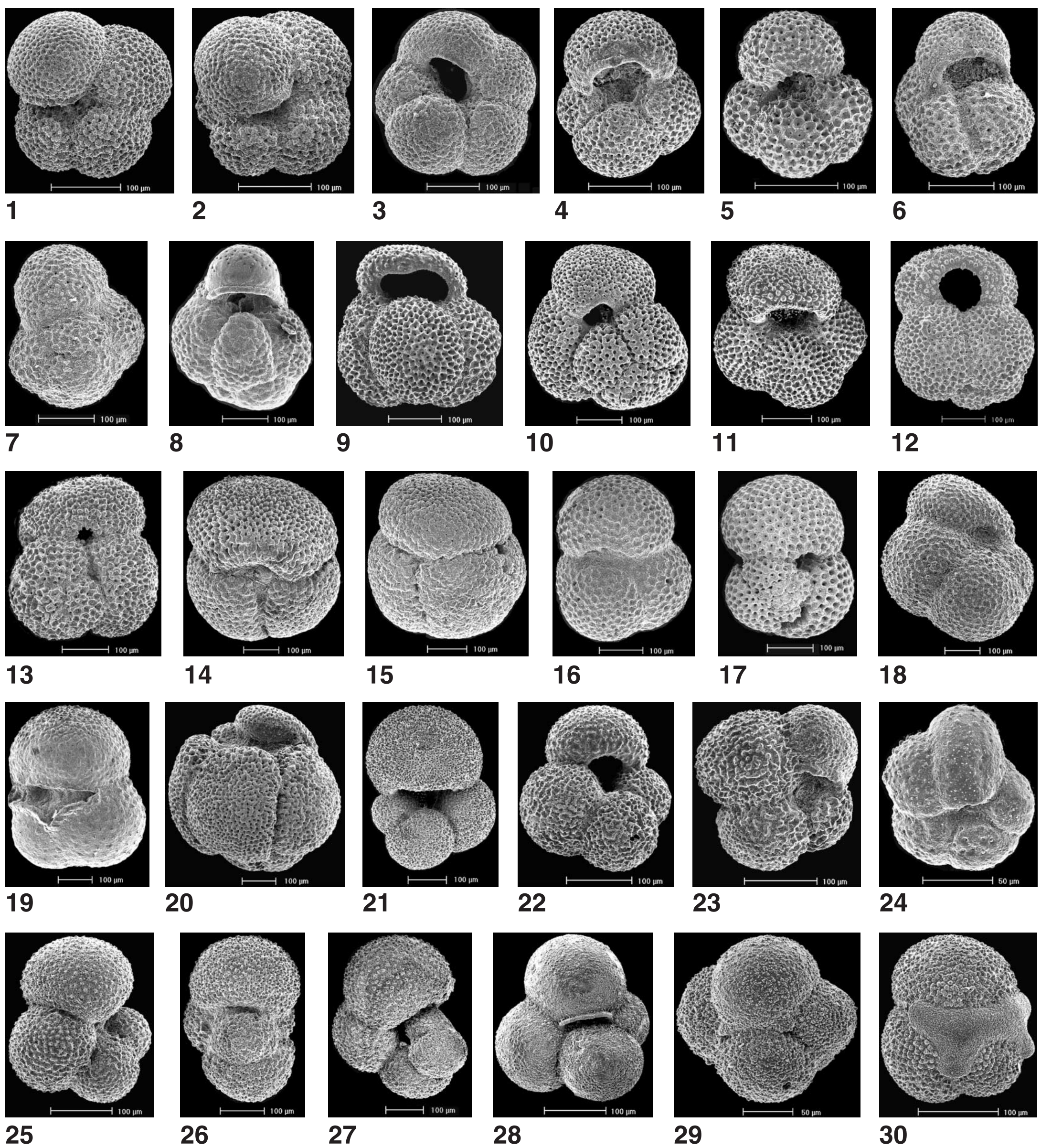

Table AT1. Counts of planktonic foraminifers, Hole 1126B. (This table is available in an **oversized format.**)

Table AT2. Counts of planktonic foraminifers, Hole 1126C. (**See table notes.** Continued on next three pages.)

	182-1126C-							182-1126C-						
Core, section, interval (cm):	12X-1, 76–78	12X-3, 75–77	13X-1, 75–77	13X-3, 75–77	13X-5, 75–77	14X-1, 75–77	14X-3, 75–77	12X-1, 76–78	12X-3, 75–77	13X-1, 75–77	13X-3, 75–77	13X-5, 75–77	14X-1, 75–77	14X-3, 75–77
Depth (mbsf):	100.66	103.65	110.25	113.25	116.25	119.85	122.85	100.66	103.65	110.25	113.25	116.25	119.85	122.85
Preservation:	G	G	G	G		G	G							
Group abundance:	A	A	A	A		A	A							
Benthic abundance (%):	5	5	5	5		5	5							
Sponge spicules:	F	A	No	C		C	A							
Cassigerinella chipolensis		3						0.00	0.85	0.00	0.00		0.00	0.00
Catapsydrax dissimilis (10701)								0.00	0.00	0.00	0.00		0.00	0.00
Catapsydrax dissimilis (no bulla)								0.00	0.00	0.00	0.00		0.00	0.00
Catapsydrax parvulus (10706)	3		1	2		4		0.86	0.00	0.28	0.54		1.17	0.00
Catapsydrax unicavus (11806)								0.00	0.00	0.00	0.00		0.00	0.00
Chiloguembelina cubensis (11816)								0.00	0.00	0.00	0.00		0.00	0.00
Dentoglobigerina altispira (10731)								0.00	0.00	0.00	0.00		0.00	0.00
Dentoglobigerina baroemoenensis								0.00	0.00	0.00	0.00		0.00	0.00
Dentoglobigerina galavisi (11901)								0.00	0.00	0.00	0.00		0.00	0.00
Dentoglobigerina globularis								0.00	0.00	0.00	0.00		0.00	0.00
Dentoglobigerina larmeui (11916)								0.00	0.00	0.00	0.00		0.00	0.00
Fohsella peripheroronda (5315)								0.00	0.00	0.00	0.00		0.00	0.00
Globigerina bulloides (10806)	40	35	42	12		37	28	11.53	9.97	11.73	3.24		10.85	8.43
Globigerina ciperoensis (12016)	5	2	7	18		10	11	1.44	0.57	1.96	4.86		2.93	3.31
Globigerina cryptomphala (1865)								0.00	0.00	0.00	0.00		0.00	0.00
Globigerina euapertura (12026)								0.00	0.00	0.00	0.00		0.00	0.00
Globigerina falconensis (10831)	35	18	33	58		49	40	10.09	5.13	9.22	15.68		14.37	12.05
Globigerina gortanii								0.00	0.00	0.00	0.00		0.00	0.00
Globigerina officinalis (12036)								0.00	0.00	0.00	0.00		0.00	0.00
Globigerina ouachitaensis (12046)								0.00	0.00	0.00	0.00		0.00	0.00
Globigerina praebulloides (12056)								0.00	0.00	0.00	0.00		0.00	0.00
Globigerina quinqueloba (10841)		4	2	7		10	15	0.00	1.14	0.56	1.89		2.93	4.52
Globigerinatheka index (12081)								0.00	0.00	0.00	0.00		0.00	0.00
Globigerinatheka subconglobata (785)								0.00	0.00	0.00	0.00		0.00	0.00
Globigerinella obesa (12106)	3	2	10	12		6		0.86	0.57	2.79	3.24		1.76	0.00
Globigerinella siphonifera (10876)								0.00	0.00	0.00	0.00		0.00	0.00
Globigerinita glutinata (10881)	7	5	8	13		12	7	2.02	1.42	2.23	3.51		3.52	2.11
Globigerinita juvenilis (12131)	5	5	11	10		8	5	1.44	1.42	3.07	2.70		2.35	1.51
Globigerinita parkerae/boweni								0.00	0.00	0.00	0.00		0.00	0.00
Globigerinita uvula (10891)								0.00	0.00	0.00	0.00		0.00	0.00
Globigerinoides bollii								0.00	0.00	0.00	0.00		0.00	0.00
Globigerinoides bulloideus								0.00	0.00	0.00	0.00		0.00	0.00
Globigerinoides conglobatus (10916)								0.00	0.00	0.00	0.00		0.00	0.00
Globigerinoides obliquus (10951)								0.00	0.00	0.00	0.00		0.00	0.00
Globigerinoides extremus								0.00	0.00	0.00	0.00		0.00	0.00
Globigerinoides kennetti								0.00	0.00	0.00	0.00		0.00	0.00
Globigerinoides parawoodi (10956)			5					0.00	0.00	1.40	0.00		0.00	0.00
Globigerinoides primordius (10961)								0.00	0.00	0.00	0.00		0.00	0.00
Globigerinoides quadrilobatus (10966)	2	1	25	14		25	30	0.58	0.28	6.98	3.78		7.33	9.04
Globigerinoides ruber (10971)				2				0.00	0.00	0.00	0.54		0.00	0.00
Globigerinoides sacculifer (10976)								0.00	0.00	0.00	0.00		0.00	0.00
Globigerinoides seigliei (10981)								0.00	0.00	0.00	0.00		0.00	0.00

Table AT2 (continued).

	182-1126C-							182-1126C-						
Core, section, interval (cm):	12X-1, 76–78	12X-3, 75–77	13X-1, 75–77	13X-3, 75–77	13X-5, 75–77	14X-1, 75–77	14X-3, 75–77	12X-1, 76–78	12X-3, 75–77	13X-1, 75–77	13X-3, 75–77	13X-5, 75–77	14X-1, 75–77	14X-3, 75–77
Depth (mbsf):	100.66	103.65	110.25	113.25	116.25	119.85	122.85	100.66	103.65	110.25	113.25	116.25	119.85	122.85
Preservation:	G	G	G	G		G	G							
Group abundance:	A	A	A	A		A	A							
Benthic abundance (%):	5	5	5	5		5	5							
Sponge spicules:	F	A	No	C		C	A							
Globigerinoides tenellus (10996)								0.00	0.00	0.00	0.00		0.00	0.00
Globigerinoides trilobus (11001)	2	1	11	15		16	12	0.58	0.28	3.07	4.05		4.69	3.61
Globoconella conica			2					0.00	0.00	0.56	0.00		0.00	0.00
Globoconella conoidea (11006) + *miotumida*	52	37	5	8		13	15	14.99	10.54	1.40	2.16		3.81	4.52
Globoconella conomiozea (11011)								0.00	0.00	0.00	0.00		0.00	0.00
Globoconella conomiozea cf.		5						0.00	1.42	0.00	0.00		0.00	0.00
Globoconella incognita (11016)								0.00	0.00	0.00	0.00		0.00	0.00
Globoconella inflata (11021)								0.00	0.00	0.00	0.00		0.00	0.00
Globoconella miozea (11026)		3	1	5		2	10	0.00	0.85	0.28	1.35		0.59	3.01
Globoconella panda (11036)								0.00	0.00	0.00	0.00		0.00	0.00
Globoconella praescitula (11041)								0.00	0.00	0.00	0.00		0.00	0.00
Globoconella sphericomiozea (11051)								0.00	0.00	0.00	0.00		0.00	0.00
Globoconella zealandica (11056)								0.00	0.00	0.00	0.00		0.00	0.00
Globoquadrina dehiscens (12156)	28	38	14	10		26	8	8.07	10.83	3.91	2.70		7.62	2.41
Globoquadrina praedehiscens (11086)								0.00	0.00	0.00	0.00		0.00	0.00
Globoquadrina sellii								0.00	0.00	0.00	0.00		0.00	0.00
Globoquadrina tapuriensis								0.00	0.00	0.00	0.00		0.00	0.00
Globoquadrina tripartita (12176)								0.00	0.00	0.00	0.00		0.00	0.00
Globoquadrina venzuelana (11096)								0.00	0.00	0.00	0.00		0.00	0.00
Globorotalia cibaoensis								0.00	0.00	0.00	0.00		0.00	0.00
Globorotalia crassaconica (5290)								0.00	0.00	0.00	0.00		0.00	0.00
Globorotalia crassaformis (11136)								0.00	0.00	0.00	0.00		0.00	0.00
Globorotalia crassula (11146)								0.00	0.00	0.00	0.00		0.00	0.00
Globorotalia exilis (11151)								0.00	0.00	0.00	0.00		0.00	0.00
Globorotalia hirsuta (11171)								0.00	0.00	0.00	0.00		0.00	0.00
Globorotalia inflata (11181)								0.00	0.00	0.00	0.00		0.00	0.00
Globorotalia juanai								0.00	0.00	0.00	0.00		0.00	0.00
Globorotalia lenguaensis								0.00	0.00	0.00	0.00		0.00	0.00
Globorotalia paralenguaensis								0.00	0.00	0.00	0.00		0.00	0.00
Globorotalia margaritae (11206)								0.00	0.00	0.00	0.00		0.00	0.00
Globorotalia menardii (11211)								0.00	0.00	0.00	0.00		0.00	0.00
Globorotalia mesotumida								0.00	0.00	0.00	0.00		0.00	0.00
Globorotalia peripheroronda			34	12		10		0.00	0.00	9.50	3.24		2.93	0.00
Globorotalia plesiotumida								0.00	0.00	0.00	0.00		0.00	0.00
Globorotalia pliozea (11276)								0.00	0.00	0.00	0.00		0.00	0.00
Globorotalia praemenardii (11281)			2	5		7	11	0.00	0.00	0.56	1.35		2.05	3.31
Globorotalia pseudomiocenica (5370)								0.00	0.00	0.00	0.00		0.00	0.00
Globorotalia puncticulata (11291)								0.00	0.00	0.00	0.00		0.00	0.00
Globorotalia scitula (11296)	1							0.29	0.00	0.00	0.00		0.00	0.00
Globorotalia spp.								0.00	0.00	0.00	0.00		0.00	0.00
Globorotalia theyeri cf.								0.00	0.00	0.00	0.00		0.00	0.00
Globorotalia tosaensis (11321)								0.00	0.00	0.00	0.00		0.00	0.00

Table AT2 (continued).

	182-1126C-							182-1126C-						
Core, section, interval (cm):	12X-1, 76–78	12X-3, 75–77	13X-1, 75–77	13X-3, 75–77	13X-5, 75–77	14X-1, 75–77	14X-3, 75–77	12X-1, 76–78	12X-3, 75–77	13X-1, 75–77	13X-3, 75–77	13X-5, 75–77	14X-1, 75–77	14X-3, 75–77
Depth (mbsf):	100.66	103.65	110.25	113.25	116.25	119.85	122.85	100.66	103.65	110.25	113.25	116.25	119.85	122.85
Preservation:	G	G	G	G		G	G							
Group abundance:	A	A	A	A		A	A							
Benthic abundance (%):	5	5	5	5		5	5							
Sponge spicules:	F	A	No	C		C	A							
Globorotalia truncatulinoides (11326)								0.00	0.00	0.00	0.00		0.00	0.00
Globorotalia tumida (11336)								0.00	0.00	0.00	0.00		0.00	0.00
Globorotalia ungulata								0.00	0.00	0.00	0.00		0.00	0.00
Globorotaloides suteri (12211)	7	5	2	4		2	5	2.02	1.42	0.56	1.08		0.59	1.51
Globorotaloides testarugosa (12216)								0.00	0.00	0.00	0.00		0.00	0.00
Globorotaloides variabilis (12226)								0.00	0.00	0.00	0.00		0.00	0.00
Hastigerina pelagica (11371)								0.00	0.00	0.00	0.00		0.00	0.00
Neogloboquadrina acostaensis								0.00	0.00	0.00	0.00		0.00	0.00
Neogloboquadrina continuosa (11416)	4	2	3	2				1.15	0.57	0.84	0.54		0.00	0.00
Neogloboquadrina dutertrei (11421)								0.00	0.00	0.00	0.00		0.00	0.00
Neogloboquadrina humerosa								0.00	0.00	0.00	0.00		0.00	0.00
Neogloboquadrina pachyderma (11441)								0.00	0.00	0.00	0.00		0.00	0.00
Orbulina bilobata (11446)								0.00	0.00	0.00	0.00		0.00	0.00
Orbulina suturalis (11451)								0.00	0.00	0.00	0.00		0.00	0.00
Orbulina universa (11456)	14	26	23	29		25	28	4.03	7.41	6.42	7.84		7.33	8.43
Paragloborotalia bella (11386)								0.00	0.00	0.00	0.00		0.00	0.00
Paragloborotalia birnageae								0.00	0.00	0.00	0.00		0.00	0.00
Paragloborotalia mayeri (11391)	1	2	11	8				0.29	0.57	3.07	2.16		0.00	0.00
Paragloborotalia opima nana (12466)								0.00	0.00	0.00	0.00		0.00	0.00
Paragloborotalia opima opima (12471)								0.00	0.00	0.00	0.00		0.00	0.00
Paragloborotalia semivera (12486)								0.00	0.00	0.00	0.00		0.00	0.00
Paragloborotalia sp.								0.00	0.00	0.00	0.00		0.00	0.00
Praeorbulina glomerosa (11471)	5	10	15	11		12	5	1.44	2.85	4.19	2.97		3.52	1.51
Praeorbulina sicana (10986)								0.00	0.00	0.00	0.00		0.00	0.00
Praeorbulina transitoria (11481)								0.00	0.00	0.00	0.00		0.00	0.00
Pseudohastigerina micra (12601)								0.00	0.00	0.00	0.00		0.00	0.00
Pulleniatina obliquiloculata (11496)								0.00	0.00	0.00	0.00		0.00	0.00
Sphaeroidinella dehiscens (11516)								0.00	0.00	0.00	0.00		0.00	0.00
Sphaeroidinellopsis disjuncta (12626)								0.00	0.00	0.00	0.00		0.00	0.00
Sphaeroidinellopsis kochi (11526)	4	2	1					1.15	0.57	0.28	0.00		0.00	0.00
Sphaeroidinellopsis seminulina (11536)			2	3				0.00	0.00	0.56	0.81		0.00	0.00
Subbotina angiporoides (12636)								0.00	0.00	0.00	0.00		0.00	0.00
Subbotina eocaena (12646)								0.00	0.00	0.00	0.00		0.00	0.00
Subbotina linaperta (12671)								0.00	0.00	0.00	0.00		0.00	0.00
Tenuitella gemma (12716)								0.00	0.00	0.00	0.00		0.00	0.00
Tenuitella munda (12726)								0.00	0.00	0.00	0.00		0.00	0.00
Tenuitella spp.	2	10	5	14		9	15	0.58	2.85	1.40	3.78		2.64	4.52
Tenuitellinata angustiumbilicata (12736)								0.00	0.00	0.00	0.00		0.00	0.00
Tenuitellinata juvenilis (12741)								0.00	0.00	0.00	0.00		0.00	0.00
Tenuitellinata prestainforthi (12746)								0.00	0.00	0.00	0.00		0.00	0.00
Turborotalia ampliapertura (12756)								0.00	0.00	0.00	0.00		0.00	0.00
Turborotalia cerroazulensis (12761)								0.00	0.00	0.00	0.00		0.00	0.00

Table AT2 (continued).

	182-1126C-							182-1126C-						
Core, section, interval (cm):	12X-1, 76–78	12X-3, 75–77	13X-1, 75–77	13X-3, 75–77	13X-5, 75–77	14X-1, 75–77	14X-3, 75–77	12X-1, 76–78	12X-3, 75–77	13X-1, 75–77	13X-3, 75–77	13X-5, 75–77	14X-1, 75–77	14X-3, 75–77
Depth (mbsf):	100.66	103.65	110.25	113.25	116.25	119.85	122.85	100.66	103.65	110.25	113.25	116.25	119.85	122.85
Preservation:	G	G	G	G		G	G							
Group abundance:	A	A	A	A		A	A							
Benthic abundance (%):	5	5	5	5		5	5							
Sponge spicules:	F	A	No	C		C	A							
Turborotalia cunialensis (12771)								0.00	0.00	0.00	0.00		0.00	0.00
Turborotalia increbescens (12776)								0.00	0.00	0.00	0.00		0.00	0.00
Turborotalita humulis (11581)								0.00	0.00	0.00	0.00		0.00	0.00
Turborotalita sp.								0.00	0.00	0.00	0.00		0.00	0.00
Zeaglobigerina apertura (11586)	4	5						1.15	1.42	0.00	0.00		0.00	0.00
Zeaglobigerina brazieri (12811)								0.00	0.00	0.00	0.00		0.00	0.00
Zeaglobigerina brazieri cf.							10	0.00	0.00	0.00	0.00		0.00	3.01
Zeaglobigerina brevis (5255)								0.00	0.00	0.00	0.00		0.00	0.00
Zeaglobigerina connecta (12816)				12			12	0.00	0.00	0.00	3.24		0.00	3.61
Zeaglobigerina decoraperta (11601)	18	23	20	15		3		5.19	6.55	5.59	4.05		0.88	0.00
Zeaglobigerina druryi	15	20	12	7		2	5	4.32	5.70	3.35	1.89		0.59	1.51
Zeaglobigerina labiacrassata (12821)								0.00	0.00	0.00	0.00		0.00	0.00
Zeaglobigerina nepenthes (11611)								0.00	0.00	0.00	0.00		0.00	0.00
Zeaglobigerina rubescens (11616)								0.00	0.00	0.00	0.00		0.00	0.00
Zeaglobigerina woodi (11621)	60	72	18	17		25	20	17.29	20.51	5.03	4.59		7.33	6.02
Zeaglobigerina spp.	10	5	13	15		5	10	2.88	1.42	3.63	4.05		1.47	3.01
Other globigerinids	20	10	20	30		23	30	5.76	2.85	5.59	8.11		6.74	9.04
Total:	347	351	358	370		341	332							

Notes: Preservation: G = good. Abundance: A = abundant, C = common, F = few, R = rare. Numbers after species names are catalog numbers from the ODP Janus database. Percentage data are given in the second half of the table.

Table AT3. Counts of planktonic foraminifers, Hole 1128B. (This table is available in an **oversized format.**)

Table AT4. Counts of planktonic foraminifers, Hole 1128C. (This table is available in an **oversized format.**)

Table AT5. Counts of planktonic foraminifers, Hole 1130A. (This table is available in an **oversized format.**)

Table AT6. Counts of planktonic foraminifers, Hole 1130B. (This table is available in an **oversized format.**)

Table AT7. Planktonic foraminifers, Hole 1132B. (See table notes. Continued on next two pages.)

	182-1130A-						
Core, section, interval (cm):	26X-1, 75–77	26X-3, 75–77	26X-5, 75–77	27X-1, 75–77	27X-2, 75–77	28X-1, 76–78	28X-2, 75–77
Depth (mbsf):	229.65	232.65	235.65	239.25	240.75	248.66	250.15
Zone:	lower Pleistocene			SN13	SN13	N16–N17	
Preservation:	P	M	P	M	M	M–G	G
Group abundance:	C	C	C	C	A	A	A
Bathymetry/size:	F	F	F				
Benthic abundance (%):	10	10	10	10	10	5	5
Acarinina aculeata (5260)							
Acarinina bullbrooki (11636)							
Acarinina collactea (11651)							
Acarinina primitiva (11691)							
Acarinina spinuloinflata (11716)							
Cassigerinella chipolensis							
Catapsydrax dissimilis (10701)							
Catapsydrax parvulus (10706)	P	P	P	P		P	P
Catapsydrax unicavus (11806)							
Chiloguembelina cubensis (11816)							
Dentoglobigerina altispira (10731)						P	
Dentoglobigerina baroemoenensis							
Dentoglobigerina galavisi (11901)							
Dentoglobigerina globularis							
Dentoglobigerina larmeui (11916)							
Fohsella peripheroronda (5315)							
Globigerina bulloides (10806)	P	F	P	P	P	P	P
Globigerina ciperoensis (12016)							
Globigerina cryptomphala (1865)							
Globigerina euapertura (12026)							
Globigerina falconensis (10831)	A	A	F	C	C	C	F
Globigerina gortanii							
Globigerina officinalis (12036)							
Globigerina ouachitaensis (12046)							
Globigerina praebulloides (12056)							
Globigerina quinqueloba (10841)	F	F	P	P	P	P	P
Globigerinatheka index (12081)							
Globigerinatheka subconglobata (785)							
Globigerinella obesa (12106)	P	P	P	P	P	P	P
Globigerinella siphonifera (10876)			P	P	P		P
Globigerinita glutinata (10881)	P	C	C	P	C	P	P
Globigerinita juvenilis (12131)	P	C	C	P	C	P	P
Globigerinita parkerae (10886)							
Globigerinita uvula (10891)							
Globigerinoides bollii							
Globigerinoides conglobatus (10916)	P						
Globigerinoides obliquus (10951)					P	R	P
Globigerinoides extremus		P			P	P	P
Globigerinoides kennetti							
Globigerinoides parawoodi (10956)							
Globigerinoides primordius (10961)							
Globigerinoides quadrilobatus (10966)							P
Globigerinoides ruber (10971)	F	P	P	P	R		
Globigerinoides sacculifer (10976)						P	P
Globigerinoides seigliei (10981)							
Globigerinoides tenellus (10996)							
Globigerinoides trilobus (11001)	P		P	P		P	P
Globoconella conoidea (11006) + *miotumida*						C	C
Globoconella conomiozea (11011)							
Globoconella incognita (11016)							
Globoconella inflata (11021)							
Globoconella miozea (11026)							
Globoconella panda (11036)							
Globoconella praescitula (11041)							
Globoconella sphericomiozea (11051)							
Globoconella zealandica (11056)							
Globoquadrina dehiscens (12156)							
Globoquadrina praedehiscens (11086)							
Globoquadrina sellii							

Table AT7 (continued).

	182-1130A-						
Core, section, interval (cm):	26X-1, 75–77	26X-3, 75–77	26X-5, 75–77	27X-1, 75–77	27X-2, 75–77	28X-1, 76–78	28X-2, 75–77
Depth (mbsf):	229.65	232.65	235.65	239.25	240.75	248.66	250.15
Zone:	lower Pleistocene			SN13	SN13	N16–N17	
Preservation:	P	M	P	M	M	M–G	G
Group abundance:	C	C	C	C	A	A	A
Bathymetry/size:	F	F	F				
Benthic abundance (%):	10	10	10	10	10	5	5
Globoquadrina tapuriensis							
Globoquadrina tripartita (12176)							
Globoquadrina venzuelana (11096)							
Globorotalia juanai						P	P
Globorotalia crassaconica (5290)							
Globorotalia crassaformis (11136)	F	P	P	P	R		
Globorotalia crassula (11146)	F	P	P	P	P		
Globorotalia exilis (11151)							
Globorotalia hirsuta (11171)							
Globorotalia inflata (11181)	P	P	F	P	P		
Globorotalia lenguaensis							
Globorotalia paralenguaensis							
Globorotalia margaritae (11206)							
Globorotalia menardii (11211)						P	
Globorotalia mesotumida						P	
Globorotalia peripheroronda							
Globorotalia plesiotumida							
Globorotalia pliozea (11276)							
Globorotalia cibaoensis						P	P
Globorotalia praemenardii (11281)							
Globorotalia pseudomiocenica (5370)							
Globorotalia puncticulata (11291)	C	F	P	P	A		
Globorotalia scitula (11296)	P		P		P	P	P
Globorotalia spp.							
Globorotalia theyeri cf.							
Globorotalia tosaensis (11321)							
Globorotalia truncatulinoides (11326)				P			
Globorotalia tumida (11336)							
Globorotalia ungulata							
Globorotaloides suteri (12211)						P	P
Globorotaloides testarugosa (12216)							
Globorotaloides variabilis (12226)							
Hastigerina pelagica (11371)							
Neogloboquadrina acostaensis						F	R
Neogloboquadrina continuosa (11416)							P
Neogloboquadrina dutertrei (11421)							
Neogloboquadrina humerosa							
Neogloboquadrina pachyderma (11441)	P	P	P	R	P		
Orbulina bilobata (11446)							
Orbulina suturalis (11451)							
Orbulina universa (11456)	P	P	P	P	P	P	P
Paragloborotalia bella (11386)							
Paragloborotalia birnageae							
Paragloborotalia mayeri (11391)							
Paragloborotalia opima nana (12466)							
Paragloborotalia opima opima (12471)							
Paragloborotalia semivera (12486)							
Praeorbulina glomerosa (11471)							
Praeorbulina sicana (10986)							
Praeorbulina transitoria (11481)							
Pseudohastigerina micra (12601)							
Pulleniatina obliquiloculata (11496)							
Sphaeroidinella dehiscens (11516)							
Sphaeroidinellopsis disjuncta (12626)							
Sphaeroidinellopsis kochi (11526)							P
Sphaeroidinellopsis seminulina (11536)						P	P
Subbotina angiporoides (12636)							
Subbotina eocaena (12646)							
Subbotina linaperta (12671)							
Tenuitella gemma (12716)							
Tenuitella munda (12726)							

Table AT7 (continued).

	182-1130A-						
Core, section, interval (cm):	26X-1, 75–77	26X-3, 75–77	26X-5, 75–77	27X-1, 75–77	27X-2, 75–77	28X-1, 76–78	28X-2, 75–77
Depth (mbsf):	229.65	232.65	235.65	239.25	240.75	248.66	250.15
Zone:	lower Pleistocene			SN13	SN13	N16–N17	
Preservation:	P	M	P	M	M	M–G	G
Group abundance:	C	C	C	C	A	A	A
Bathymetry/size:	F	F	F				
Benthic abundance (%):	10	10	10	10	10	5	5
Tenuitella spp.							
Tenuitellinata angustiumbilicata (12736)							
Tenuitellinata juvenilis (12741)							
Tenuitellinata prestainforthi (12746)							
Turborotalia ampliapertura (12756)							
Turborotalia cerroazulensis (12761)							
Turborotalia cunialensis (12771)							
Turborotalia increbescens (12776)							
Turborotalita humulis (11581)							
Zeaglobigerina apertura (11586)				P		P	P
Zeaglobigerina brazieri (12811)							
Zeaglobigerina brevis (5255)							
Zeaglobigerina connecta (12816)			P				
Zeaglobigerina decoraperta (11601)					P	P	P
Zeaglobigerina druryi						P	
Zeaglobigerina labiacrassata (12821)							
Zeaglobigerina nepenthes (11611)						P	
Zeaglobigerina rubescens (11616)							
Zeaglobigerina woodi (11621)				P	P	A	A
Zeaglobigerina spp.	P	R	P	P	P	P	P
Other globigerinids:							
Comments:			Mixed			No *dehiscens*	Transported *Elphidium*

Notes: Preservation: G = good, M = moderate, P = poor. Abundance: A = abundant, C = common, F = few, R = rare. Size: F = fine. Numbers after species names are catalog numbers from the ODP Janus database.

Table AT8. Counts of planktonic foraminifers, Hole 1134A. (This table is available in an **oversized format.**)

Table AT9. Counts of planktonic foraminifers, Hole 1134B. (This table is available in an **oversized format.**)